THE OHIO STATE UNIVERSITY

Cyclic Behavior and Modeling of Prequalified Rigid Steel Connections

Authors:

Baris Kasapoglu, Ph.D. student (Department of Civil, Environmental and Geodetic Engineering)

Ali Nassiri, Ph.D. (Department of Integrated Systems Engineering)

Halil Sezen, Ph.D. (Department of Civil, Environmental and Geodetic Engineering)

April 2023

Introduction

It is a challenge to analyze and determine the behavior of a structural steel connection when it is subjected to a variety of loading conditions using conventional analytical methods. Finite Element Analysis (FEA) is a useful tool for numerically modeling physical details that are too complex for regular analytical approaches. IDEA StatiCa is a steel connection design software that can be used to model and analyze all types of welded and bolted connections, base plates, footings, and anchoring systems.

The objective of this project is to evaluate the behavior of seismic steel connections obtained from the IDEA StatiCa software package considering load resistance, rotation capacity, and moment-rotation response. For this purpose, the following steps were taken in the project:

- Four different prequalified rigid steel connections that can be used as part of intermediate moment frame (IMF) and special moment frame according to AISC 358 (2016), and one moment connection to be used as part of ordinary moment frame according to AISC 341 were selected. Namely these connections are:
    - Reduced beam section (RBS) moment connection
    - End plate moment (EPM) connection
    - Welded unreinforced flange-welded web (WUF-W) moment connection
    - Welded unreinforced flange-bolted web (WUF-B) moment connection
    - Double-tee moment connection
- For each connection type, one experimental study was chosen from the literature, and one of the tested specimens was selected as a baseline model, and five additional variation specimens were either selected from the same test or created to be examined.
- Following the requirements given in AISC 341 (2016), AISC 358 (2016), and AISC 360 (2016), the design checks were performed for each connection type, and flexural capacities were calculated.
- The same specimens were modelled and analyzed in IDEA StatiCa, and their moment capacities, and failure modes were calculated.
- For the baseline model of each connection type, moment rotation analysis was performed using IDEA StatiCa and the calculated moment plastic rotation curve was compared with the experimentally measured moment plastic rotation relationship given in the test report.
- To compare the IDEA StatiCa results with traditional FEA approach, the equivalent ABAQUS model was developed for the baseline model of each connection type. Stress and strain distributions as well as moment rotation relationships were compared.
- The results obtained from the tests, AISC design calculations, IDEA StatiCa, and ABAQUS were evaluated, and recommendations were provided.

Chapter 1 Reduced Beam Section (RBS) Moment Connection

1.1. Introduction

RBS is one of the prequalified moment connections permitted to be used in seismic region by AISC as a part of intermediate moment frame (IMF) and special moment frame (SMF) systems if the requirements listed in AISC 358 Chapter 5 are satisfied. The beam flanges at the certain distance away from column face are trimmed with an intent of that yielding and plastic hinge occur within the reduced section.

In this chapter, first, one test specimen for reduced beam section (RBS) moment connection was selected from the experimental study conducted by Uang et al. (2000) at C. L. Powell Structural Research Laboratories, University of California at San Diego. It was modeled and analyzed in IDEA StatiCa and ABAQUS by representing the test condition. Numerically obtained results were compared with the test observations and the design strength capacity calculated following the requirements of AISC 341, 358 and 360. Then, five additional variations were developed, and their capacities were calculated using IDEA StatiCa and based on AISC code requirements. At the end the results were compared.

1.2. Experimental Study

Four identical test specimens were subjected to different loading histories to investigate the effects of loading sequence and lateral bracing as a part of SAC project. Among them, the first test specimen, LS-1, was selected to be studied in this research since it has more available data in the literature. The connection details are shown in Figure 1.1.

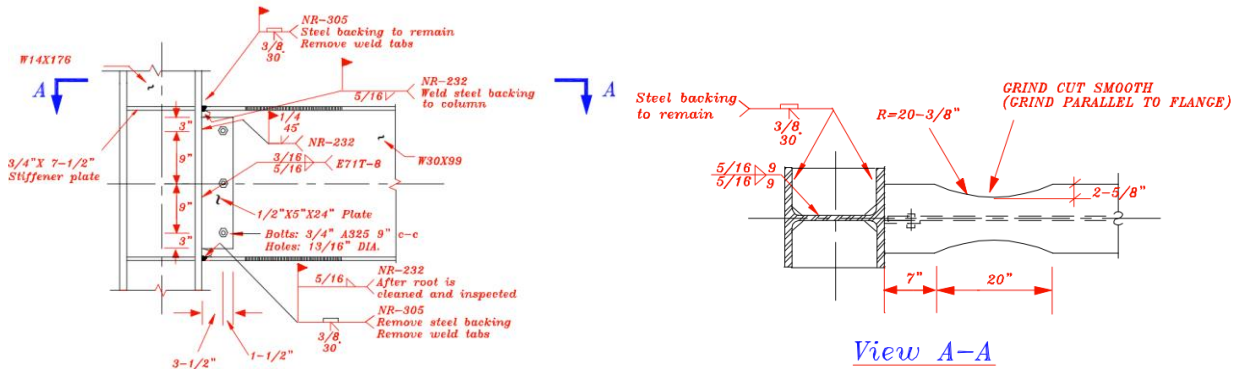

Figure 1.1: Connection details (Uang et al., 2000)

Sizes of the beam and column are W30X99 and W14X176, respectively, and both are made from ASTM A992 Steel. Web and flange of the beam are welded to column flange using a complete-joint-penetration (CJP) groove weld as specified in AISC 358. Welding procedure details and measured material properties are presented in Table 1.1. Continuity plate with a thickness of. 3/4 in. and a corner clip of 1.79 in. is made from ASTM A572 Grade 50. It is welded to the flange of column using CJP groove weld and to the web of column with 5/16 in. double fillet. Shear tab is used for erection purpose and removed before testing.

Table 1.1: Material and specimen details

Member	Size	Grade	Yield Stress (ksi)		Ultimate Strength (ksi)	
			mill certs.	coupon tests*	mill certs.	coupon tests*
Beam	W30X99	A992	56.0	54.7 flange 58.0 web	74.0	71.9 flange 74.8 web
Column	W14X176	A992	64.0		84.0	

The standard SAC-multi-step loading history is applied at the end of the beam which is 149 in. away from the column centerline by hydraulic actuator. The column is laterally restrained and the top and bottom of the column are restricted to strong wall and floor. Test setup and applied loading history are presented in Figure 1.2.

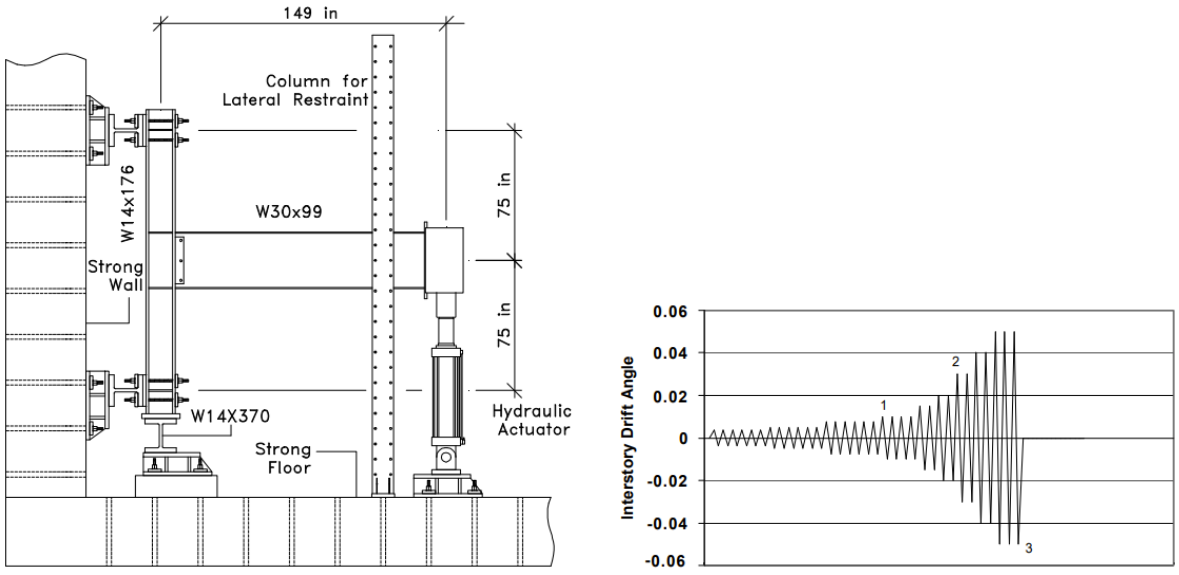

(a) (b)

Figure 1.2: (a) Test setup; and (b) loading history (Uang et al., 2000)

The main observations made during the test by the researchers are as follows:

- Significant yielding develops in the RBS region
- Moderate yielding occurred in the column panel zone
- Buckling of the beam was observed during the 3% drift cycles
- Test is stopped after three cycles at 5% drift

Actuator force-displacement and global moment-plastic rotation relations as well as photos after the peak of the third cycle of 5% drift are presented in Figures 1.3 and 1.4.

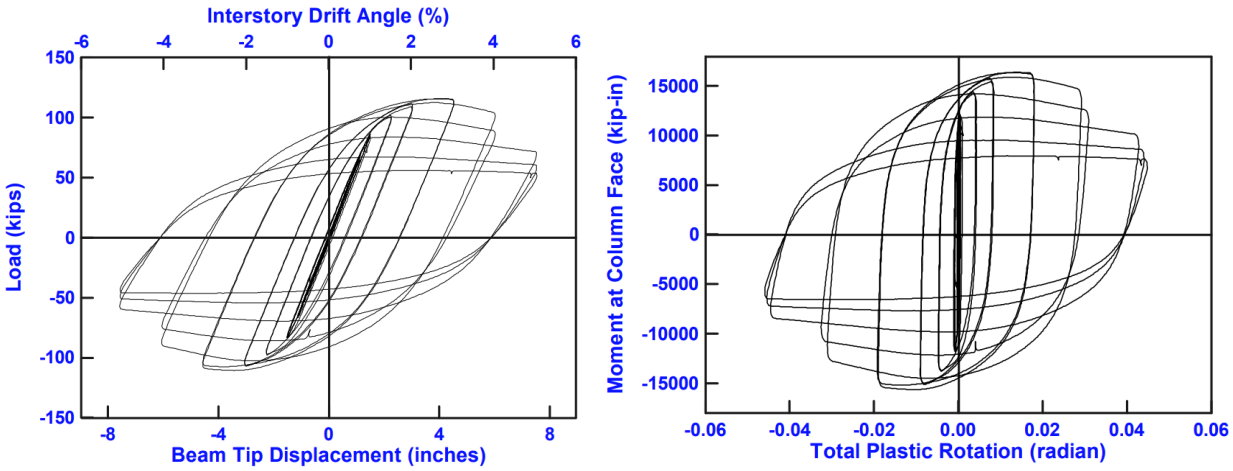

(a) (b)

Figure 1.3: (a) Actuator force-displacement; and (b) global moment-plastic rotation relations (Uang et al., 2000)

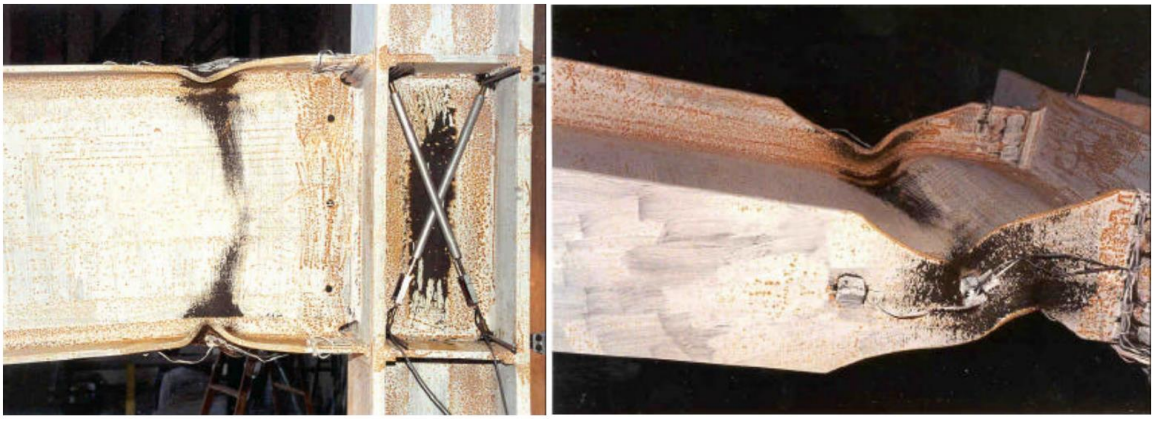

Figure 1.4: Specimen after testing (Uang et al., 2000)

1.3 Code Design Calculations

The following design checks outlined in AISC 358 were performed for the selected test specimen, and five additional variations were developed.

- Check the prequalification limits for column and beam (AISC 358 Section 5.3)
- Check RBS dimensions (AISC 358 Eq. 5.8-1-5.8-3)
- Check that prob. max. moment at the face of the column, M_f, does not exceed available strength $\phi_d M_{pe}$. (ANSI/AISC 358 Eq. 5.8-8)
- Check beam shear strength (AISC 360-16, Eq. J4-3)
- Check beam web-to-column connection (AISC 358 Eq. 5.8-9)
- Check the beam web-to-column connection. (AISC 358 Section 5.6)
- Check continuity plate requirements. (AISC 358 Chapter 2)
- Check column-beam relationship. (AISC 358 Section 5.4)

- Check shear strength of panel zone (AISC 358 Section 5.4)
- Check flexural strength at the centerline of the RBS (AISC Specification F2-1)

It is assumed that frame system satisfies the requirements of SMF. For the calculation of shear force at the center of RBS, V_{RBS}, the distance between column centerlines, L, is assumed to be equal to 360 in. For design calculation of the test specimen, the material properties based on the mill test report were used for beam and column while material properties given in AISC Table Manual Table 2-5 were used for the continuity plate. For comparison purpose, it is intended to represent test condition with a tip load on the beam which is 149 in. away from the column centerline. The self-weight of the beam is neglected. It is assumed that the load combination 6 from ASCE/SEI 7 Section 12.4.2.3 is governing, and the required flexural and shear strength at the face of the column and the centerline of the RBS region are as follows:

- $V_{u@RBS}$ = 40 kip (at the centerline of the RBS)
- $V_{u@FOC}$ = 40 kip (at the face of the column)
- $M_{u@RBS}$ = 4976 kips-in (at the centerline of the RBS)
- $M_{u@FOC}$ = 5656 kips-in (at the face of the column)

AISC limitations were checked for the baseline test specimen (LS-1) and presented in Table 1.2 (for details, see Appendix A).

Table 1.2: AISC Design Checks for the baseline specimen (LS-1)

AISC Design Checks	**LS-1**
Prequalification limits for column and beam	OK
RBS dimensions	OK
Moment at the face of the column > Plastic moment of the beam	OK
Beam shear strength	OK
Beam web-to-column connection	OK
Continuity plate (double-sided fillet weld)	**Not OK**
Column-beam relationships	OK
Panel zone strength	OK
Flexural strength	OK

It is observed that the amount of the weld between the continuity plate and column web (5/16 in. double-sided fillet) is less than the required amount of double-sided fillet weld of 1/2 in. according to AISC Manual Eq. 8-2a. Although this connection would not be allowed to be used in SMF system according to the updated AISC requirements, but it is seen from the test observation that it has no significant effect on the yielding first occurring on RBS cut of the beam. Flexural strength of the RBS cut of the beam is determined according to AISC 360 Eq. F2-1, AISC 358 Eq. 5.8-4 and using ϕ_d of 1.0 (for ductile limit) specified in AISC 358 Section 2.4.1 as follows

$M_n = M_p = F_y \cdot Z_x$ (AISC 360 Eq. F2-1)

$Z_{RBS} = Z_x - 2 \cdot c \cdot t_f \cdot (d - t_f)$ (AISC 358 Eq. 5.8-4)

$\phi_d = 1.0$ (AISC 358 Section 2.4.1)

where

- M_n : the nominal flexural strength of beam
- M_p : plastic moment of beam
- F_y : specified minimum yield stress
- Z_x: plastic section modulus of beam taken about X-axis
- Z_{RBS} : plastic section modulus of center of reduced beam taken about X-axis
- d : depth of beam
- c : depth of cut at beam section
- t_f : thickness of flange of beam
- ϕ_d : Resistance factor for ductile limit

Nominal and available flexural strength at the center of RBS cut of the baseline specimen can be computed as follows:

$M_{n@RBS} = F_y \cdot Z_{RBS}$ = (56 ksi)·(209.9in.^{3}) = 11,754 kips-in.

$\phi M_{n@RBS}$ = (1.0)·(11,754 kips-in.) = 11,754 kips-in.

Five additional variations were developed as presented in Table 1.3. For the first three variations, size of the column and beam elements were varied with respect to baseline model while the last two variations were varied with respect to variation 2. To be able to have a need of column-web doubler plate, it is assumed that there is another beam with the same size connected to column on the other side. The length of the column is equal to 400 in. while the length of the column centerlines are assumed to be equal to 400 in. and 300 in., respectively. Material properties of column and beam (ASTM A992) and continuity plate (ASTM A572 Grade 50) from AISC Manual Tables 2-4 and 2-5 are as follows:

ASTM A992

F_y = 50 ksi

F_u = 65 ksi

ASTM A572 Grade 50

F_y = 50 ksi

F_u = 65 ksi

The design checks were performed following the same procedure shown in Table 1.4. The calculated design capacities are presented in Table 1.5 (for details of Var-4, see Appendix B).

Table 1.3: Properties of variations

Properties	**LS-1**	**Var-1**	**Var-2**	**Var-3**	**Var-4**	**Var-5**
Column	W14X176	W14X176	W14X176	*W18X192*	*W12X170*	*W12X136*

Thickness of doubler plate	-	-	-	-	3/8 in.	1/2 in.
Beam	W30X99	*W27X94*	*W24X68*	W30X99	*W24X68*	*W24X68*
Beam cut - a [in.]	7	6	5	7	5	5
Beam cut - b [in.]	20	19	17	20	17	17
Beam cut - c [in.]	2.63	2	2	2.63	2	2
stiffener plate - thickness [in.]	0.75	0.75	0.75	0.75	0.75	0.75
stiffener plate - depth [in.]	7.5	7.5	7.5	7.5	7.5	7.5
stiffener plate - length [in.]	9	9	9	9	9	9
stiffener plate - double-sided weld [in.]	0.31	0.31	0.31	0.31	0.31	0.31

Table 1.4: Design checks for the variations

AISC Design Checks	**Var-1**	**Var-2**	**Var-3**	**Var-4**	**Var-5**
Prequalification limits for column and beam	OK	OK	OK	OK	OK
RBS dimensions	OK	OK	OK	OK	OK
Moment at the face of the column > Plastic moment of the beam	OK	OK	OK	OK	OK
Beam shear strength	OK	OK	OK	OK	OK
Beam web-to-column connection	OK	OK	OK	OK	OK
Continuity plate (double-sided fillet weld)	**Not OK**	**Not OK**	**Not OK**	**Not OK**	**Not OK**
Column-beam relationships	OK	OK	OK	OK	OK
Panel zone strength	OK	OK	OK	OK	OK
Flexural strength	OK	OK	OK	OK	OK

Table 1.5: Design capacities of the variations

Variations	Column size	Beam size	thickness of doubler plate	Available flexural design strength at centerline of the RBS cut of beam (kips-in.)
Var-1	W14X176	*W27X94*	-	9,978
Var-2	W14X176	*W24X76*	-	6,146
Var-3	*W18X192*	W30X99	-	11,750
Var-4	*W12X170*	*W24X76*	3/8 in.	6,146
Var-5	*W12X136*	W30X99	0.5 in.	6,146

1.4. IDEA StatiCa Analysis

Two different analyzes were performed in IDEA StatiCa. The first one is to investigate the capacity of the baseline specimen under the test condition while the second one is to compute moment-rotation relationship of the connection. First, the test specimen was modeled in IDEA StatiCa. Then, material properties of mill certificate were introduced and overstrength coefficients, R_y and R_t, were set equal to 1.0 (see Figure 1.5). Also, all LRFD resistance factors were set to 1.0 as shown Figure 1.6.

Figure 1.5: Material properties of the test specimen in IDEA StatiCa; a) beam, b) column

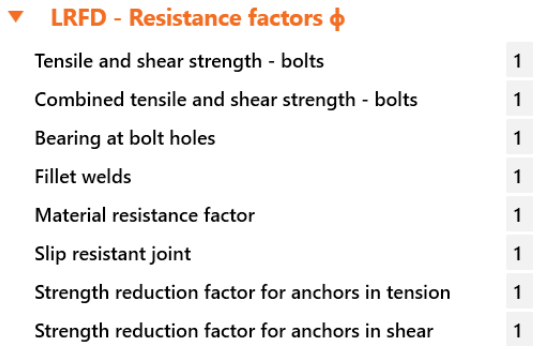

Figure 1.6: LRFD resistance factors in IDEA StatiCa

1.4.1 Capacity analysis

For the capacity calculation, “EPS” analysis type was chosen. Then, “Loads in equilibrium” option was selected to represent the test setup conditions under “Design”. In this selection, internal forces at each node of the frame should be introduced to the system. Default column length of IDEA StatiCa model is equal to 194.55 in. $(2\cdot(4+1.25)\cdot b_c+d_b)$. Since the current version of IDEA StatiCa does not allow to change the length of column, it is assumed that the column length of the IDEA model is equal to the length of test setup (150 in.). It is assumed that the column is fixed at both ends as presented in Figure 1.7(a), the loads to be applied to the model using “loads in equilibrium option” (Figure 1.7(b)) can be calculated as follows:

$V = P \cdot (149 \text{ in.})/150 \text{ in.}$

$M = P \cdot (149 \text{ in.})/2$

$N = P$

where

- P: vertical load applied on the beam at the position of 149 in.
- V: shear applied at the column ends
- N: axial load applied at the bottom of the column
- M: moment applied at the column ends

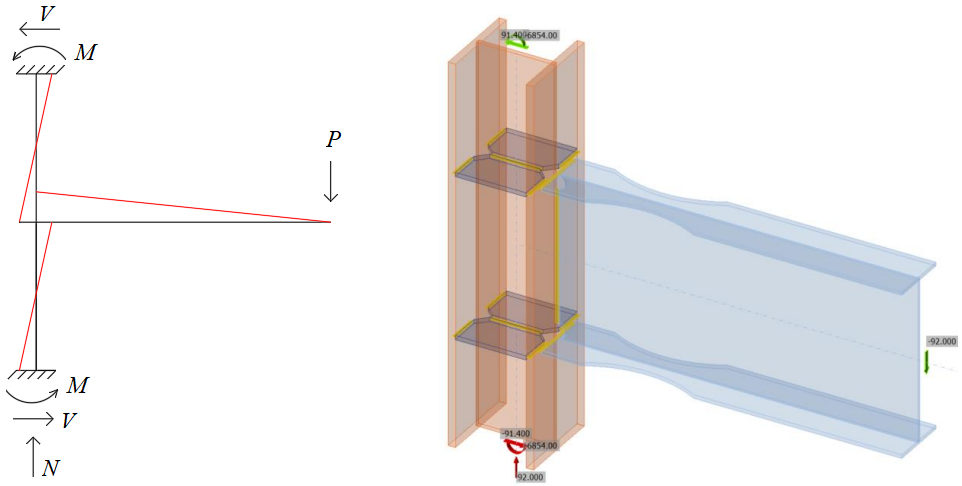

Figure 1.7: (a) Loads in the frame system, and (b) Loads in IDEA StatiCa when P = 92 kips

After incremental loading applied in IDEA StatiCa by updating all loads at each step, it was observed that yielding starts at RBS region of the bottom flange when vertical load, P, applied on the beam at 149 in. away from the column centerline reached 92 kips. The distance between the load application point and the center of RBS cut, L_{RBS}, can be calculated by subtracting the half of the column depth and the distance between center of RBS cut and column face from the 149 in. as:

$L_{RBS} = 149 \text{ in.} - (15.2 \text{ in.}/2) - 17 \text{ in.} = 124.4 \text{ in.}$

The moment value at the center of RBS cut, $M_{yRBS\text{-}IDEA}$, produced from the applied vertical load, P, can be calculated as:

$M_{yRBS\text{-}IDEA} = P \cdot L_{RBS} = M_{yRBS\text{-}IDEA} = (124.4 \text{ in.}) \cdot (92 \text{ kips}) = 11{,}445 \text{ kips-in.}$ (Figure 1.8)

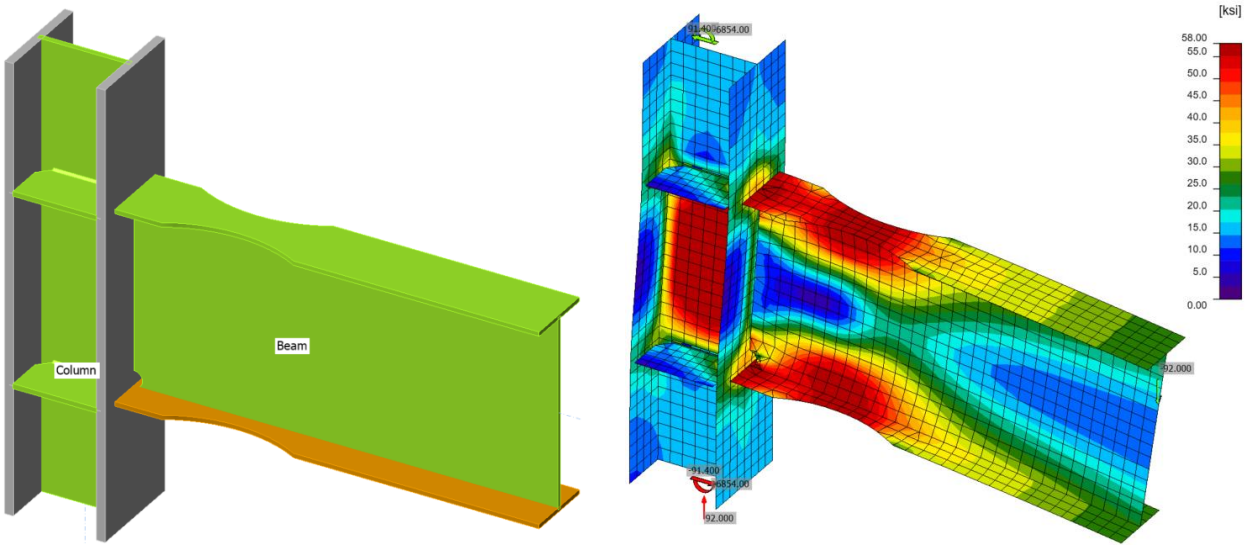

Figure 1.8: IDEA StatiCa model for LS-1

IDEA StatiCa models for the five additional variation connections (See Table 1.3) were developed using the AISC specified material properties given in AISC Manual Tables 2-4 and 2-5 shown in Figure 1.9.

General	
Name	A992
Physical properties	
m [pcf]	491
E [ksi]	29007.5
ν	0.3
G [ksi]	11156.7
α [-/°F]	0
λ [W/(m.K)]	45
c [kJ/(kg.K)]	0.49
Properties specific to American standard	
fu [ksi]	65.0
fy [ksi]	50.0
Ry [-]	1.10
Rt [-]	1.10

General	
Name	A992
Physical properties	
m [pcf]	491
E [ksi]	29007.5
ν	0.3
G [ksi]	11156.7
α [-/°F]	0
λ [W/(m.K)]	45
c [kJ/(kg.K)]	0.49
Properties specific to American standard	
fu [ksi]	65.0
fy [ksi]	50.0
Ry [-]	1.10
Rt [-]	1.10

Figure 1.9: Material properties for the variations in IDEA StatiCa; a) beam, b) column

Following the same procedure, the capacities of five variation connections were computed using IDEA StatiCa shown in Table 1.6 and Figures 1.10-1.14.

Table 1.6: Design capacities of the variations

Variations	Column size	Beam size	Thickness of doubler plate (in.)	Available flexural design strength at centerline of the RBS cut of beam (kip-in.)
Var-1	W14X176	*W27X94*	-	9,644
Var-2	W14X176	*W24X68*	-	6,587

Var-3	*W18X192*	W30X99	-	10,490
Var-4	*W12X170*	*W24X68*	3/8	6,587
Var-5	*W12X136*	*W24X68*	0.5	6,587

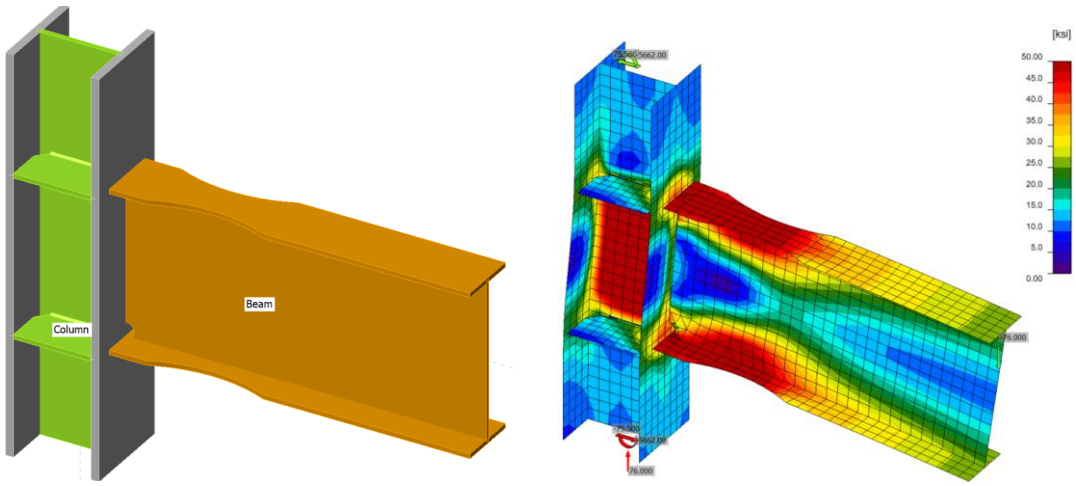

Figure 1.10: IDEA StatiCa model for variation 1

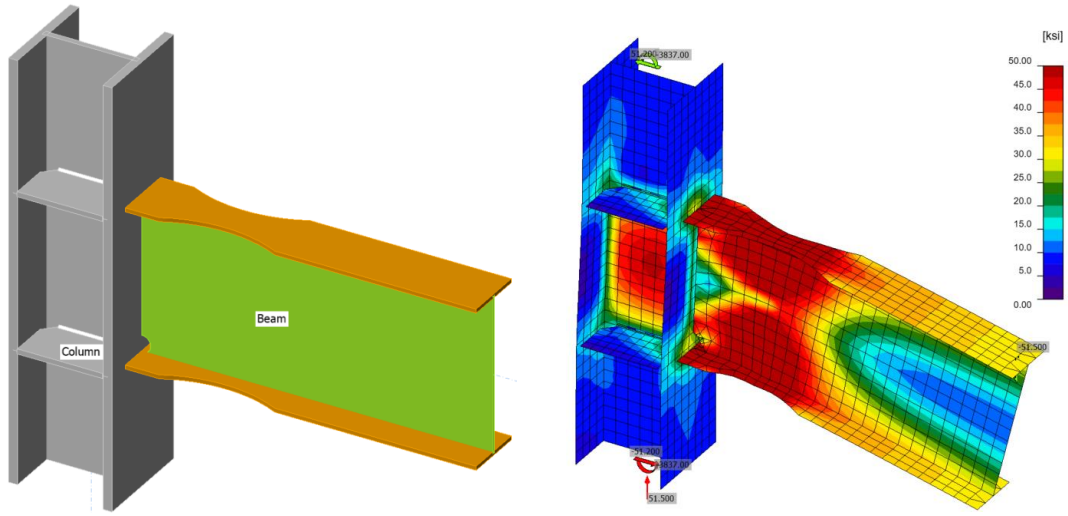

Figure 1.11: IDEA StatiCa model for variation 2

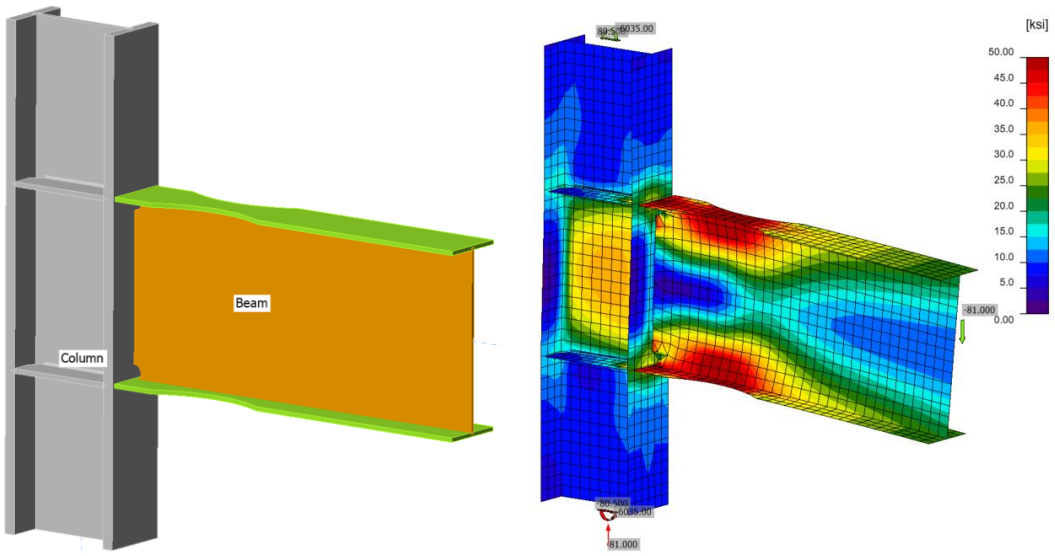

Figure 1.12: IDEA StatiCa model for variation 3

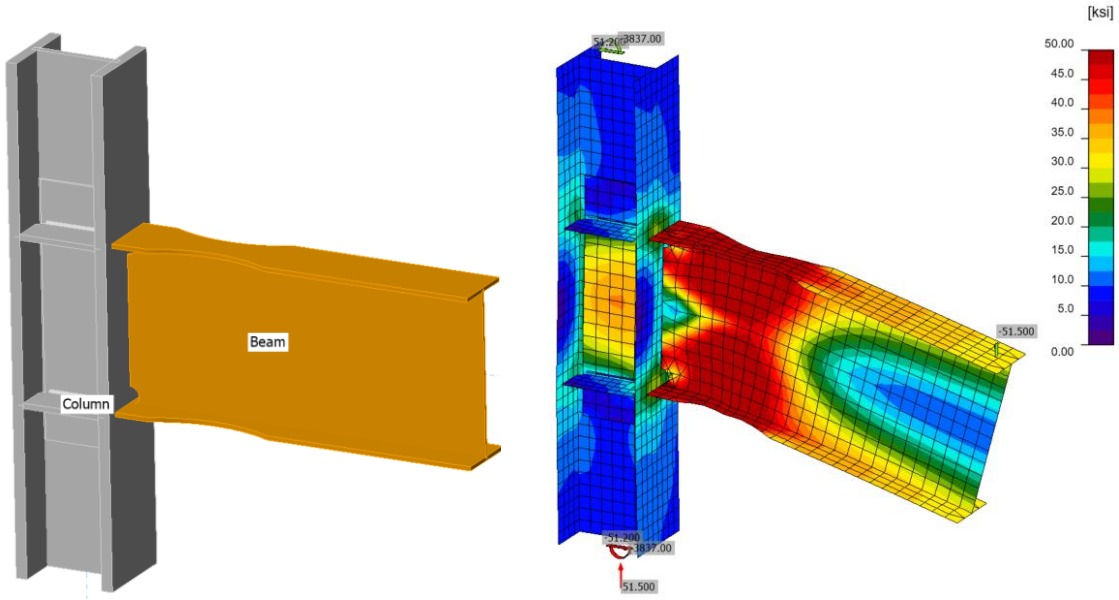

Figure 1.13: IDEA StatiCa model for variation 4

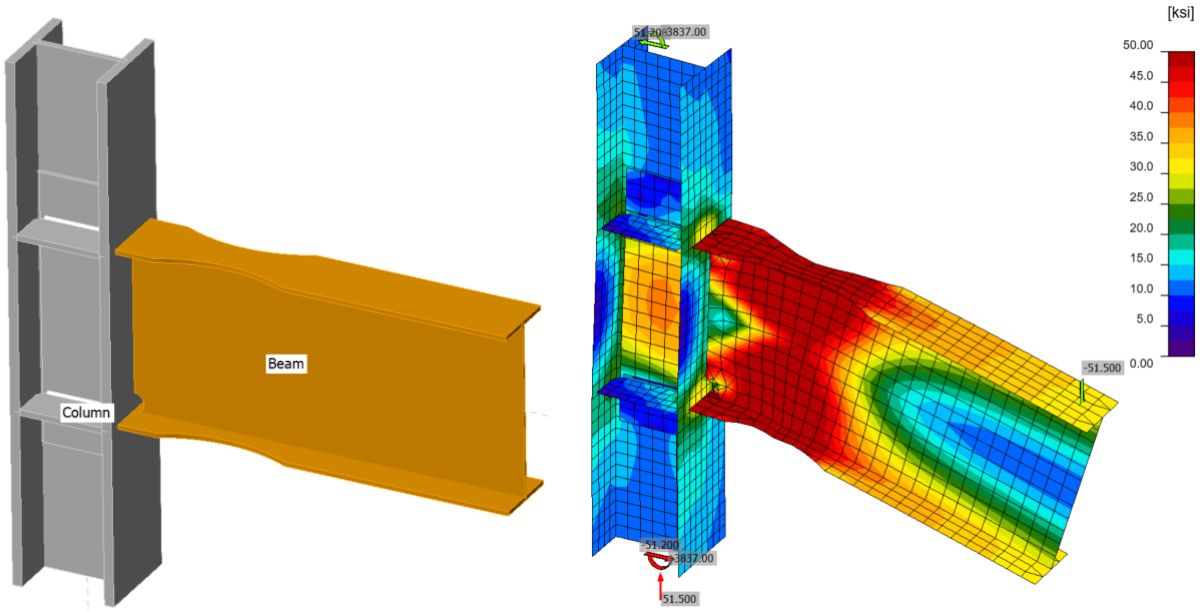

Figure 1.14: IDEA StatiCa model for variation 5

1.4.2 Moment-rotation analysis

Moment-rotation analysis is computed with "ST" (abbreviation for stiffness) analysis type. The maximum vertical force applied during the experiment, 115 kips, was applied at the beam position of 0 (zero) in. in negative z direction (V_z = -115 kips), and the corresponding moment of 17,135 kips-in. (115 kips×149 in.) is applied around Y axis (M_y = 17,135 kips-in.) as presented in Figure 1.15.

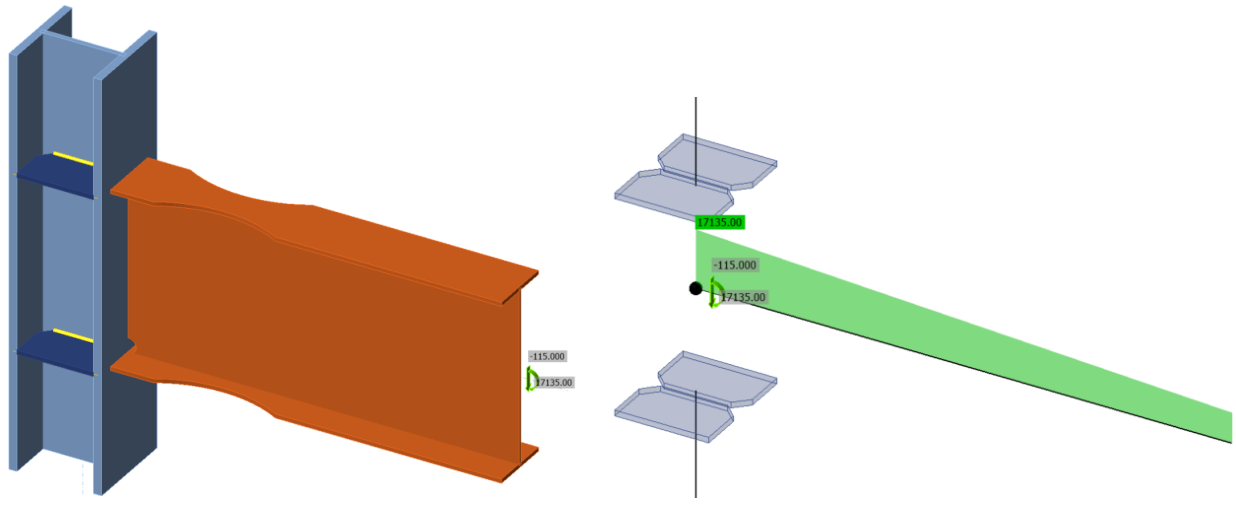

Figure 1.15: IDEA StatiCa ST analysis: (a) solid view: (b) wireframe view

Under these loads, the moment-rotation graph excluding elastic rotation of beam and column was obtained as shown in Figure 1.16 where:

- Sj: moment-rotation curve shown with
- Sj,R: limit value – rigid joint
- Sj,P: limit value – nominally pinned joint
- Sj,ini: initial rotational stiffness

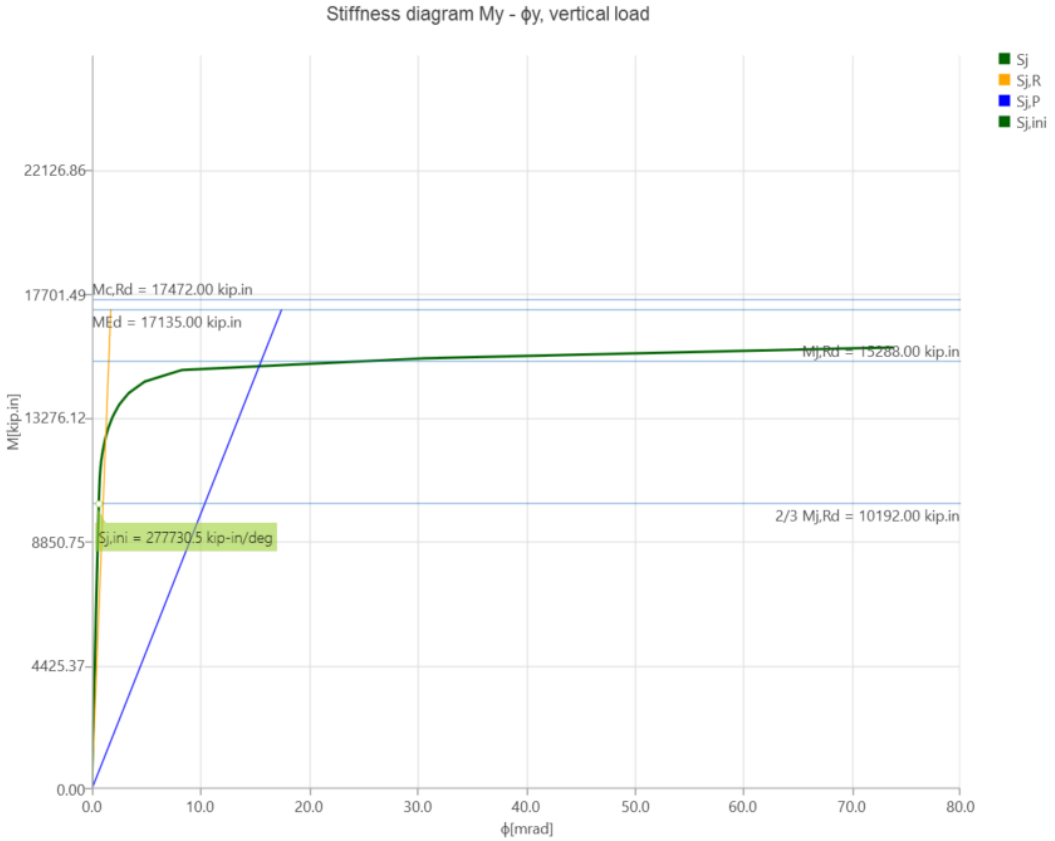

Figure 1.16: Moment-rotation relationship calculated by IDEA StatiCa

1.5. ABAQUS Analysis

In this section, the results from IDEA StatiCa were compared to the ABAQUS software package (version 2021). ABAQUS is a robust general-purpose FEA code suitable for analyzing whole ranges of statics, dynamics, and nonlinear problems.

In this study, the IDEA StatiCa model developed in Section 1.4.2 for the moment-rotation analysis was chosen as a base model. The CAD model for the FEA analysis was generated using the IDEA StatiCa's viewer platform. Numerical simulations with almost identical conditions (i.e., in terms of material properties, boundary conditions, and loading) were carried out using both IDEA StatiCa and ABAQUS.

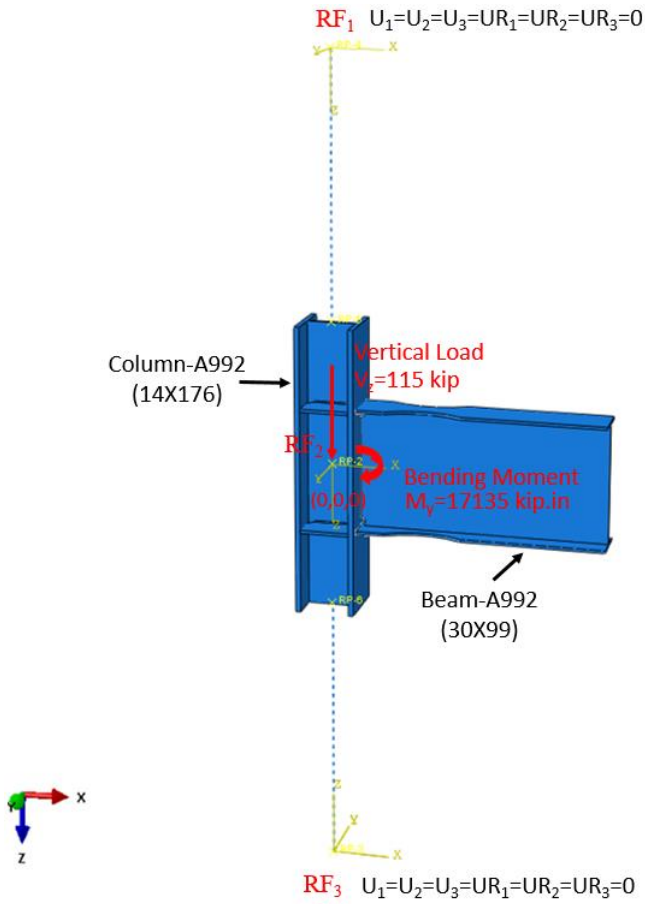

Figure 1.17: Model setup in ABAQUS

In ABAQUS, the element size and type were chosen to be 5 mm and C3D8R (3D stress, 8-node linear brick, reduced integration), respectively. In the ABAQUS model, the vertical load of 115 kips and the corresponding moment of 17,135 kips-in. (around Y axis) were applied to a defined reference point (i.e., RF_2) as shown in Figure 1.17. The calculated length of the column in IDEA StatiCa is 194.55in as described in Section 1.4.1. Therefore, to mimic the identical column length in ABAQUS, two reference points (i.e., RF_1 and RF_3) were introduced 97.245 in. away from the center of the column along the Z axis in both directions. These two reference points were fixed in all directions and were connected to the top and bottom faces of the column using a connector builder module in ABAQUS. The tie constraint was applied between the weld lines and the attaching parts. The material behavior was modeled using bi-linear plasticity in ABAQUS. Other parameters, including density, elastic modulus, and Poisson's ratio, were taken from the IDEA StatiCa materials library. The numerical simulation was carried out on four processors (Intel Xenon (R) CPU E5-2698 v4 @ 2.20GHz) and took approximately 45 minutes to finish. Figure 1.18 compares the predicted von-Mises stress and plastic strain between the IDEA StatiCa and ABAQUS models.

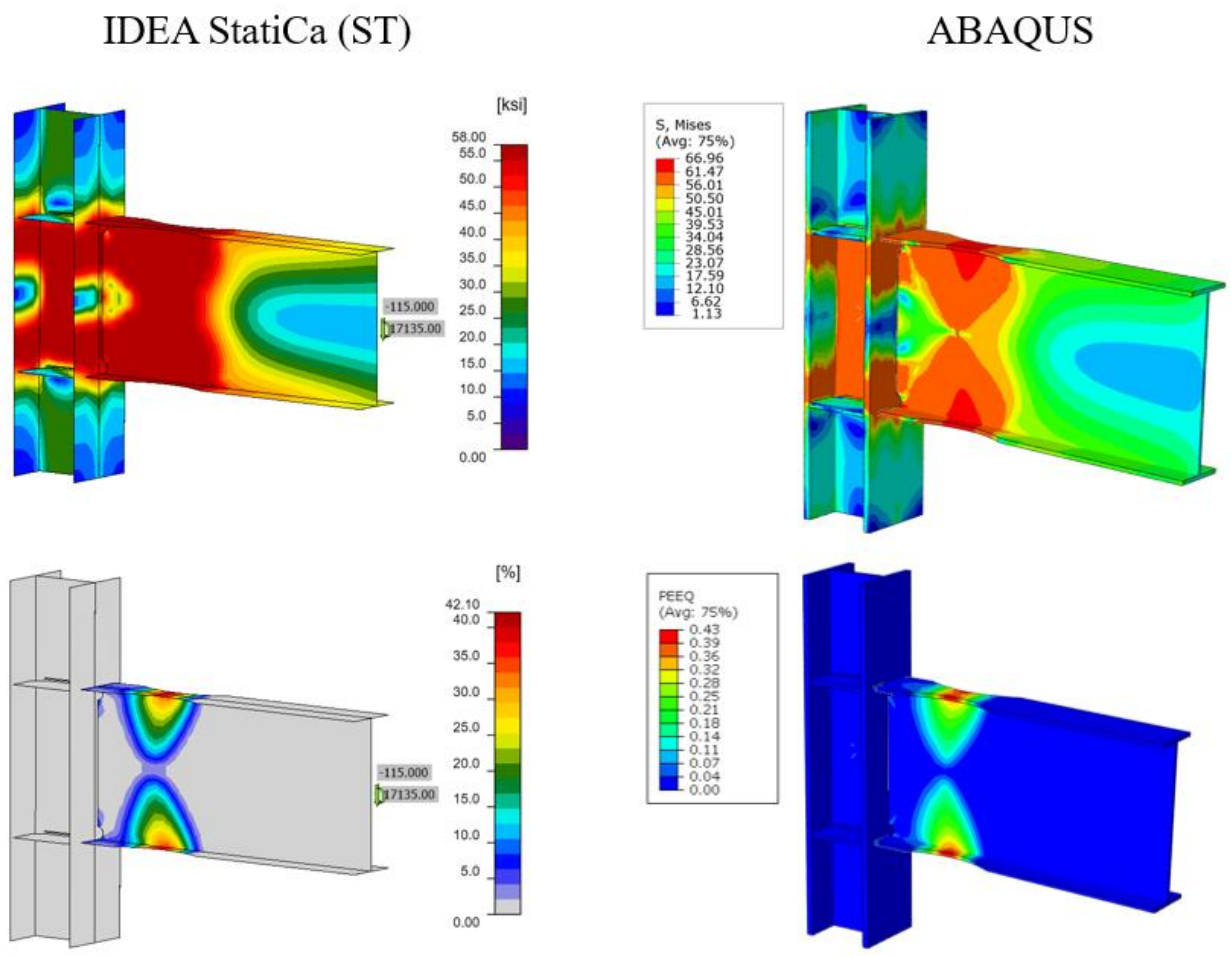

Figure 1.18: Comparison of the predicted von Mises stress (top row) and plastic strain (bottom row) between IDEA StatiCa and ABAQUS models

The maximum predicted stress in IDEA StatiCa is 68 ksi (on top and bottom of the reduced section of the beam) while the ABAQUS model shows the maximum stress of 66.96 ksi at the same location. The slightly different stress distribution is likely due to the utilization of finer mesh in the ABAQUS model and the simplified CAD model in IDEA StatiCa. Also, the maximum predicted plastic strain in IDEA StatiCa and ABAQUS are 41.3% and 43%, respectively.

Figure 1.19 depicts the comparison of the moment-rotation curve between the two software.

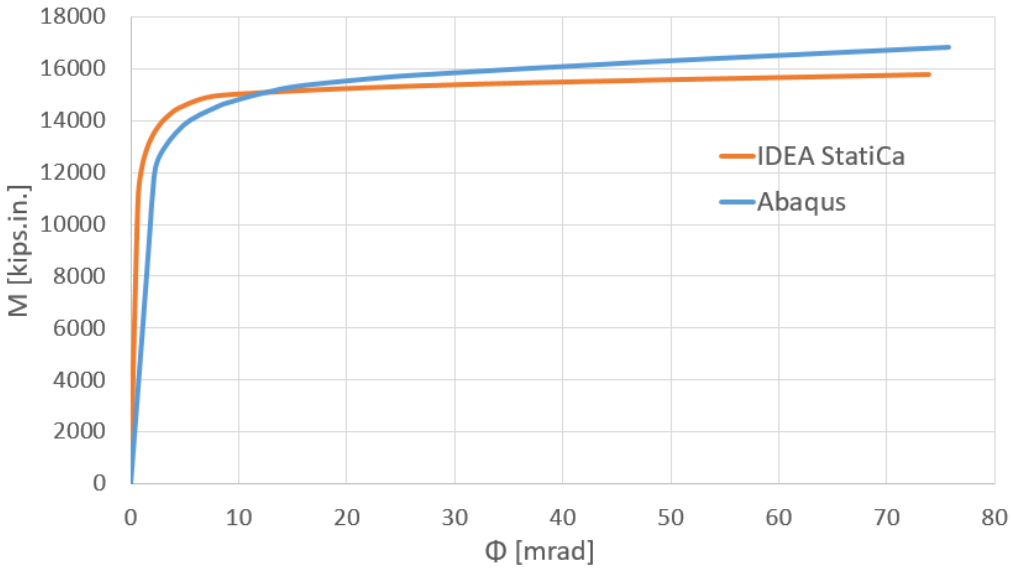

Figure 1.19: Moment-rotation comparison between IDEA StatiCa and ABAQUS

Note that in Figure 19, the blue curve (i.e., result from ABAQUS) represents the rotation of the beam which was measured at the intersection of the column and beam. Both models offer comparable initial stiffness estimations. The minor discrepancy could be associated with how that rotation is measured in each software, the difference in element types (i.e., solid element in ABAQUS versus shell element in IDEA StatiCa), and the employment of the tie constraint in ABAQUS to represent the welds.

1.6 Summary and Comparison of Results

Tip load leading yielding at RBS cut calculated using IDEA StatiCa is 92 kips. The flexural design capacity of test specimen calculated following AISC code requirement was divided by the distance from the center of RBS cut to the actuator and the corresponding tip load was calculated as 94.5 kips (11,754 kips-in./124.4 in.). These two values are shown in the graph of force-displacement history presented in the test report, and the three sources (Test observation, AISC calculation and IDEA StatiCa) were compared in Figure 1.20. The capacity of the connection found by IDEA StatiCa is about 3% less than the one calculated based on AISC procedure. Although it is hard to say when yielding started from force-displacement history, it seems that both approaches capture yielding point very well.

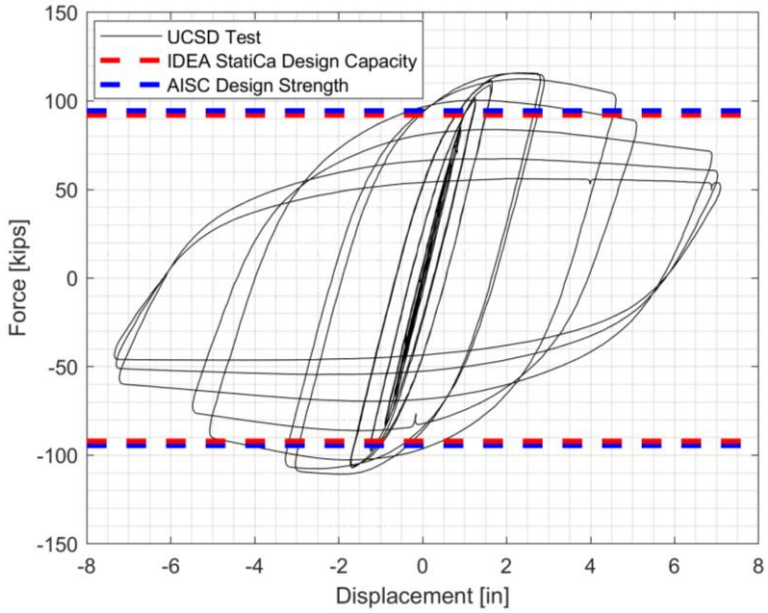

Figure 1.20: Force-displacement relationship

Moment-rotation relationship provided by IDEA StatiCa includes only plastic rotations. To be able compute plastic rotation, test researchers calculated elastic rotations for panel zone, beam and column analytically, and shared in the test output file. Using these data, elastic moment-rotation relationship was obtained, and added to the plastic moment-rotation curve of IDEA StatiCa to compare with the measured moment-rotation relationship as shown in Figure 1.21.

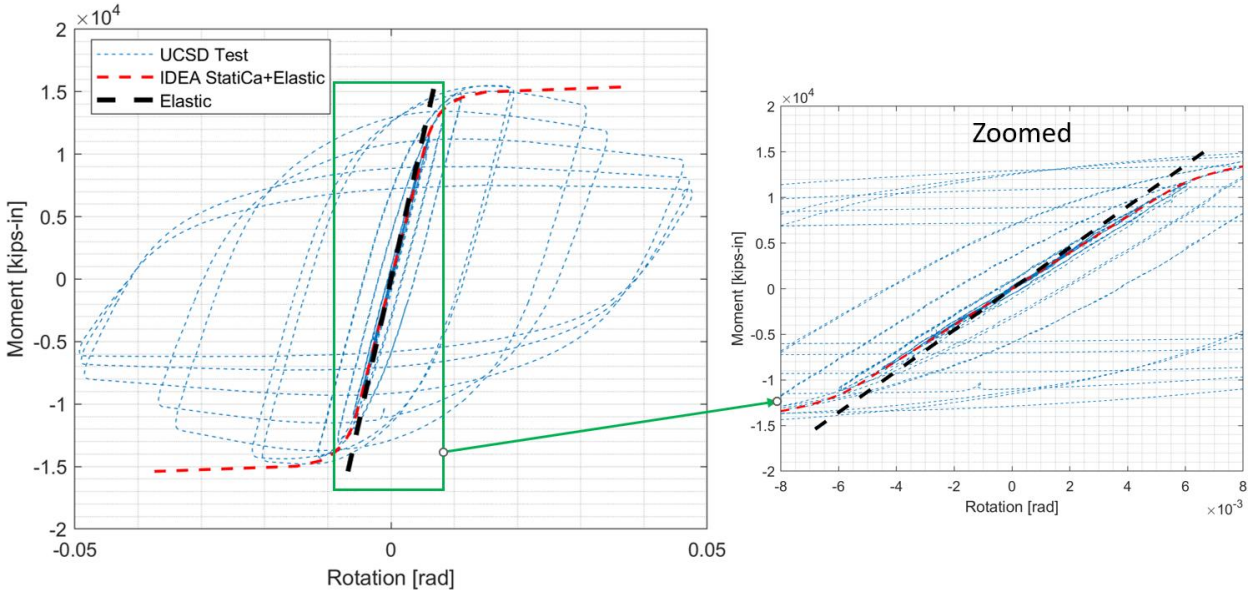

Figure 1.21: Moment-rotation comparison

IDEA StatiCa shows very good initial stiffness and yielding estimation. The difference after yielding can be attributed to the bilinear material model used by IDEA StatiCa. It resulted in the strain-hardening of the steel material measured during the test is not captured by IDEA StatiCa.

Flexural capacity of the test specimen and five variations calculated using IDEA StatiCa and following AISC code requirement are presented in Table 1.7. The differences in the calculated capacities are less than 4%.

Table 1.7: Flexural capacity of the test specimen and five variations

Specimen No	Column size	Beam size	Available flexural capacity of beam calculated using AISC procedure (kip-in.)	Available flexural capacity of beam calculated using IDEA StatiCa (kip-in.)
LS-1	W14X176	W30X99	11,754	11,445
Var-1	W14X176	W27X94	9,644	9,454
Var-2	W14X176	W24X68	6,587	6,407
Var-3	W18X192	W30X99	10,490	10,076
Var-4	W12X170	W24X68	6,587	6,407
Var-5	W12X136	W24X68	6,587	6,407

In conclusion, based on the analyzes performed in this chapter, there was good agreement in capturing the yielding capacity of the RBS connection using IDEA StatiCa.

References

Uang, C., Yu, K., and Gilton, C. (2000) Cyclic Response of RBS Moment Connections: Loading Sequence and Lateral Bracing Effects, *Report No. SSR-99/13*, C. L. Powell Structural Research Laboratories, University of California at San Diego.

AISC (2016), "Specification for Structural Steel Buildings," American Institute of Steel Construction ANSI/AISC 360-16, Chicago, Illinois.

AISC (2016), "Prequalified Connections for Special and Intermediate Steel Moment Frames for Seismic Applications, including Supplement No. 1," American Institute of Steel Construction ANSI/AISC 358-16, Chicago, Illinois.

AISC (2016), "Seismic Provisions for Structural Steel Buildings," American Institute of Steel Construction ANSI/AISC 341-16, Chicago, Illinois.

AISC (2020), "Seismic Design Manual," 3rd edition, American Institute of Steel Construction, Chicago.

AISC (2017), “Steel Construction Manual,” 15th edition, American Institute of Steel Construction, Chicago, Illinois.
ABAQUS 2021, Dassault Systemes Simulia Corporation, Providence, RI, USA.
IDEA StatiCa s.r.o., Sumavska 519/35, Brno, 602 00 Czech Republic; https://www.ideastatica.com/support-center/general-theoretical-background

Chapter 2. Bolted Unstiffened and Stiffened Extended End Plate Moment (EPM) Connections

2.1. Introduction

Bolted unstiffened and stiffened extended end plate moment (EPM) connection is another prequalified connection permitted to be used in high seismic regions by AISC 358 (2016) Chapter 6. In this chapter, six tested EPM specimens were selected from the literature. Their flexural capacities were calculated using IDEA StatiCa and following the AISC design procedure, and the results were compared with observations made during the experiments. Also, one of the specimens was selected as a baseline model, and moment-rotation analysis was performed using the IDEA StatiCa and ABAQUS for this connection. The numerically obtained moment rotation curves were compared with each other. Moreover, the moment-plastic rotation relationship obtained through IDEA StatiCa analysis was compared with the experimentally measured one provided in the test report.

2.2 Experimental Study

Six EPM specimens were subjected to cycling loading, and their responses were investigated at Virginia Polytechnic Institute and State University as part of the SAC steel project (Sumner et al., 2000). The test identification (ID) of "4E-1.25-1.5-24" was selected as the baseline model and the other specimens with IDs of "4E-1.25-1.125-24", "8ES-1.25-2.5-36", "8ES-1.25-1-30", "8ES-1.25-1.75-30", and "8ES-1.25-1.25-36" were selected as variation connections and numbered respectively. The properties of the specimens are presented in Table 2.1, and the configurations of the six connections are shown in Figures 2.1 through 2.3.

Table 2.1: Properties of the EPM specimens

Specimen No.	Beam	Column	Doubler plate thickness (in.)	Continuity plate thickness (in.)	Number of bolts (Grade)	End-plate thickness (in.)	End-plate stiffener thickness (in.)
Baseline	W24x68	W14x120	1/2	5/8	Four (A490)	1 1/2	-
Var-1	W24x68	W14x120	1/2	5/8	Four (A325)	1 1/8	-
Var-2	W36x150	W14x257	3/4	-	Eight (A490)	2 1/2	3/4
Var-3	W30x99	W14x193	3/8	5/8	Eight (A325)	1	1/2
Var-4	W30x99	W14x193	3/8	5/8	Eight (A490)	1 3/4	1/2
Var-5	W36x150	W14x257	3/4	-	Eight (A325)	1 1/4	3/4

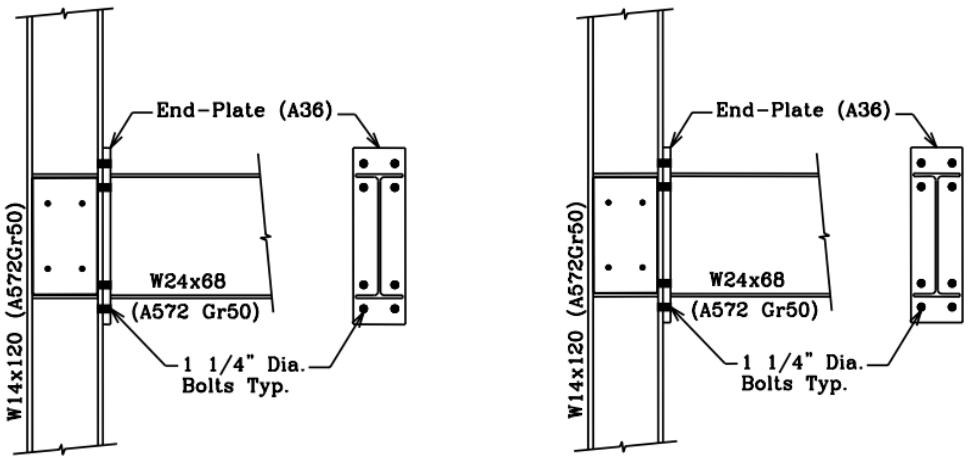

Figure 2.1: Left) Configuration of baseline model; Right) configuration of Variation 1 (Sumner et al., 2000)

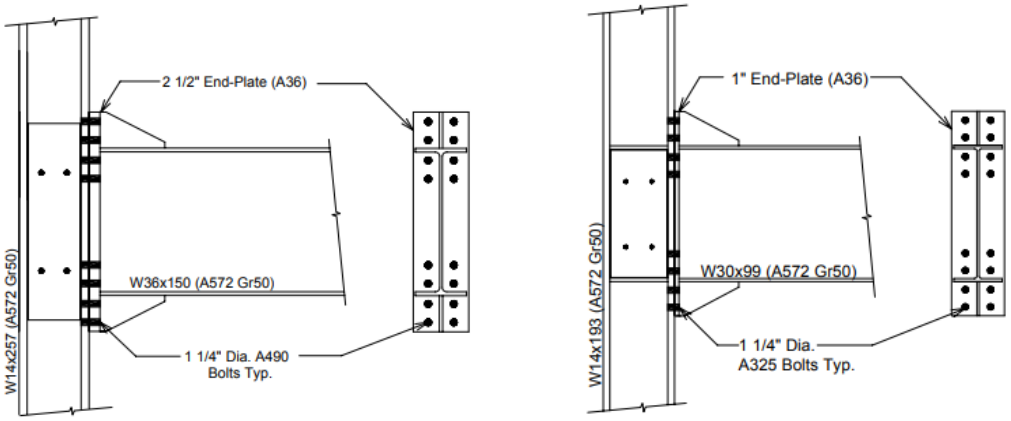

Figure 2.2: Left) Configuration of Variation 2; Right) configuration of Variation 3 (Sumner et al., 2000)

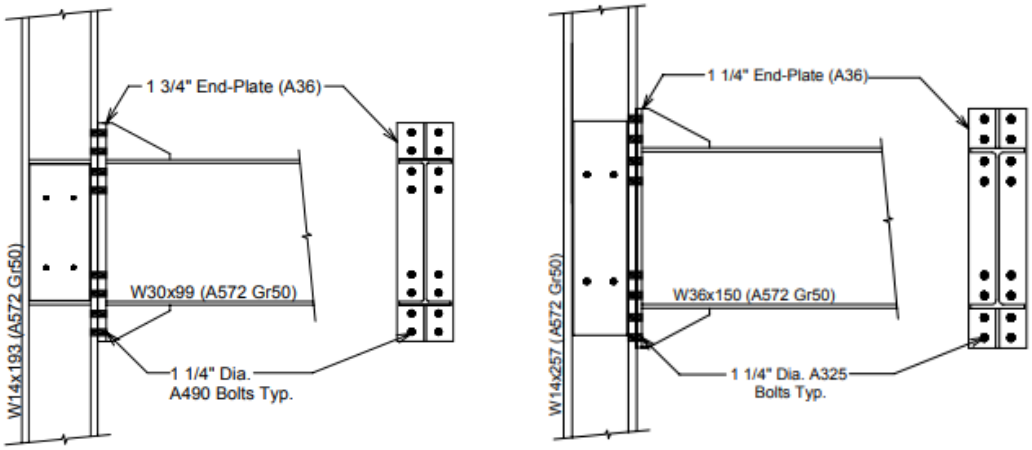

Figure 2.3: Left) Configuration of Variation 4; Right) configuration of Variation 5 (Sumner et al., 2000)

The baseline model and Variation 1 (Var-1) are four-bolt unstiffened extended EPM connections while the others are eight-bolt stiffened extended EPM connections. All bolts have a diameter of 1 1/4 in., and the bolt grades vary from ASTM A325 (f_{nt} = 90 ksi) to A490 (f_{nt} = 113 ksi) where f_{nt} is nominal tensile strength. Each connection has one sided doubler plate plug welded to the column web and 5/16 in. double sided fillet weld between beam web and end plate. The measured material properties for the beam flange, column flange and end plate are presented in Table 2.2.

Table 2.2: Material properties of selected EPM specimens

Specimen No.	Section	Yield stress (ksi)	Ultimate stress (ksi)
Baseline	W14x120 (column flange)	52.0	70.6
	W24x68 (beam flange)	53.6	70.7
	1 1/2 in. end plate	38.1	68.8
Var-1	W14x120 (column flange)	52	70.6
	W24x68 (beam flange)	53.6	70.7
	1 1/8 in. end plate	37.9	63.4
Var-2	W14x257 (column flange)	51.2	68.3
	W36x150 (beam flange)	54.5	70.4
	2 1/2 in. end plate	38.2	72.3
Var-3	W14x193 (column flange)	55.5	74.3
	W30x99 (beam flange)	54.9	70.8
	1 in. end plate	37.8	60.8
Var-4	W14x193 (column flange)	55.5	74.3
	W30x99 (beam flange)	54.9	70.8
	1 3/4 in. end plate	37.2	63.4
Var-5	W14x257 (column flange)	51.2	68.3
	W36x150 (beam flange)	54.5	70.4
	1 1/4 in. end plate	40.5	67.1

The baseline model was designed to develop 110% of the nominal plastic moment capacity of the beam ($M = F_y Z$, where F_y is yield stress and Z is the plastic section modulus of beam). During testing, initial yielding occurred in the web and both flanges of the beam, and severe local buckling of the beam was observed during further cycles (Figure 2.4).

Variation 1 was designed with a thinner end plate and less strong bolts compared to the baseline model to develop 80% of the nominal plastic moment capacity of the beam. Initial yielding occurred in the beam web followed by yielding of the end plate (Figure 2.5). As the number of cycles increased, it was observed that the specimen failed due to the bolt ruptures and no local buckling of the beam was observed. The baseline and Variation 1 specimens were tested using the

same test setup. The load was applied to the beam at a distance of 14 ft 1 3/4 in. from the column centerline. The photos after testing and moment-total plastic rotation relationships which include plastic rotations of the beam, column, and panel zone are illustrated in Figures 2.4 and 2.5 for the baseline model and Variation 1, respectively.

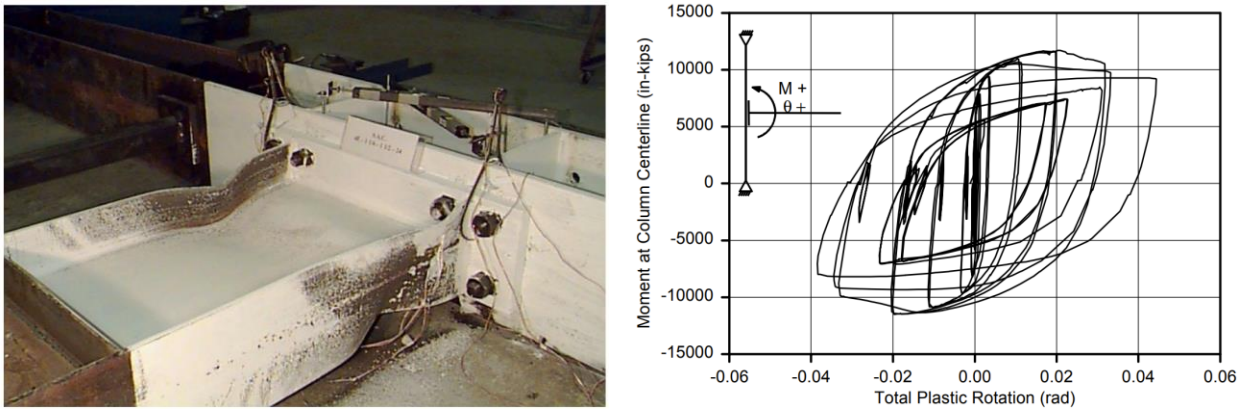

Figure 2.4: Left) Baseline model after testing; Right) moment-total plastic rotation relationship (Sumner et al., 2000)

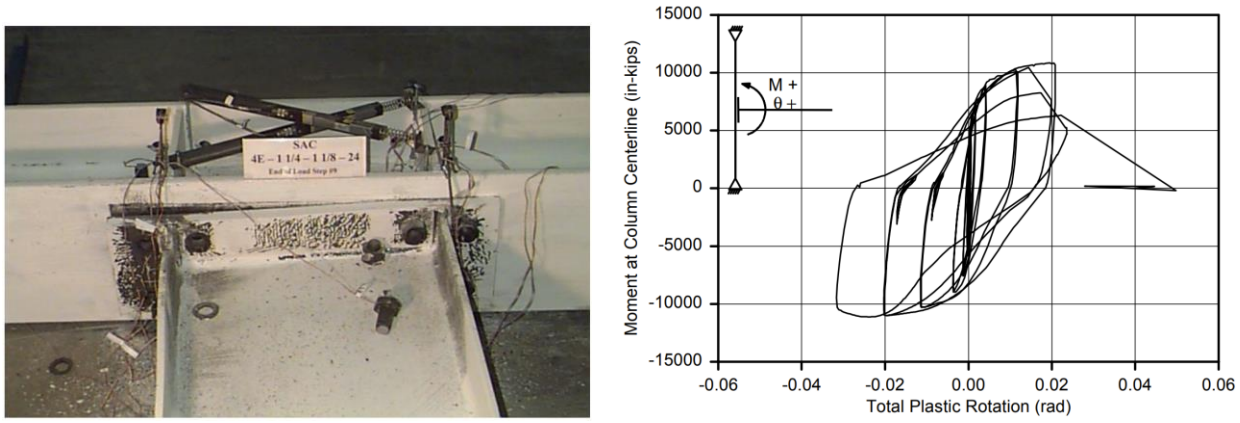

Figure 2.5: Left) Variation 1 after testing; Right) moment-total plastic rotation relationship (Sumner et al., 2000)

Variation 2 connection specimen was designed to develop 110% of the nominal plastic moment capacity of the beam. Initial yielding occurred in the end plate stiffener. Full yielding of the beam flanges and end plate stiffener was observed followed by local buckling of the beam flanges, beam web, and column web doubler plate (Figure 2.6).

Variation 3 was designed to develop 80% of the nominal plastic moment capacity of the beam. The initial yielding occurred in the beam flanges at the base of the stiffeners and in the end plate between the inner rows of the bolts. During the further cycles, severe yielding in the end plate and end plate stiffener was observed and local buckling in the beam flanges was reported (Figure 2.7).

The moment-total plastic rotation relationships for Variation 2 and 3 specimens are shown in Figures 2.6 and 2.7, respectively.

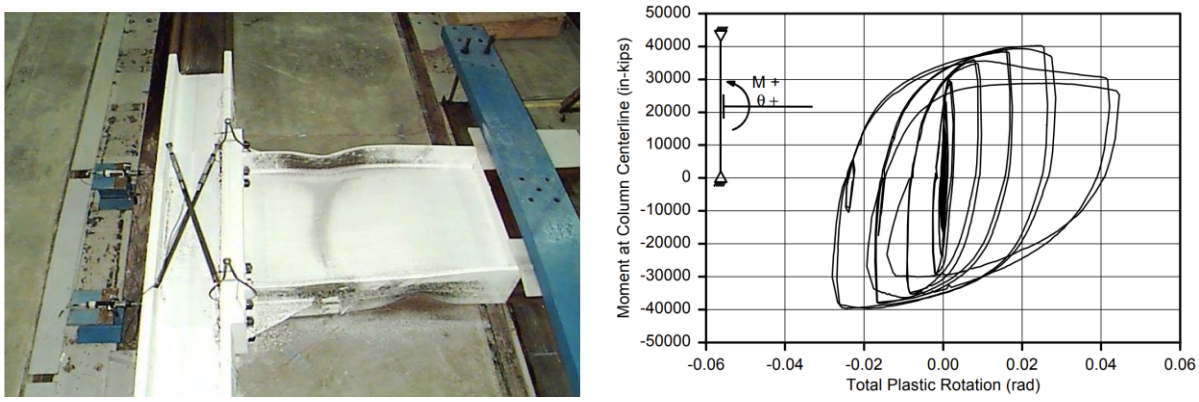

Figure 2.6: Left) Variation 2 after testing; Right) moment-total plastic rotation relationship (Sumner et al., 2000)

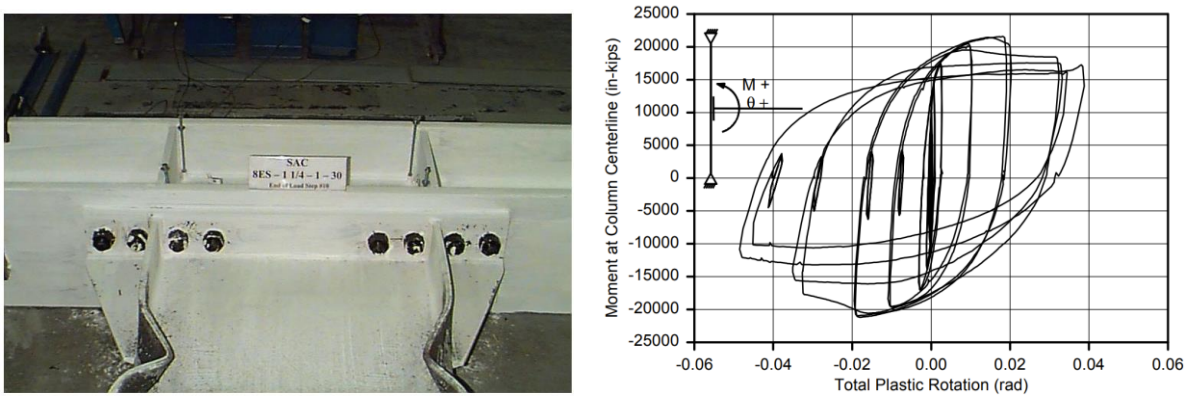

Figure 2.7: Left) Variation 3 after testing; Right) moment-total plastic rotation relationship (Sumner et al., 2000)

Variation 4 was designed to develop 110% of the nominal plastic moment capacity of the beam with a thicker end plate and the stronger bolts compared to Variation 3. The initial yielding occurred in the beam flanges and in the doubler plate. Severe local flange buckling in the beam flanges was observed and no yielding occurred in the end plate and end plate stiffener during the experiment (Figure 2.8). Note that these two specimens were evaluated in the same test setup, and the loading was applied to the tip of the beam at a distance of 20 ft and 1 1/4 in. from the column centerline.

Variation 5 was designed to develop 110% of the nominal plastic moment capacity of the beam with a thicker end plate and stronger bolts compared to Variation 2. The initial yielding was observed in the end plate stiffener. During the continued cycles, bolt rupture was observed (Figure 2.9). The loading was applied to the beam at a distance of 22 ft and 1 13/16 in. from the column

centerline. The measured moment-total plastic rotation relationships are shown in Figures 2.8 and 2.9 for Variations 4 and 5, respectively.

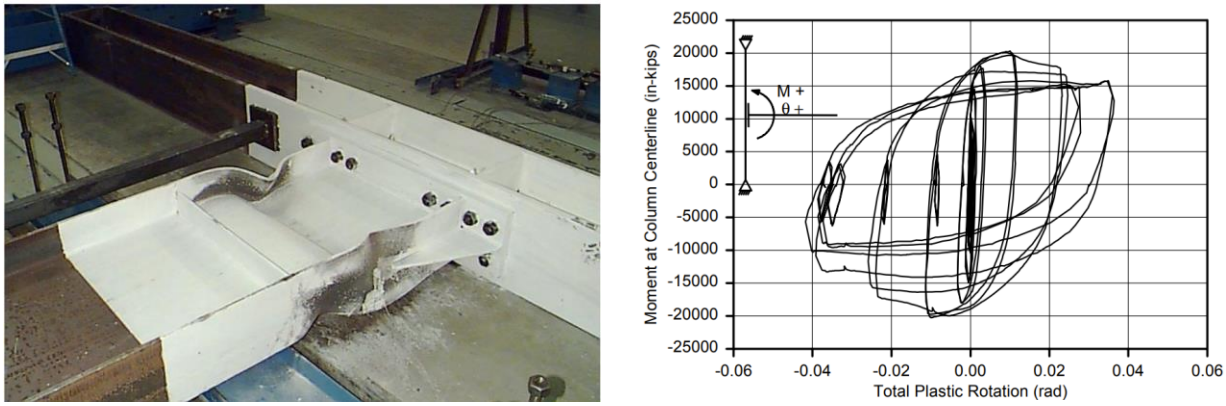

Figure 2.8: Left) Variation 4 after testing; Right) moment-total plastic rotation relationship (Sumner et al., 2000)

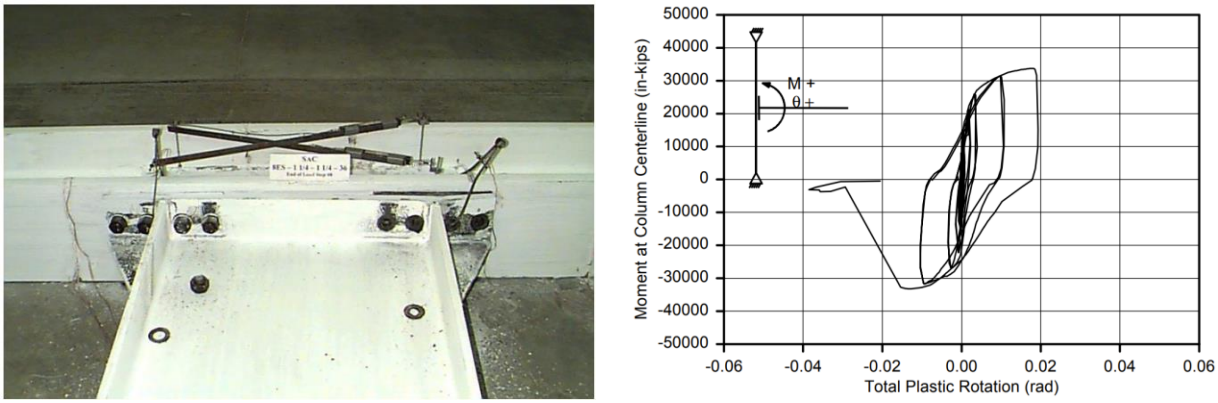

Figure 2.9: Left) Variation 5 after testing; Right) moment-total plastic rotation relationship (Sumner et al., 2000)

2.3 Code Design Calculations

The procedure outlined in Section 6.8 of AISC 358 (2016) for EPM connections were followed, and the following checks were performed for the six specimens.

- Check prequalification limits (AISC 358 (2016) Sec. 6.3)
- Check that probable maximum moment at the face of the column, M_f, does not exceed available strength $\phi_d M_{pe}$. (AISC 358 (2016) Eq. 6.8-1)
- Check the bolt diameters (AISC 358 (2016) Eq. 6.8-3)
- Check the end plate thickness (AISC 358 (2016) Eq. 6.8-5)
- Check shear yielding of the extended portion of the end plate for four-bolt extended unstiffened end plate (AISC 358 (2016) Eq. 6.8-7)

- Check shear rupture of the extended portion of the end plate for four-bolt extended unstiffened end plate (AISC 358 (2016), Eq. 6.8-7)
- Check end-plate stiffener thickness (AISC 358 (2016), Eq. 6.8-9)
- Check stiffener width-to-thickness ratio (AISC 358 (2016), Eq. 6.8-10)
- Check bolt shear rupture strength (AISC 358 (2016), Eq. 6.8-11)
- Check bolt-bearing/tear-out failure of the end plate and column (AISC 358 (2016), Eq. 6.8-12)
- Check the weld between beam web and end plate (AISC Design Guide 4 (2003), Sec. 4.2.13)
- Check the column flange for flexural yielding (AISC 358 (2016), Eq. 6.8-13)
- Check the local column web yielding strength of the unstiffened column web at the beam flanges (AISC 358 (2016), Eq. 6.8-16-17)
- Check the unstiffened column web buckling strength at the beam compression flange (AISC 358 (2016), Eq. 6.8-18-20)
- Check the unstiffened column web crippling strength at the beam compression flange (AISC 358 (2016), Eq. 6.8-21-24)
- Check the panel zone (AISC 358 (2016), Section 6.4(1))

It is assumed that the frame system satisfies the design requirements of special moment frames (SMF). The distance between the column centerlines, L, is assumed to be equal to 360 in. in the six specimens considered here (Table 2.1). The measured beam flange and column flange properties were used for the beam, column respectively while the measured end plate properties were used for end plate. It is also assumed that the material properties of rest of the plates (end plate stiffener, continuity plate, doubler plate) are identical with the measured properties of the end plate (See Table 2.2). The nominal tensile strength (f_{nt}) and shear strength (f_{nv}) given by AISC Table J3.2 were used for A325 and A490 bolts (threads are excluded) presented in Table 2.3.

Table 2.3: Nominal strength of bolts

Bolt type	Nominal tensile strength (f_{nt})	Nominal shear Strength (f_{nv})
A325	90 ksi	68 ksi
A490	113 ksi	84 ksi

The summary of the AISC 358 (2016) design checks of the six specimens is presented in Table 2.4. The details of the design calculations and checks are provided in Appendices C and D.

Table 2.4: AISC 358 (2016) design checks for the specimens

AISC design checks	Baseline	Var-1	Var-2	Var-3	Var-4	Var-5
Bolt diameter	OK	Not OK	Not OK	OK	OK	Not OK
End plate thickness	OK	Not OK	OK	Not OK	OK	Not OK
End plate stiffener thickness	-	-	Not OK	Not OK	Not OK	Not OK

Yielding of the extended portion of the end plate	OK	Not OK	-	-	-	-
Shear rupture of the extended portion of the end plate	OK	OK	-	-	-	-
Compression bolt shear rupture	OK	OK	OK	OK	OK	OK
Bolt-bearing/tear-out failure of the end plate and column flange	OK	OK	OK	OK	OK	OK
Weld - between beam web and end plate	OK	OK	Not OK	Not OK	Not OK	Not OK
Column flange thickness	OK	OK	OK	OK	OK	OK
Continuity plate requirement	Required	Required	Required	Required	Required	Required
Continuity plate thickness	OK	OK	-	OK	OK	-
Continuity plate weld	Not OK	Not OK	-	Not OK	OK	-
Column-beam relationships	OK	OK	Not OK	Not OK	Not OK	Not OK
Panel zone	OK	OK	OK	OK	OK	OK

The design guidelines provided in AISC 358 (2016) Section 6.8 for extended stiffened and unstiffened end plate moment connections ensure that yielding does not occur on the connection side (e.g., in end plate or bolts). However, some of the checks performed for the test specimens were not satisfied. Therefore, further investigation may be necessary to investigate the failure modes and moment capacities of the EPM connections satisfying the requirements of AISC 358 (2016) standard.

According to Borgsmiller (1995) and AISC Steel Design Guide 4 (DG 4) (2003), controlling the damage limit state of an EPM connection can be predicted if the following limit states are known:

1- Moment strength of beam
2- Yield moment strength of end plate
3- Yield moment strength of column flange
4- Tensile rupture strength of bolts

If no prying moment tensile rupture strength is less than or equal to 90% of the yield moment strengths of the end plate and column flange, thick plate behavior is expected. In other words, if the applied moment is larger than this, the end plate behaves as a thin plate and prying action is required to be considered in the bolts (AISC DG 4, 2003). The moment strength of the beam at plastic hinge location, $M_{by@ph}$, the yield moment strength of the end plate, M_{ply}, the yield moment

strength of the column flange, M_{cf}, and no prying moment for the bolt strength (bolt tensile rupture limit), M_{bnp}, are calculated as follows:

$$M_{by@ph} = F_{yb} Z_{bx} \tag{2.1}$$

$$M_{ply} = Y_p F_{epy} {t_p}^2 \tag{2.2}$$

$$M_{cf} = Y_c F_{cy} {t_{cf}}^2 \tag{2.3}$$

$$M_{bnp} = 2F_{nt} \left(\pi \frac{{d_{bolt}}^2}{4} \right) (h_0 + h_1) \tag{2.4}$$

where F_{yb} is yield stress of beam, Z_{bx} is plastic section modulus of beam, Y_p is end plate yield line mechanism parameter, F_{epy} is yield stress of end plate, t_p is end plate thickness, Y_c is column flange yield line mechanism parameter, F_{cy} is yield stress of column, t_{cf} is column flange thickness, F_{nt} is nominal tensile stress of bolt, d_{bolt} is bolt diameter, h_0 is distance from centerline of compression flange to the tension-side outer bolt row, and h_i is distance from centerline of compression flange to the centerline of the i^{th} tension bolt row. Plastic moment capacity of the beam at column face can be calculated by considering the additional moment resulting from the shear force at the plastic hinge location as follows:

$$M_{by@foc} = M_{by@ph} + VS_h \tag{2.5}$$

where $M_{by@foc}$ is flexural moment capacity of beam at column face, S_h is the distance between the column face and plastic hinge, and V is shear force on the beam at plastic hinge location. In Section 6.8 of AISC 358 (2016), S_h is defined as the lesser of $d_b/2$ or $3b_{bf}$ for an unstiffened EPM connection and $L_{st} + t_p$ for a stiffened EPM connection where d_b is depth of beam, b_{bf} is width of beam, L_{st} is length of stiffener, and t_p is end plate thickness. For the cantilever beam used in the six specimens, V is constant and equal to the applied load. Using Equations 2.1 through 2.5, the strengths of the test specimens were calculated and the controlling or the smallest moment capacity, M_n was determined and presented in Table 2.5.

Table 2.5: Summary of capacity calculations

Specimen No.	S_h (in.)	V (kips)	$M_{by@ph}$ (Kips-in.)	$M_{by@foc}$ (kips-in.)	M_{ply} (kips-in.)	M_{cf} (kips-in.)	M_{bnp} (kips-in.)	M_n (kips-in.)
Baseline	11.85	61.35	9,487	**10,214**	15,492	15,872	12,821	10,214
Var-1	11.85	54.50	9,487	10,133	**8,669**	15,872	10,210	8,669
Var-2	19	135.20	31,665	**34,234**	135,864	72,890	38,780	34,234
Var-3	14	73.80	17,129	18,162	**17,327**	68,814	25,650	17,327
Var-4	14.75	82.55	17,129	**18,347**	52,214	68,814	32,210	18,347
Var-5	17.75	101.60	31,665	33,468	35,997	72,890	**30,890**	30,890

2.4 IDEA StatiCa Analysis

The six tested specimens were modeled in IDEA StatiCa. The aim was to simulate the behavior of the experiment. Their moment capacities and failure modes were identified using stress, strain analysis type. The measured material properties reported in Sumner et al. (2000) were used and resistance factors were set to 1.0. For the baseline model, the moment-rotation relationship was obtained using the connection stiffness analysis type (i.e., ST) in IDEA StatiCa.

2.4.1 Analysis of Baseline Model

IDEA StatiCa model was developed for the baseline model. The measured material properties were introduced, and the overstrength coefficients, R_y and R_t, were set equal to 1.0 (see Figure 2.10). Also, all LRFD resistance factors were set to 1.0. To obtain the loads at the column centerline, a beam-column frame model was developed in SAP2000 using the lengths of column and beam in the test setup. The columns were fixed at both ends and a shear force of 59.00 kips was applied at a distance of 14 ft 1 3/4 in. from the centerline of the column. Shear and moment diagrams were obtained as shown in Figure 2.11. In this way, the loads at the nodes were calculated from the SAP2000 model, and the calculated loads were applied to the IDEA StatiCa model using the "loads in equilibrium" option at the beam position equal to zero which indicates the column centerline.

General	
Name	beam_A572 Gr.50
Physical properties	
m [pcf]	491
E [ksi]	29007.5
ν	0.3
G [ksi]	11156.7
α [-/°F]	0
λ [W/(m.K)]	45
c [kJ/(kg.K)]	0.49
Properties specific to American standard	
fu [ksi]	70.7
fy [ksi]	53.6
Ry [-]	1.00
Rt [-]	1.00

General	
Name	End_plate_A36
Physical properties	
m [pcf]	491
E [ksi]	29007.5
ν	0.3
G [ksi]	11156.7
α [-/°F]	0
λ [W/(m.K)]	45
c [kJ/(kg.K)]	0.49
Properties specific to American standard	
fu [ksi]	68.8
fy [ksi]	38.1
Ry [-]	1.00
Rt [-]	1.00

General	
Name	column_A572 Gr.50
Physical properties	
m [pcf]	491
E [ksi]	29007.5
ν	0.3
G [ksi]	11156.7
α [-/°F]	0
λ [W/(m.K)]	45
c [kJ/(kg.K)]	0.49
Properties specific to American standard	
fu [ksi]	70.6
fy [ksi]	52.0
Ry [-]	1.00
Rt [-]	1.00

Figure 2.10: Material properties in IDEA StatiCa

For the capacity calculation, the stress/strain design analysis (i.e., EPS) with "loads in equilibrium" option was selected in IDEA StatiCa. The loads were gradually increased until any of the following is achieved:

1) 5% of plastic strain in plates (beam, column, end plate and stiffener)
2) 100% strength capacity in bolts
3) 100% strength capacity in welds

When shear force and the corresponding moment values were increased to 61.35 kips and 10,414 kips-in., respectively, (with all loads proportionally being in equilibrium) 5% of the plastic strain limit was reached in the beam flange (Figure 2.12). Using “ST” analysis, the moment-rotation relationship was obtained and is shown in Figure 2.13.

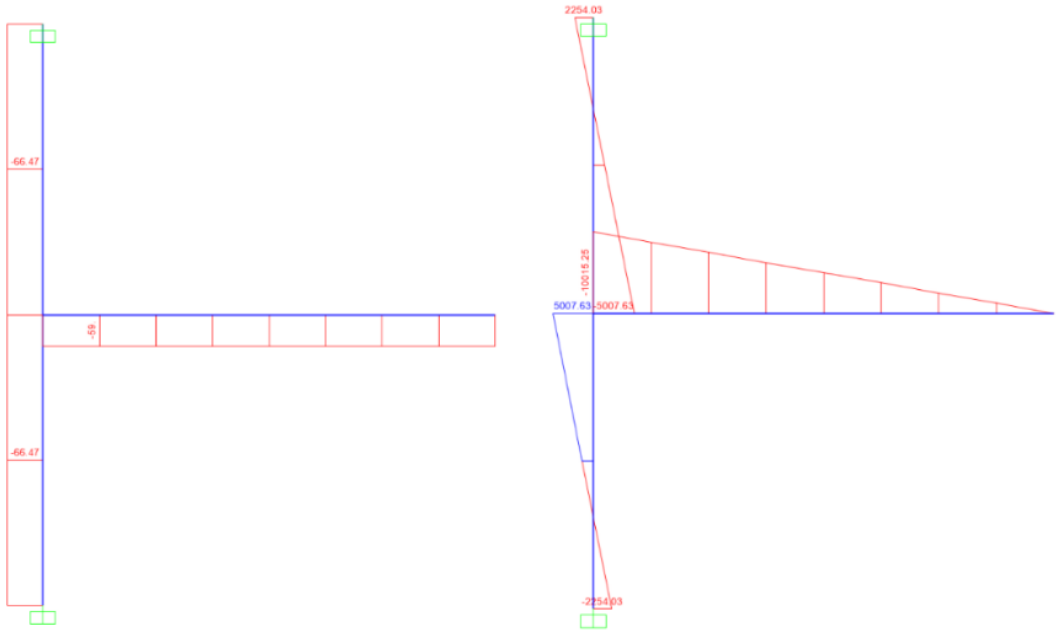

Figure 2.11: Shear force and moment diagram (SAP2000)

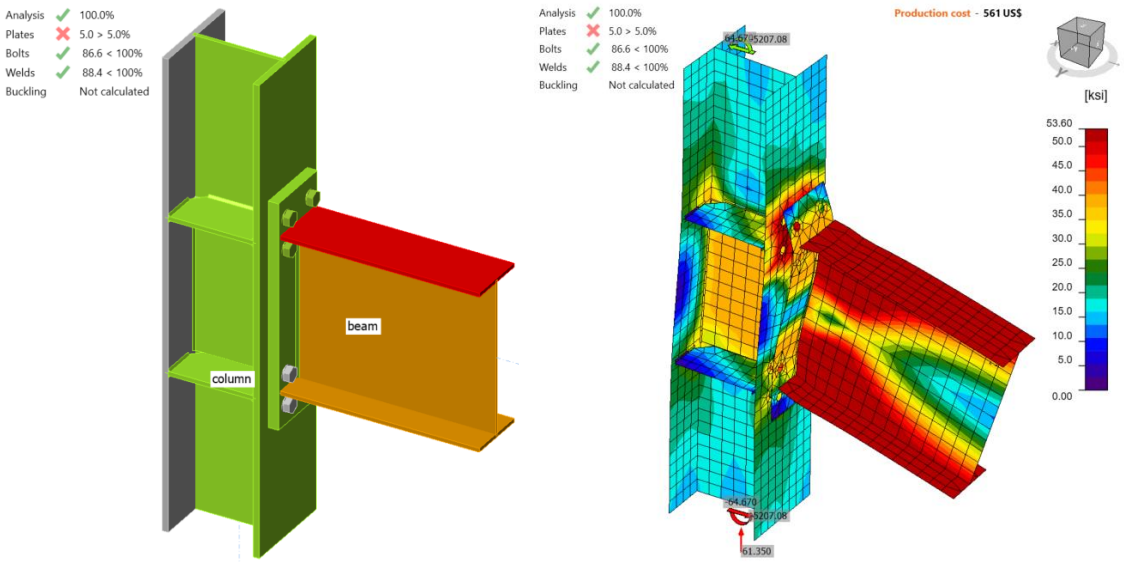

Figure 2.12: IDEA StatiCa model for Baseline Model under the moment of 10,414 kips-in.

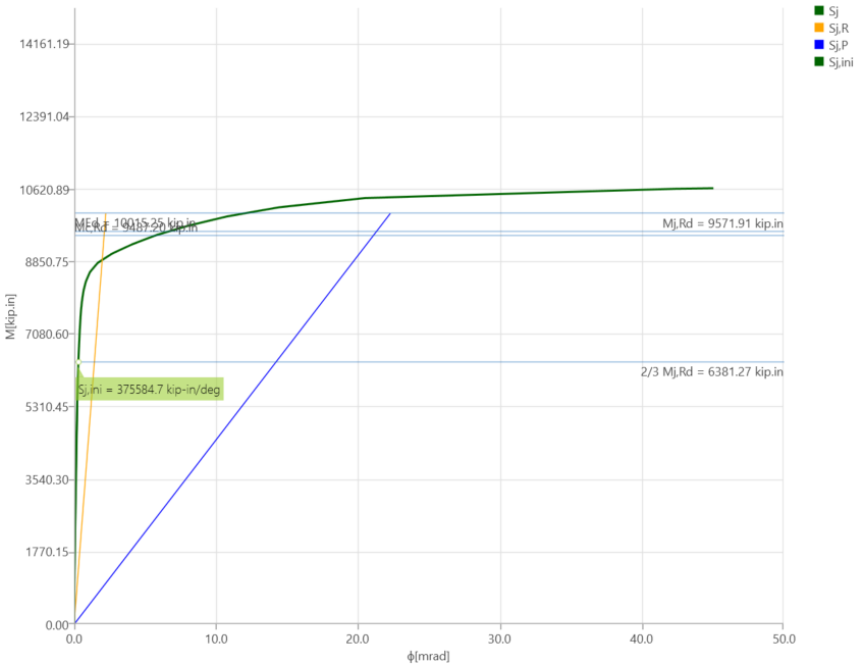

Figure 2.13: Moment-rotation relationship for Baseline Model

2.4.2 Analysis of Variation 1

Following the same procedure described for the baseline model, IDEA StatiCa model was developed for the specimen Variation 1 (Figure 2.1). During the incremental loading, it was observed that the inner bolts reached their tensile rupture capacities when the shear force and the corresponding moment were 54.20 kips and 9,200 kips-in., respectively (Figure 2.14). Also, the deformed shape of the model shows that the prying action occurred in the end plate when the capacity was achieved.

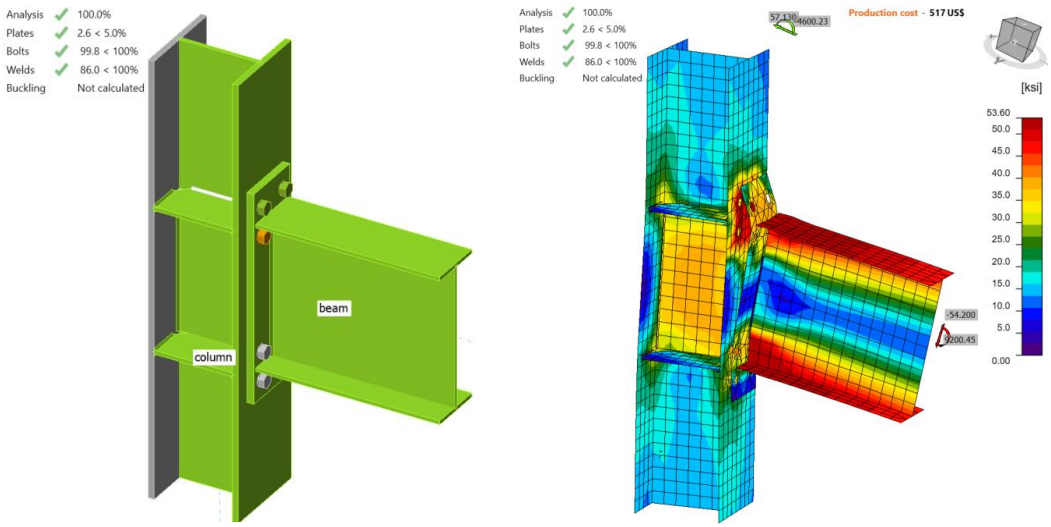

Figure 2.14: IDEA StatiCa model for Variation 1 under the moment of 9,200 kips-in.

2.4.3 Analysis of Variation 2

Following the same procedure described for the baseline model, IDEA StatiCa analysis was performed for the specimen Variation 2. It was observed that the fillet weld between beam web and end plate reached its strength capacity when the shear force and the corresponding moment were 135.20 kips and 35,938 kips-in., respectively (Figure 2.15).

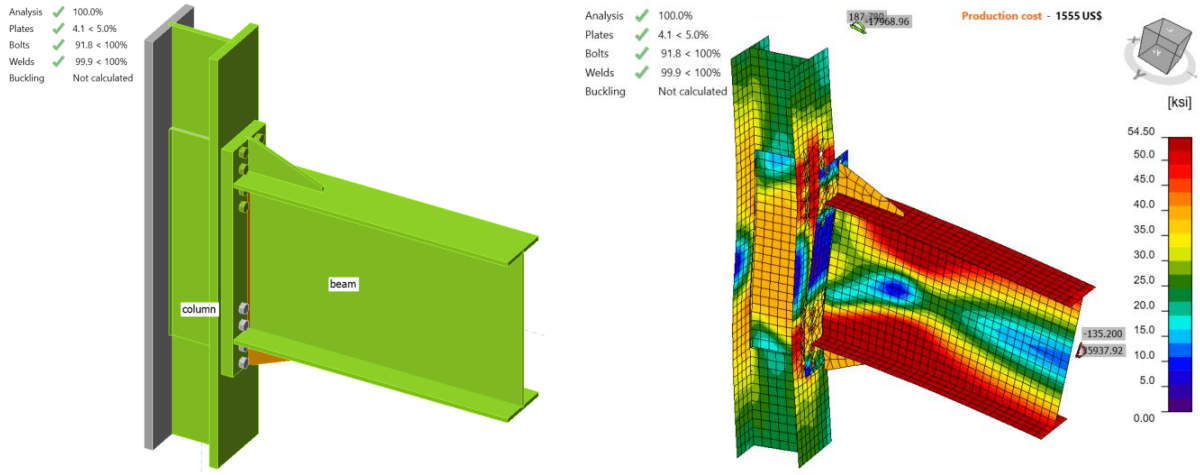

Figure 2.15: IDEA StatiCa model for Variation 2 under the moment of 35,938 kips-in.

2.4.4 Analysis of Variation 3

Following the same procedure, the moment strength capacity of the specimen Variation 3 was calculated in IDEA StatiCa. The incremental loading was stopped when any of the failure limit was achieved. The fillet weld between beam web and end plate reached its strength capacity when the shear force and the corresponding moment were 73.80 kips and 17,804 kip-in., respectively (Figure 2.16).

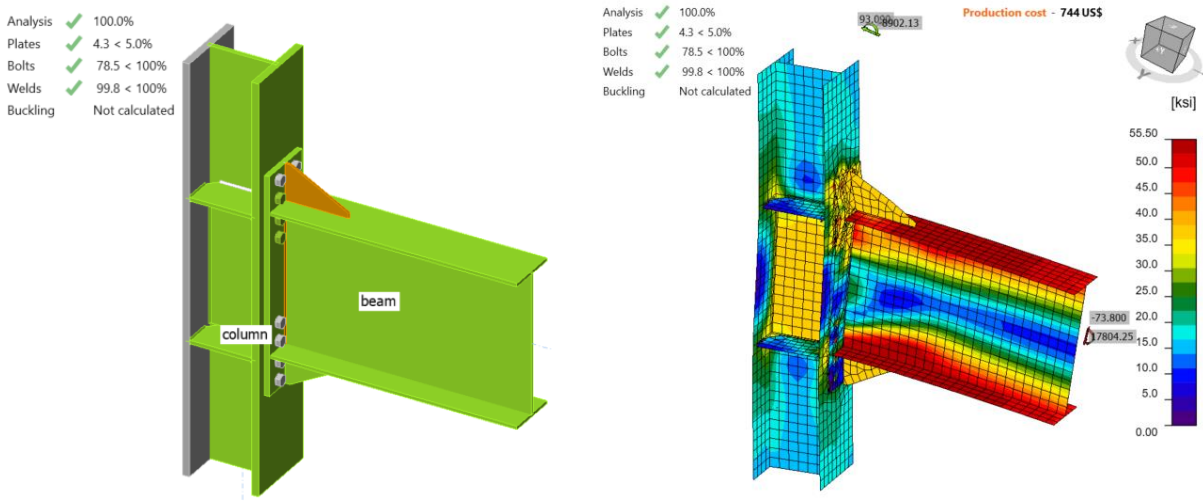

Figure 2.16: IDEA StatiCa model for Variation 3 under the moment of 17,804 kips-in.

2.4.5 Analysis of Variation 4

IDEA StatiCa analysis was performed for Variation 4 following the same steps. It was observed that 5% of the plastic strain limit was reached in the beam flange when shear force of 82.55 kips and the corresponding moment of 19,915 kips-in. were reached (Figure 2.17).

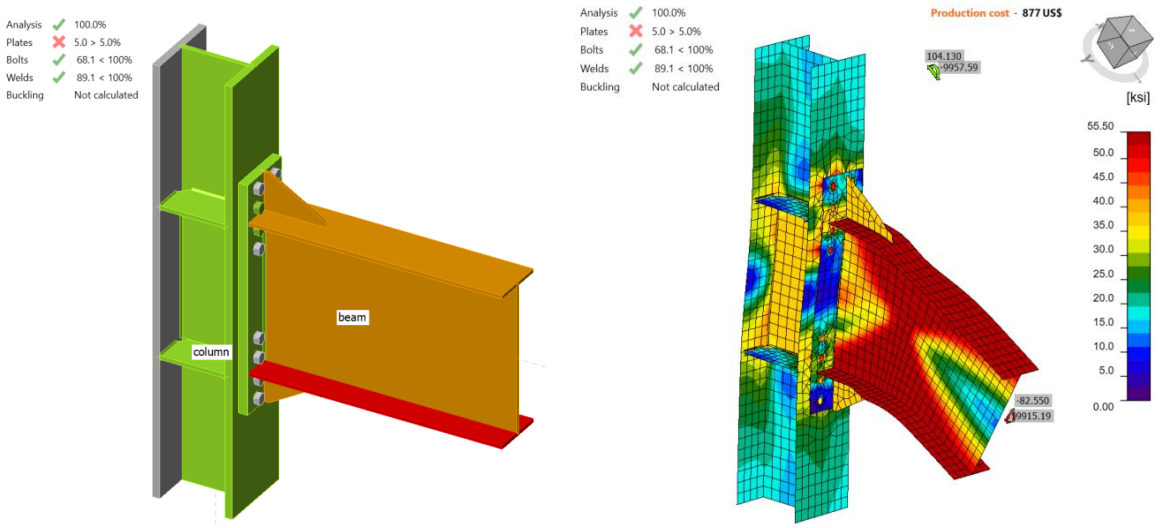

Figure 2.17: IDEA StatiCa model for Variation 4 under the moment of 19,915 kips-in.

2.4.6 Analysis of Variation 5

Following the same procedure, IDEA StatiCa model was developed for Variation 5, and its moment strength capacity was calculated. It was observed that 5% plastic strain occurred in the end plate stiffener when shear force of 101.60 kips and the corresponding moment of 27,007 kip-in. were reached (see Figure 2.18).

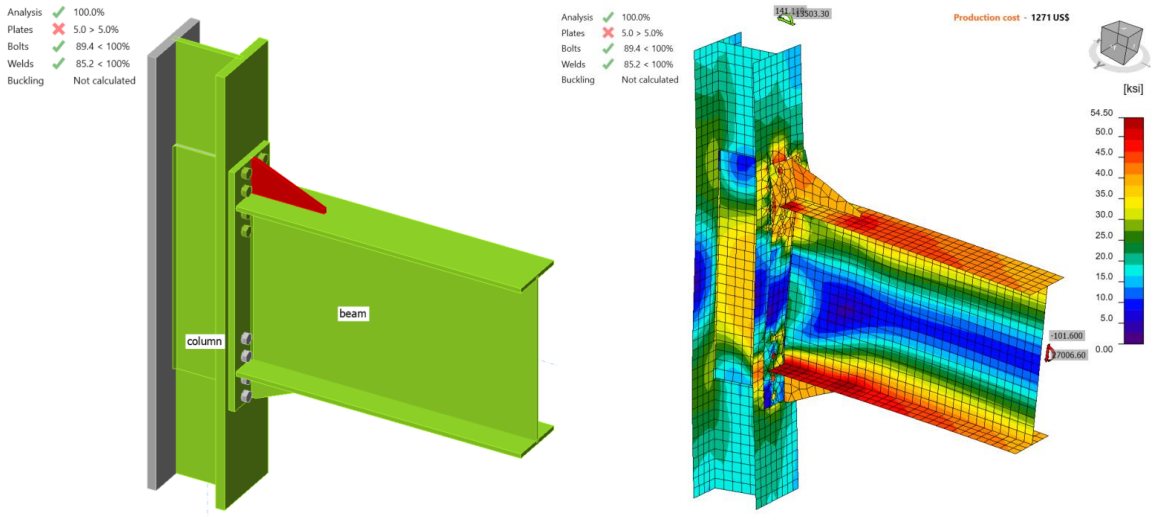

Figure 2.18: IDEA StatiCa model for Variation 5 under the moment of 27,007 kips-in.

The six specimens were analyzed using IDEA StatiCa and their moment capacities at the column centerline were calculated by representing their test conditions. To compare the moment capacities with the ones calculated following the AISC 358 procedure, the moment capacities at the column face were calculated using Eq. 2.6 and presented in Table 2.6.

$$M_{y@foc} = M_{y@cc} - V\frac{d_c}{2} \tag{2.6}$$

where $M_{y@foc}$ is moment capacity at the column face, $M_{y@cc}$ is moment capacity at the column centerline, V is shear force, and d_c is depth of column.

Table 2.6: Moment capacity calculated by IDEA StatiCa

Specimen No	$M_{y@cc}$ (kips-in.)	$M_{y@foc}$ (kips-in.)
Baseline	10,414	9,969
Var-1	9,200	8,808
Var-2	37,453	34,829
Var-3	19,951	17,232
Var-4	19,915	19,275
Var-5	29,372	26,173

2.5. ABAQUS Analysis

In this section, the baseline model developed in Section 2.4.1 was constructed again using ABAQUS software (version 2022) and results were compared with IDEA StatiCa. The CAD model for the finite element analysis was generated using the IDEA StatiCa's viewer platform. The eight bolts and all 26 weld lines in four different lengths were then added to the assembly using the CAD interface in ABAQUS. The same vertical load of 59 kips and the corresponding moment of 100,15.25 kips-in. (around Y axis) were applied to a defined reference point (i.e., RF_1) as shown in Figure 2.19. The analytical length of the column in IDEA StatiCa was 178.05 in. Therefore, to mimic the identical column length in ABAQUS, two other reference points (i.e., RF_2 and RF_3) were introduced 89.025 in. away from the center of the column along the Z axis in both directions (see Figure 2.19). These two reference points were fixed in all directions and were connected to the top and bottom faces of the column using a connector builder module in ABAQUS. In ABAQUS, the element size was chosen to be between 2.5-5 mm after mesh sensitivity analysis. The 3D stress, 8-node linear brick reduced integration (i.e., C3D8R) element type was selected.

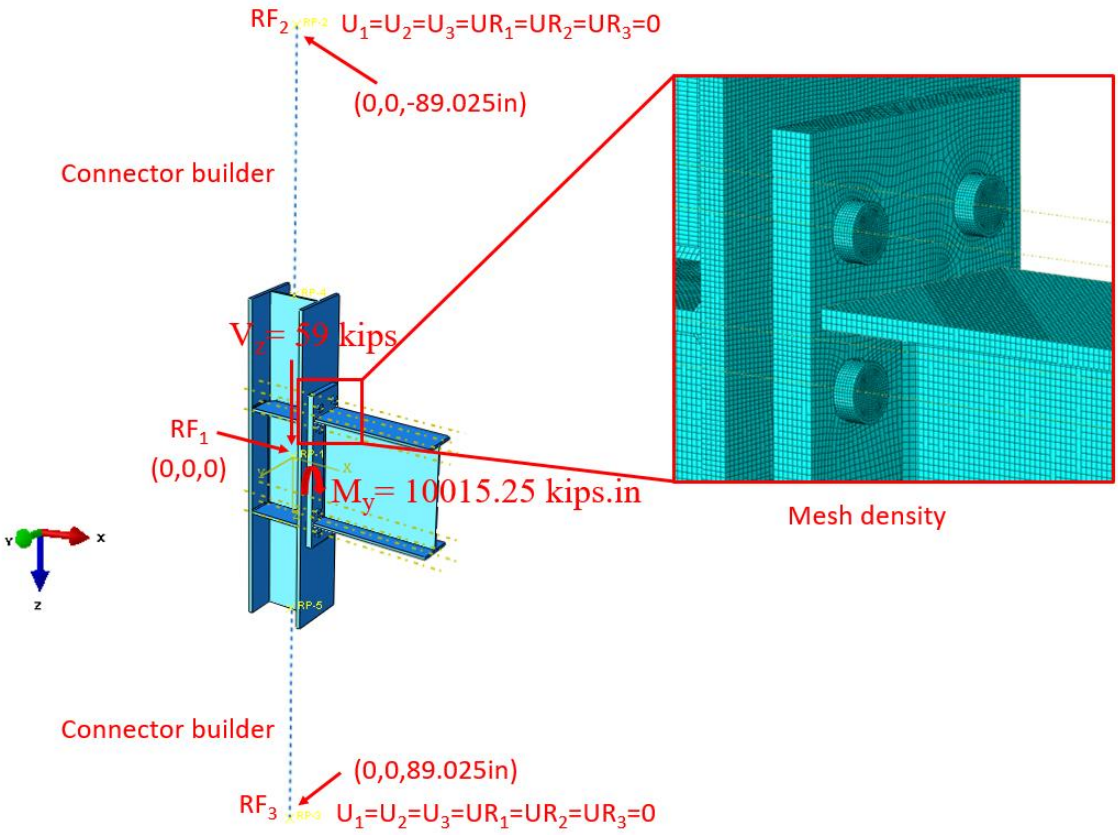

Figure 2.19: Model setup in ABAQUS

The tie constraint was applied between the weld lines and the attaching parts. The material behavior was modeled using bi-linear plasticity in ABAQUS. Other parameters, including density, elastic modulus, and Poisson's ratio were taken from the IDEA StatiCa materials library. The numerical simulation was carried out on four processors (Intel Xenon (R) CPU E5-2698 v4 @ 2.20GHz) and took approximately 75 minutes to finish. Figure 2.20 compares the calculated von-Mises stress and plastic strain between the IDEA StatiCa and ABAQUS.

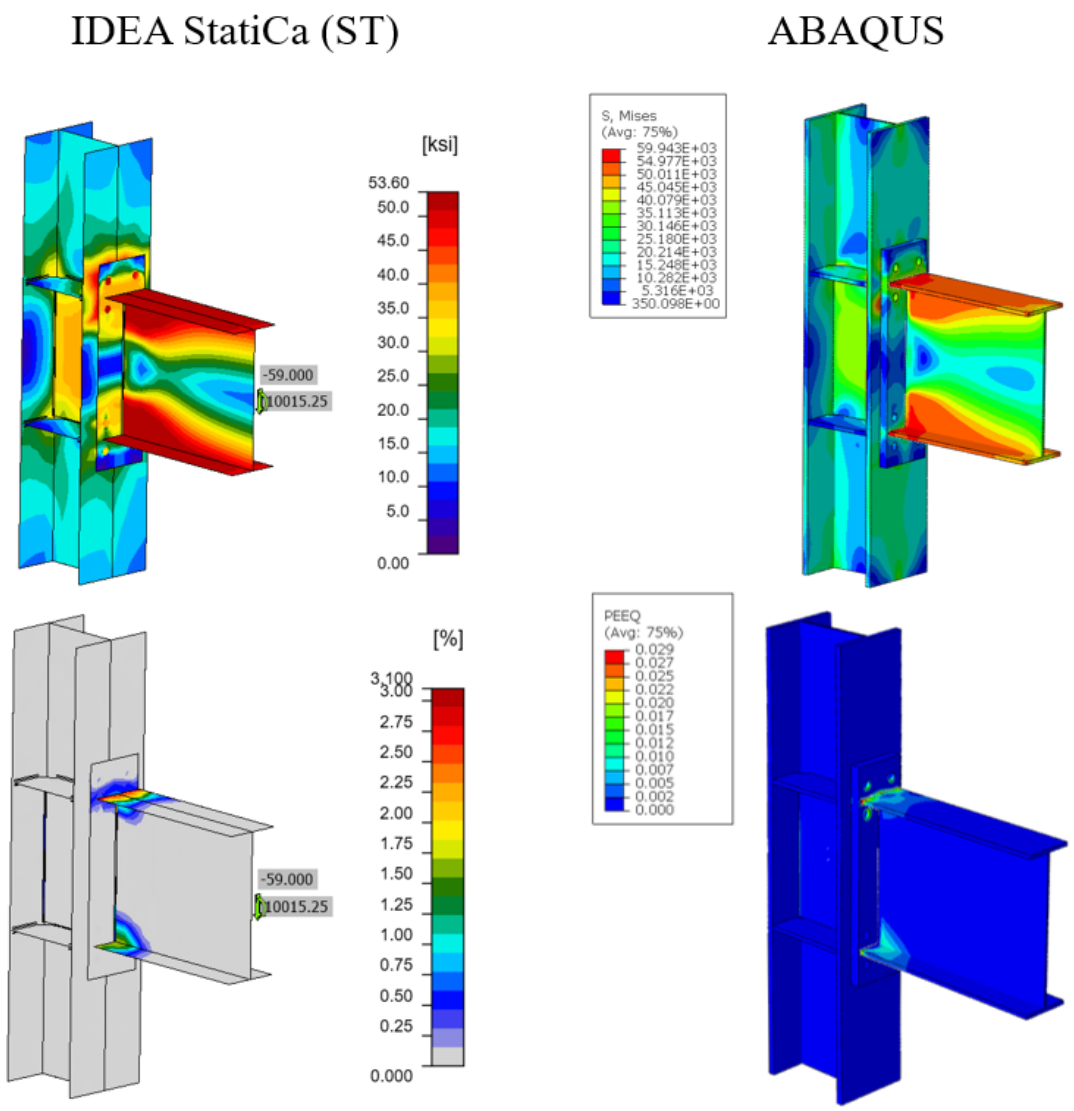

Figure 2.20: Comparison of the predicted von Mises stress (top row) and plastic strain (bottom row) between IDEA StatiCa and ABAQUS models

The maximum predicted stress in IDEA StatiCa was 54.40 ksi (on the beam top flange) while the ABAQUS model shows a maximum stress of 59.94 ksi at the same location. The slightly different stress distribution is likely due to the utilization of finer mesh in the ABAQUS model, the way that shear and tensile forces are being transferred between the bolt and plates as well as the simplified CAD model in IDEA StatiCa. Also, the maximum calculated plastic strain in IDEA StatiCa and ABAQUS were 3.1% and 2.9%, respectively (both at the beam top flange). Figure 2.21 depicts the comparison of the moment-rotation curve between the two software with respect to the column centerline.

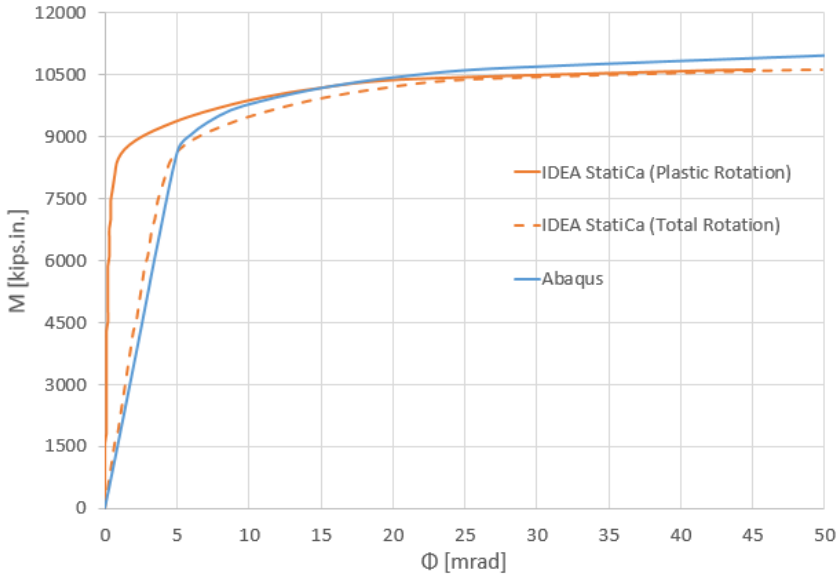

Figure 2.21: Moment-rotation comparison between IDEA StatiCa and ABAQUS

Note that in Figure 2.21, to obtain the total rotation by IDEA StatiCa (shown by dashed orange line), the linear column rotation at the column centerline was calculated using SAP2000 and then added to the default plastic rotation curve reported by IDEA StatiCa (shown by solid orange line). Both models offer comparable initial stiffness estimations. The minor discrepancy could be associated with the difference in the element types (i.e., solid element in ABAQUS versus shell element in IDEA StatiCa), the difference in load transferring between the bolts and plates, and the employment of the tie constraint in ABAQUS to represent the welds.

2.6 Summary and Comparison of Results

The six tested EPM connections were investigated using IDEA StatiCa and following the AISC design procedure. Also, the results from IDEA StatiCa baseline model were compared with those from the equivalent ABAQUS model. The calculated flexural moment capacities using IDEA StatiCa and AISC procedure are presented in Figure 2.22.

The connection of the baseline model was designed to develop 110% of the plastic moment capacity of the beam. As expected, it was reported that severe flange buckling occurred in the beam (Figure 2.4). Similarly, IDEA StatiCa and code-based design calculations identified the same failure mode. The moment capacity corresponding to 5% of the plastic strain limit computed by IDEA StatiCa is slightly less than the moment strength of the beam calculated following the AISC procedure (9,969 kips-in. versus 10,216 kips-in. in Figure 2.22). Also, the moment-rotation comparison was performed for the baseline model. The moment-plastic rotation curve was extracted from the test report and compared with the one provided by IDEA StatiCa as shown in Figure 2.23.

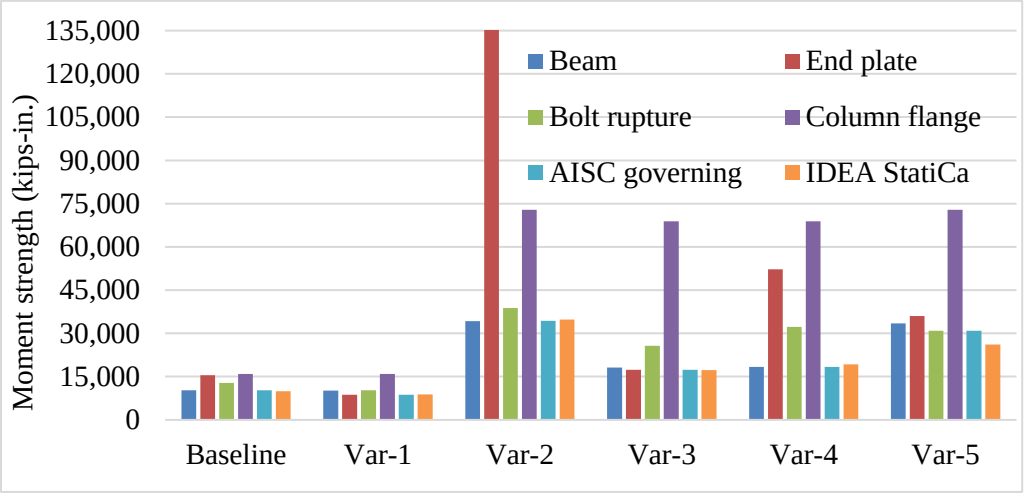

Figure 2.22: Moment capacity calculated by IDEA StatiCa and AISC procedure

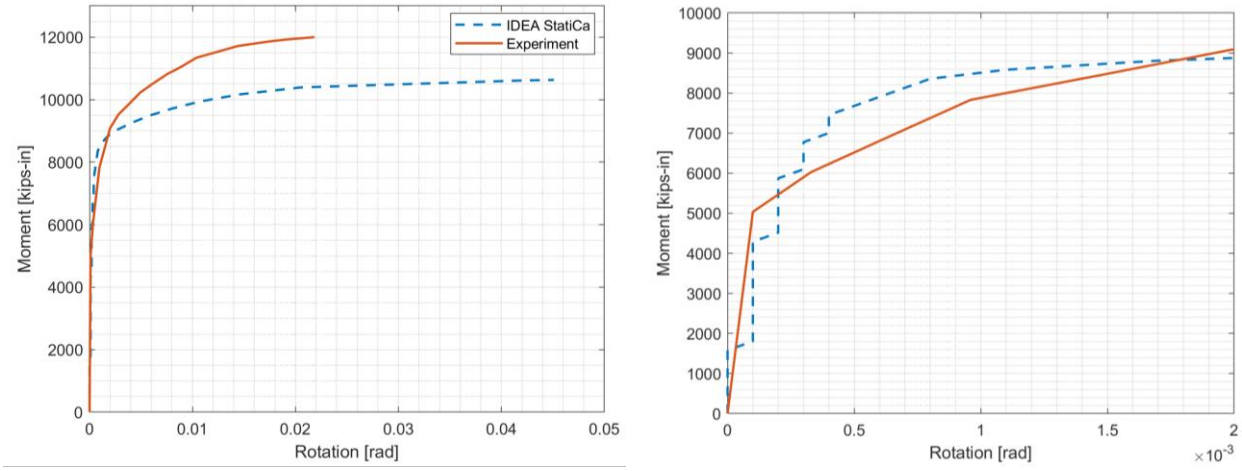

Figure 2.23: Moment-rotation comparison

During the test of Variation 1, it was observed that the specimen failed due to the bolt rupture. Similarly, IDEA StatiCa analysis for the same connection indicated that the inner bolts reached their tensile capacities (8,808 kips-in.). On the other hand, according to AISC design calculations, the minimum end plate thickness requirement was not satisfied and the controlling limit state was the end plate yield strength with moment strength of 8,669 kips-in. (note that bolt rupture strength was calculated by excluding effects of prying). Since the moment strength of end plate (8,669 kips-in.) is less than 110% of the no prying bolts tension rupture strength (10,210 kips-in.), prying action is expected to occur in the bolts and thus decreasing the bolt rupture capacity calculated with the assumption that no prying occurs in the bolts. In this example, IDEA StatiCa shows its capability in calculating bolt rupture capacity including the effects of prying on strength capacity of bolts while AISC 358 doesn't permit prying action in bolts with the minimum thickness requirement of end plate.

It was stated in the test report of Variation 2 that initial yielding occurred in the end plate stiffener and severe local buckling was observed in the beam (Figure 2.6). IDEA StatiCa analysis showed that the specimen failed due to the fillet weld between the beam web and end plate (reached its strength capacity at 34,829 kips-in.). Similarly, AISC design checks confirmed that the fillet weld does not have enough strength (0.313 in. double sided weld was used while 0.46 in. was required). Following AISC design procedure, the moment strength was calculated as 34,323 kips-in. controlled by beam failure.

Regarding Variation 3, it was reported that the initial yielding occurred in the end plate stiffener followed by the end plate and beam yielding (Figure 2.7). According to the code-based calculations, the moment strength capacity of the specimen was 17,327 kips-in. controlled by end plate yield. Also, the specimen didn't satisfy the required minimum size of the weld between the beam web and end plate (0.313 in. double sided weld was used while 0.38 in. was required). On the other hand, IDEA StatiCa analysis showed that the specimen failed due to the inadequate weld strength between the beam web and end plate (17,232 kips-in.).

For Variation 4, it was reported that severe local buckling occurred in the beam at the end of the experiment (Figure 2.8). Similarly, the moment strength of the beam is the governing limit state based on AISC design calculations. Likewise, the first member exceeding the 5% of plastic strain limit was the beam flange in IDEA StatiCa. The reason IDEA StatiCa calculated a slightly larger moment capacity than the one calculated following the AISC procedure (19,275 kips-in. versus 18,346 kips-in. in Figure 2.22) can be attributed to the contribution of the end plate stiffener.

In the test report of Variation 5, it was stated that the initial yielding occurred in the end plate stiffener and the specimen failed due to the bolt rupture which is the controlling limit state according to AISC design calculations. On the other hand, the IDEA StatiCa model failed due to end plate stiffener which didn't satisfy the minimum thickness requirement of end plate stiffener. The reason IDEA StatiCa computed a less moment capacity than the one calculated following the AISC procedure (26,173 kips-in. versus 30,890 kips-in. in Figure 2.22) can be associated with the insufficient thicknesses of end plate (1.25 in. while 1.40 in. is required) and end plate stiffener (0.75 in. while 0.84 in. is required) based on AISC design checks. It should be noted that Variation 5 is the only specimen among the covered six EPM connections that didn't satisfy both requirements.

References

AISC (2016), "Prequalified Connections for Special and Intermediate Steel Moment Frames for Seismic Applications, including Supplement No. 1," American Institute of Steel Construction ANSI/AISC 358-16, Chicago, Illinois.

Sumner, E. A., Mays, T. W. and Murray, T. M. (2000), Cyclic Testing of Bolted Moment End-Plate Connections, *Research No. CE/VPI-ST-00/03*, Virginia Polytechnic Institute and State University, Blacksburg, VA.

Borgsmiller, J. T. (1995), Simplified Method for Design of Moment End-Plate Connections, Department of Civil Engineering, Virginia Polytechnic Institute and State University, Blacksburg, VA.

AISC Steel Design Guide 4 (2003), "Extended End-plate Moment Connections Seismic and Wind Applications," American Institute of Steel Construction, Chicago, Illinois.

Chapter 3. Welded Unreinforced Flange-Welded Web (WUF-W) Connections

3.1. Introduction

The third prequalified connection covered in this verification study is welded unreinforced flange-welded web (WUF-W) moment connection. In this chapter, similarly to the previous chapters, six experimentally investigated steel connections were selected from the literature to be compared their flexural moment strengths obtained using IDEA StatiCa and AISC design procedure. In addition, the moment-rotation comparison between IDEA StatiCa and ABAQUS was performed for one of the specimens selected as a baseline model.

3.2 Experimental Study

Ricles et al. (2000) conducted a series of experiments to investigate seismic performance of ductile welded unreinforced flange connections at Lehigh University. For this purpose, six exterior and five interior full-scale connections were subjected to cycling loading. Although the weld and geometric details of none of the tested specimens necessarily satisfy the requirements of the latest AISC 358 (2016), this experimental study was selected to be examined in this verification study because of the following reasons:

- There is no experimental investigation conducted in the U.S. for WUF-W with the specimens that satisfy all requirements outlined in AISC 358 (2016)
- Being one of the experimental studies that formed that basis of prequalification requirements of WUF-W moment connections in AISC 358 (2016)
- This experimental research was sponsored by SAC Joint Venture with funding from the Federal Emergency Management Agency (FEMA) to evaluate the improved details of WUF-W moment connections. SAC research program was implemented to improve the steel connection design and performance after poor performance was observed in some connections after the 1994 Northridge earthquake.

The test setup for interior connections is illustrated in Figure 3.1. The length between beam support and the column centerline was 177 in. (4.50 m), and the length from the actuator to the bottom support of the column was 156 in. (3.96 m). Among 11 tested connections, six of them were chosen to be covered in this verification study. The geometric and material properties of the selected six connections are presented in Tables 3.1 and 3.2, and the configurations of the specimens are shown in Figures 3.2 through 3.4.

Table 3.1: Properties of the WUF-W specimens

Specimen No.	Beam	Column	Shear plate size (in.)	Doubler plate thickness (in.)	Continuity plate thickness (in.)
Baseline (T1)	W36x150	W14x311	5/8x5x30.5	-	1.0
T5	W36x150	W14x311	5/8x5x30.5	1/2 (one side)	-

C1	W36x150	W14x398	5/8x5x30.5	3/4 (both sides)	-
C2	W36x150	W14x398	5/8x5x30.5	3/8 (both sides)	1.0
C3	W36x150	W27x258	5/8x5x30.5	3/8 (both sides)	-
C4	W36x150	W27x258	5/8x5x30.5	3/4 (both sides)	1.0

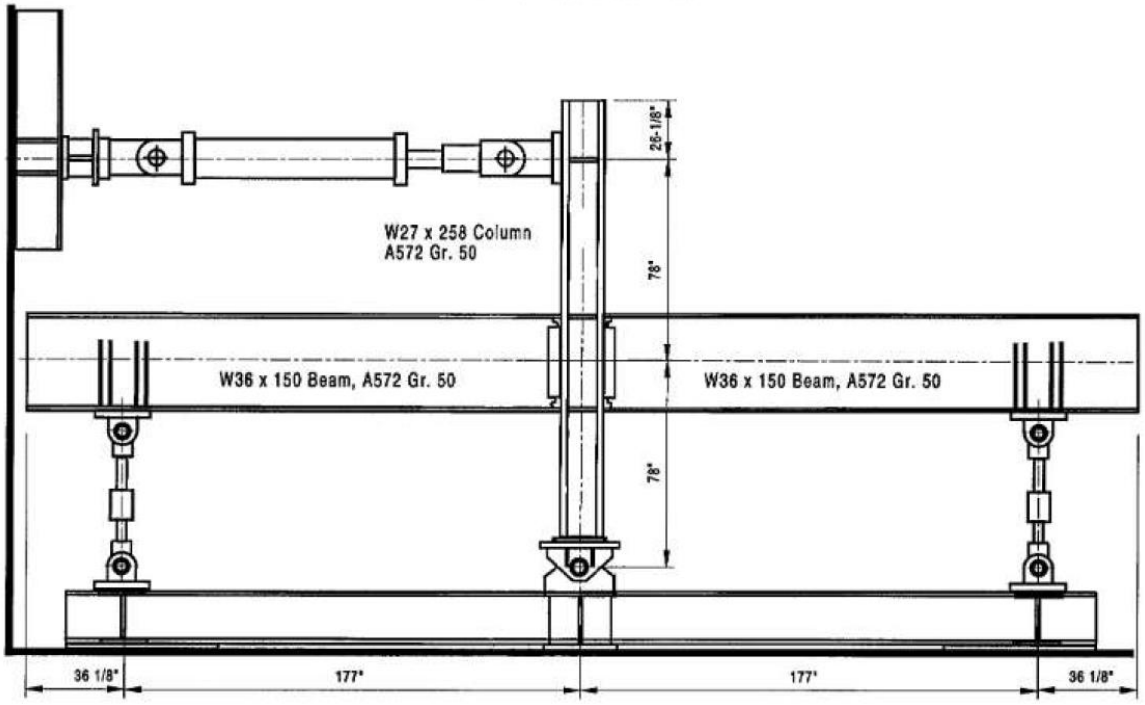

Figure 3.1: Test setup (Ricles et al., 2000)

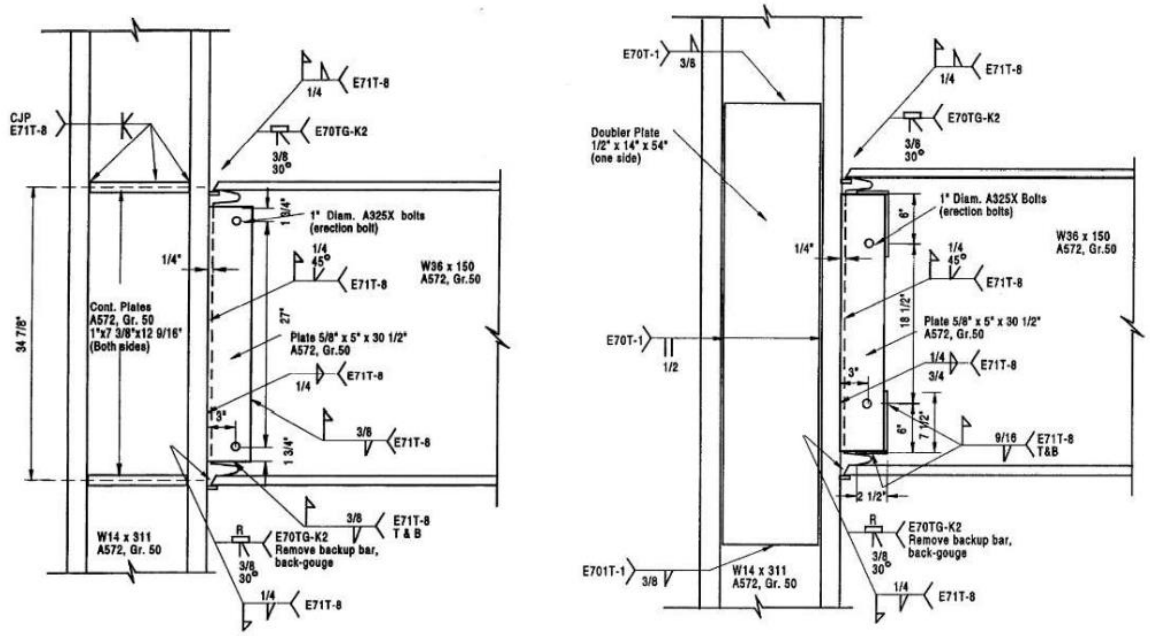

Figure 3.2: Left) Configuration of baseline model T1; Right) configuration of Specimen T5 (Ricles et al., 2000)

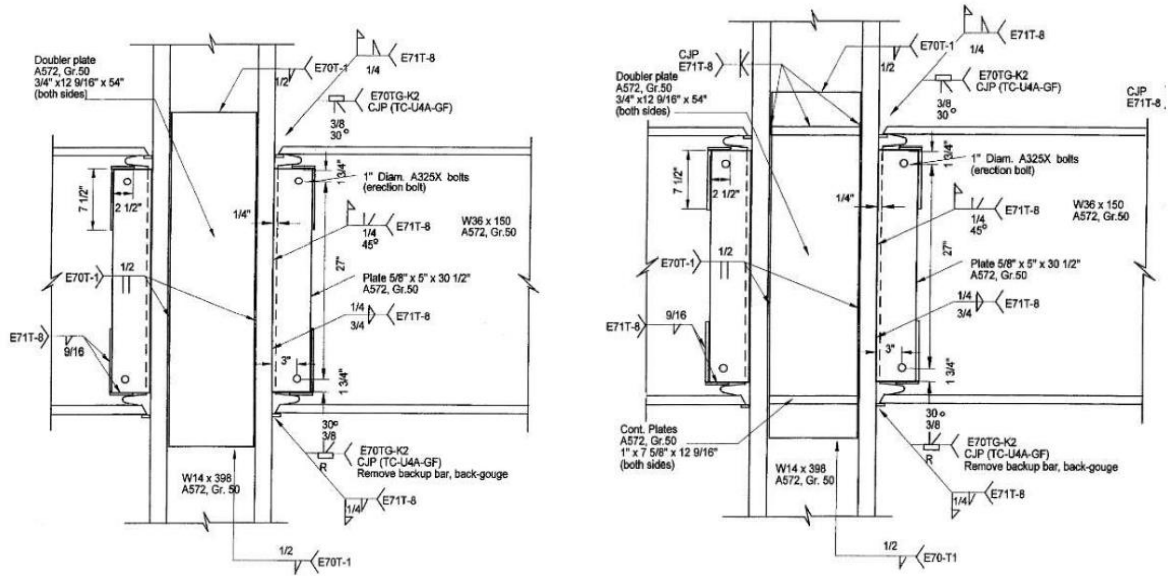

Figure 3.3: Left) Configuration of Specimen C1; Right) configuration of Specimen C2 (Ricles et al., 2000)

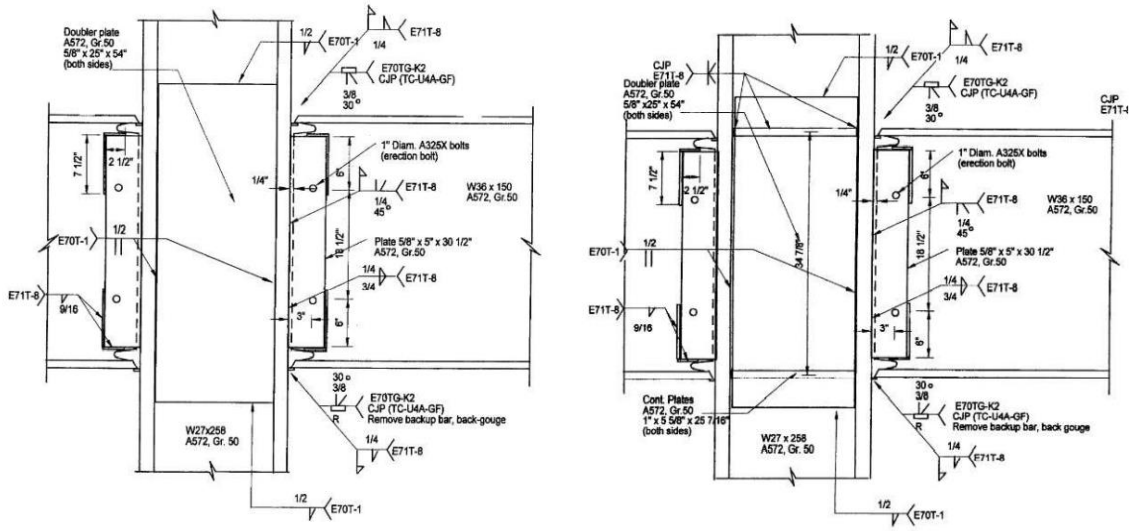

Figure 3.4: Left) Configuration of Specimen C3; Right) configuration of Specimen C4 (Ricles et al., 2000)

Table 3.2: Measured material properties of the WUF-W specimens (Ricles et al., 2000)

Specimen No.	Section	Yield stress (ksi)	Ultimate stress (ksi)
Baseline (T1)	Column (flange)	47.3	69.5
	Beam (flange)	55.1	71.6

	Shear tab	51.3	75.5
	Continuity plate	38.2	62.9
T5	Column (flange)	47.3	69.5
	Beam (flange)	55.1	71.6
	Shear tab	51.3	75.5
	Doubler plate	53.0	72.0
C1	Column (flange)	53.2	72.4
	Beam (flange)	56.7	72.5
	Shear tab	51.3	75.5
	Doubler plate	57.1	76.7
C2	Column (flange)	53.2	72.4
	Beam (flange)	56.7	72.5
	Shear tab	51.3	75.5
	Doubler plate	57.1	76.7
	Continuity plate	53.0	70.9
C3	Column (flange)	50.2	73.3
	Beam (flange)	55.1	71.6
	Shear tab	51.3	75.5
	Doubler plate	64.5	85.2
C4	Column (flange)	50.2	73.3
	Beam (flange)	55.1	71.6
	Shear tab	51.3	75.5
	Doubler plate	64.5	75.5
	Continuity plate	64.5	85.2

The baseline model (specimen T1) and specimen T5 are exterior connections whereas the others are interior ones that consist of identical beams and connections attached to the same column from each horizontal side (see Figure 3.1). Since the identical connections showed almost the same performance during the testing, only one of their after-test photos and moment-rotation relationships are shared below for each interior specimen covered in this study (specimens C1, C2, C3, and C4).

The beam web of the baseline model was groove welded to the column flange and a supplementary weld was provided continuously around the edges of the shear tab. It was reported that the groove weld between the shear tab and column flange was cracked during 2% drift cycles, and beam flanges were cracked during 4% drift cycles as shown in Figure 3.5. Specimen T5 was designed differently from the baseline model with a doubler plate, a partial weld between the shear tab and beam web, a larger fillet weld size between the shear tab and column flange, and without a continuity plate. It was reported that the ductile fracture occurred in the beam flange during 6% cycles (see Figure 6).

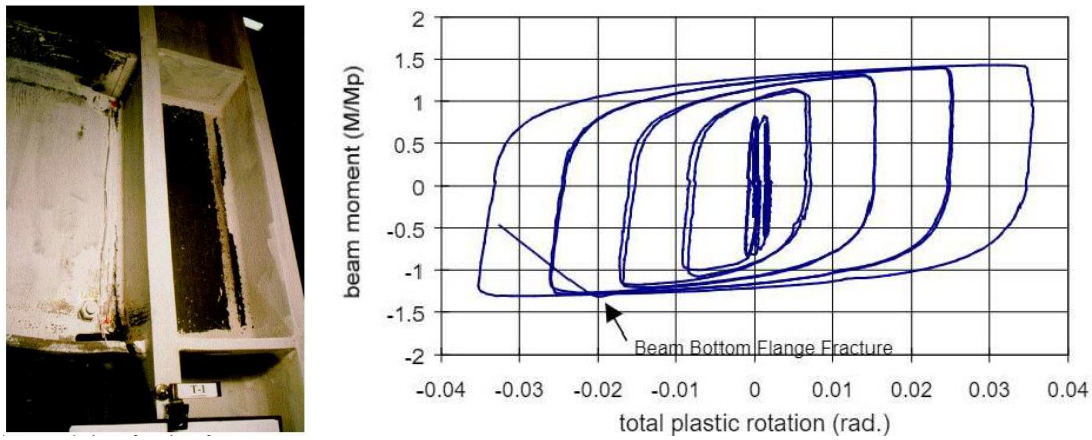

Figure 3.5: Left) Baseline model (T1) after testing; Right) moment-total plastic rotation relationship (Ricles et al., 2000)

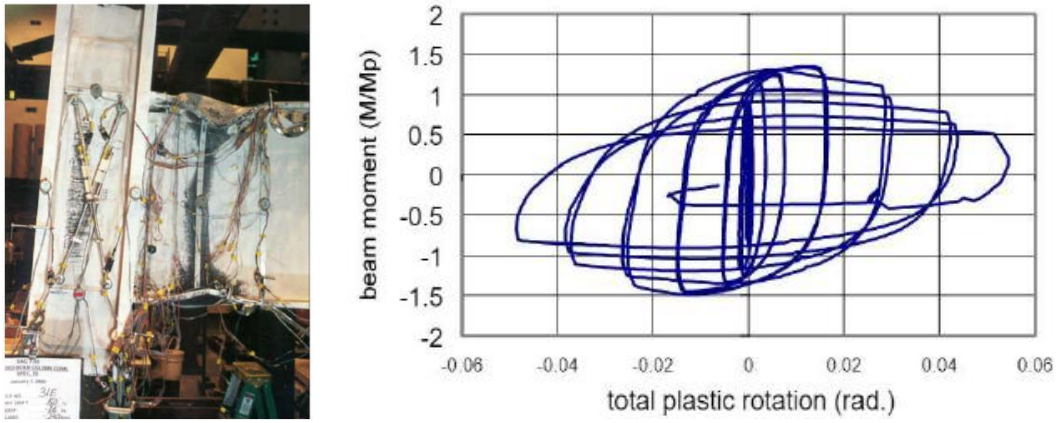

Figure 3.6: Left) Specimen T5 after testing; Right) moment-total plastic rotation relationship (Ricles et al., 2000)

Specimen C1 was one of the four interior connections covered in this study. It had a larger column size and thicker doubler plate compared to specimen T5. Ductile fracture was observed at the first cycle of 5% drift on the west beam top flange and the second cycle of 5% drift on the east beam top flange illustrated in Figure 3.7., Specimen C2, differently from specimen C1, was designed with a continuity plate and with a thinner doubler plate. Experimental results showed that specimen C2 failed during cycles of 6% drift due to the ductile fracture on both beam flanges as shown in Figure 3.8.

Specimen C3 consisted of a deeper and thinner column compared to the first four specimens. It was stated in the test report that the ductile fracture of west beam flange was observed during the first cycle of 5.5% story drift as shown in Figure 3.9. Specimen C4 had thicker doubler and

continuity plates in addition to the configuration of specimen C3. During the experiment, ductile fracture occurred at the end of 6% drift cycle (Figure 3.10).

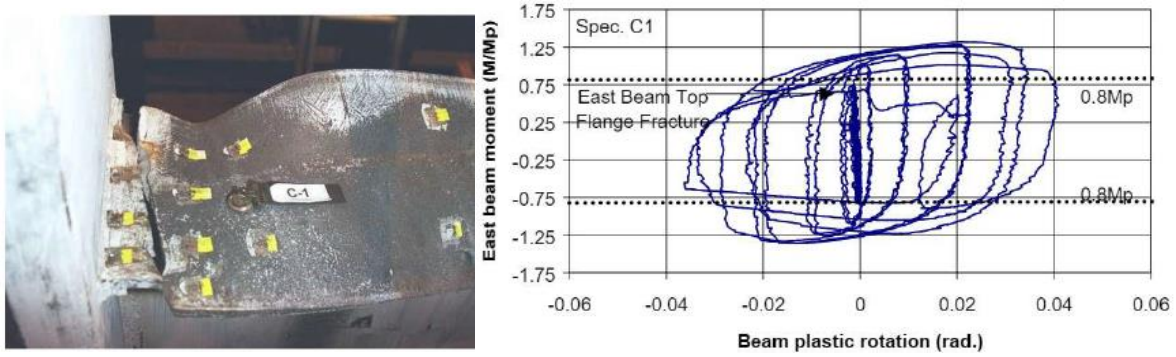

Figure 3.7: Left) Specimen C1 after testing; Right) moment-total plastic rotation relationship (Ricles et al., 2000)

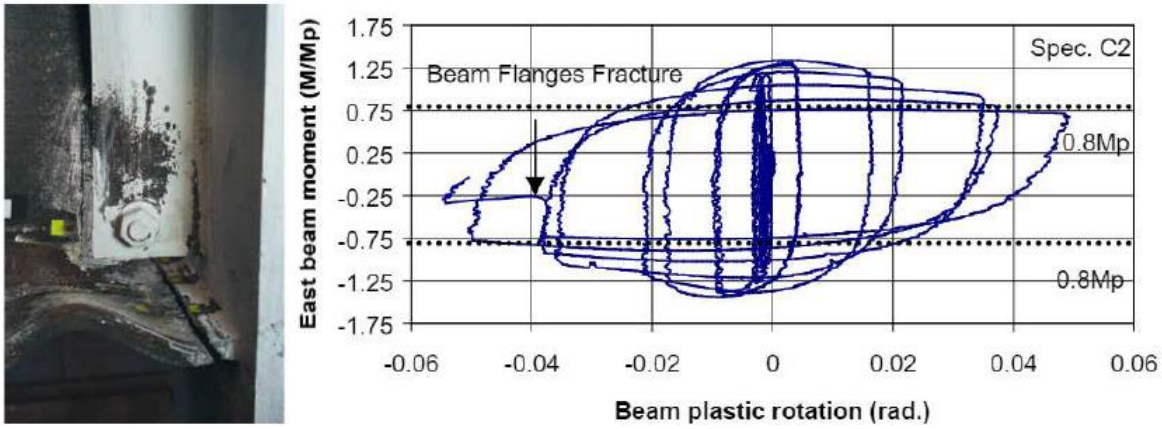

Figure 3.8: Left) Specimen C2 after testing; Right) moment-total plastic rotation relationship (Ricles et al., 2000)

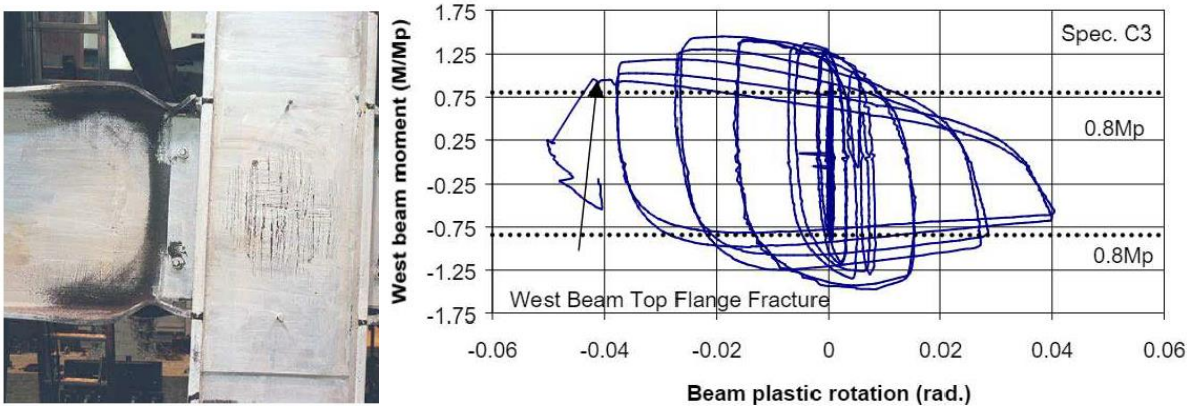

Figure 3.9: Left) Specimen C3 after testing; Right) moment-total plastic rotation relationship (Ricles et al., 2000)

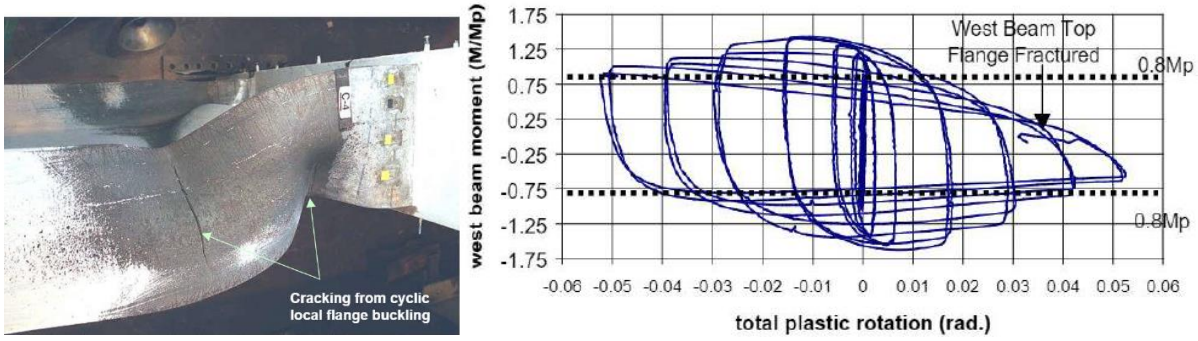

Figure 3.10: Left) Specimen C4 after testing; Right) moment-total plastic rotation relationship (Ricles et al., 2000)

3.3 Code Design Calculations

The procedure outlined in Section 8.7 of AISC 358 (2016) for WUF-W connections were followed, and the following checks were performed for the six specimens.

- Check beam geometric limitations (AISC 358 Sec. 8.3.1)
- Check column geometric limitations (AISC 358 Sec. 8.3.2)
- Check beam design shear strength (AISC 358, Sec. 8.7)
- Check flexural strength (AISC 360, Eq. F2-1)
- Check continuity plate requirements (AISC 341, Sec.E3.6f.2)
- Check column-beam strength relationship (AISC 358 Section 8.4)
- Check beam flange to column flange welds (AISC 358 Section 8.5)
- Check weld access hole geometry (AWS D1.8/D1.8M)
- Check beam web-to-column connection (AISC 358 Section 8.6)

The summary of the AISC 358 (2016) design checks of the six specimens is presented in Table 3.3. The details of the design calculations and checks are provided in Appendices E and F.

Table 3.3: AISC 358 (2016) design checks for the specimens

Design Checks	Baseline (T1)	T5	C1	C2	C3	C4
Beam geometric limitations	OK	OK	OK	OK	OK	OK
Column geometric limitations	OK	OK	OK	OK	OK	OK
Beam design shear strength	OK	Not OK	Not OK	Not OK	Not OK	Not OK

Beam flexural strength	OK	OK	OK	OK	OK	OK
Continuity plate requirements	Not OK	-	-	Not OK	-	Not OK
Column-beam strength relationships	OK	OK	OK	OK	OK	OK
Beam flange-to-column flange connection	OK	OK	OK	OK	OK	OK
Weld access hole geometry	Not OK	Not OK	Not OK	Not OK	Not OK	Not OK
Beam web-to-column connection	Not OK	OK	OK	OK	OK	OK
Panel Zone	OK	OK	OK	Not OK	OK	OK

It is assumed that plastic hinge occurs at the face of the column in accordance with Section 8.7 in AISC 358 (2016). The moment strength of the beam at plastic hinge location, $M_{by@ph}$, can be calculated using Equation 3.1.

$$M_{by@ph} = F_{yb} Z_{bx} \quad (3.1)$$

where F_{yb} is yield stress of beam, Z_{bx} is plastic section modulus of beam. The plastic moment capacities of the specimens were calculated and presented in Table 3.4.

Table 3.4: Plastic moment capacities of the specimens calculated following AISC design procedure

Specimen No	Plastic moment capacity (kips-in.)
Baseline	32,013
T5	32,013
C1	32,943
C2	32,943
C3	32,013
C4	32,013

3.4 IDEA StatiCa Analysis

The selected six specimens were modeled in IDEA StatiCa with the aim of simulating the behavior of the experiments. Their moment capacities and failure modes were identified using stress-strain analysis type (i.e., EPS). The measured material properties given in Ricles et al. (2000) (see Table 3.2) were introduced to the software, and resistance factors were set to 1.0. Using the connection stiffness analysis type (i.e., ST) in IDEA StatiCa, the moment-rotation relationship was calculated for the baseline model.

3.4.1 Analysis of Baseline Model

IDEA StatiCa model was developed for the baseline model. The measured material properties were introduced, and the overstrength coefficients, R_y and R_t, were set equal to 1.0 (see Figure 3.11). Also, all LRFD resistance factors were set to 1.0 to compare the calculated actual response of the connections with that measured during the laboratory experiment (Ricles et al., 2000). To obtain the loads at the column centerline, a beam-column frame model was developed in SAP2000 using the lengths of column and beam in the test setup. Pin support was used at the bottom of the column and roller support was used at the end of the beam.

To calculate the moment capacity of the baseline model, an incremental loading was applied using stress, strain analysis (i.e., EPS) with "loads in equilibrium" option in IDEA StatiCa model until any of following was achieved:

4) 5% of plastic strain in plates
5) 100% strength capacity in bolts
6) 100% strength capacity in welds

The weld between the shear tab and column flange reached its strength capacity when the shear force and the corresponding moment values were 167.70 kips and 29,700 kips-in., respectively (Figure 3.11). Using "ST" analysis, the moment-rotation relationship was obtained and is shown in Figure 3.12.

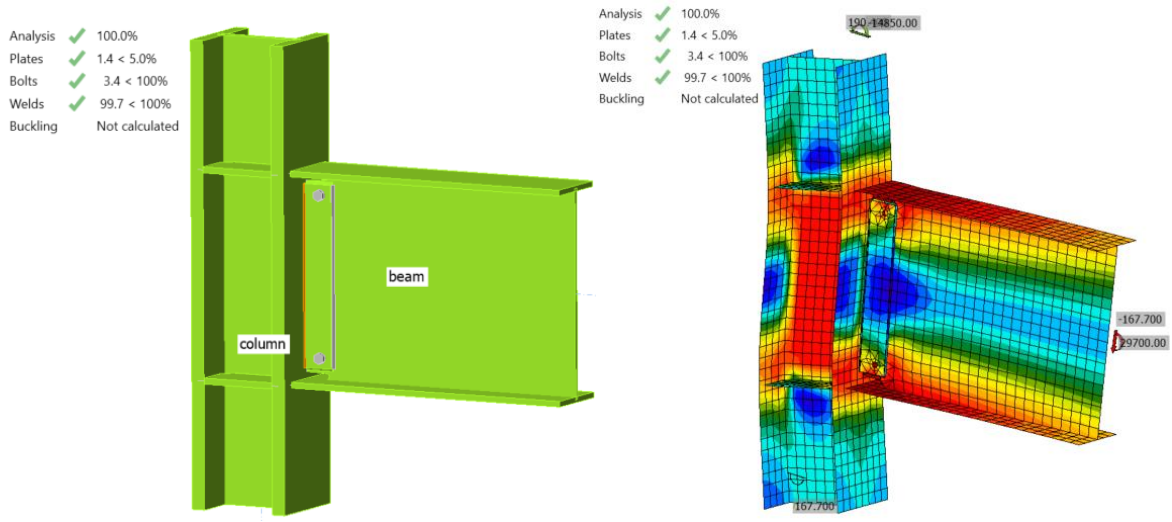

Figure 3.11: IDEA StatiCa model for baseline model

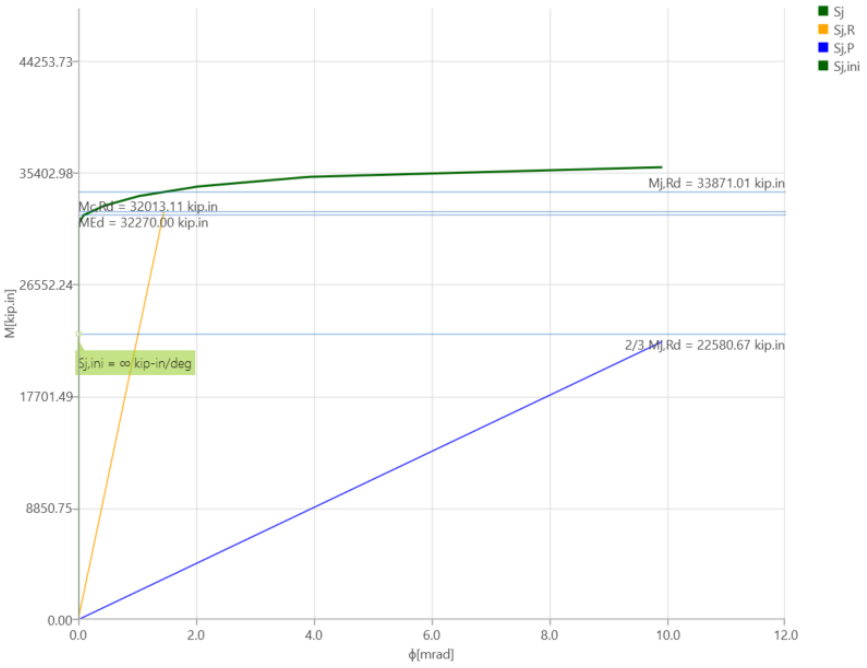

Figure 3.12: Moment-rotation relationship for the baseline model

3.4.2 Analysis of Variation Specimens

IDEA StatiCa analysis was performed for specimen T5 following the procedure explained for the baseline model. It was observed that the beam web reached 5% plastic strain when the shear force and the corresponding moment were 205.70 kips and 36,420 kips-in., respectively (Figure 3.13).

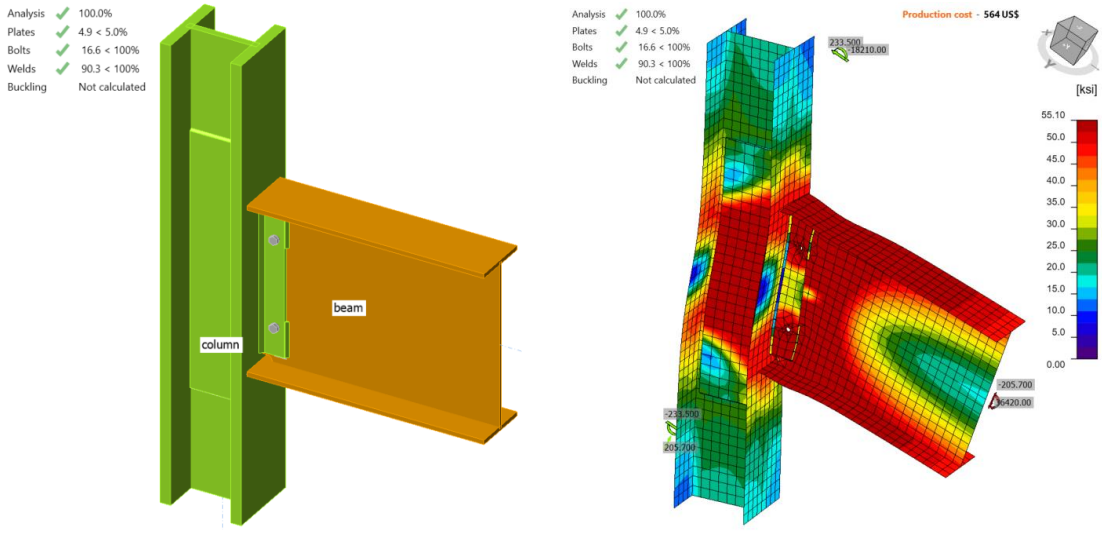

Figure 3.13: IDEA StatiCa model for Specimen T5

Specimen C1 was modelled and analyzed in IDEA StatiCa following the same procedure. It was observed that the beam web reached 5% plastic strain when the shear force and the corresponding moment were 212.60 kips and 37,650 kips-in., respectively (Figure 3.14).

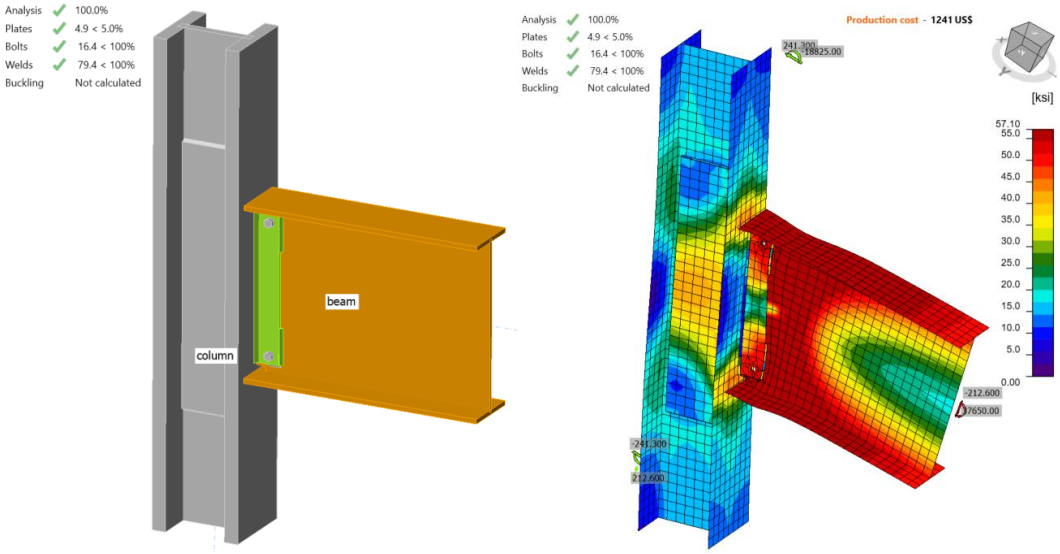

Figure 3.14: IDEA StatiCa model for Specimen C1

Following the same procedure described in this section, IDEA StatiCa analysis was performed for specimen C2. It was observed that the beam web reached 5% plastic strain when the shear force and the corresponding moment were 212.60 kips and 37,650 kips-in., respectively (Figure 3.15).

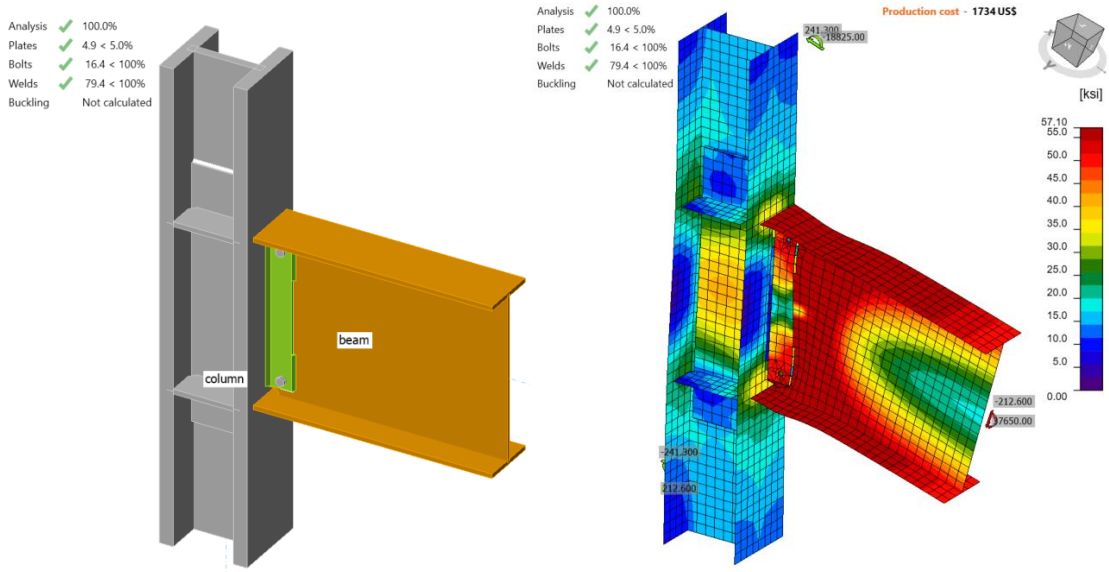

Figure 3.15: IDEA StatiCa model for Specimen C2

Following the same procedure, IDEA StatiCa analysis was performed for specimen C3. It was observed that the beam web reached 5% plastic strain when the shear force and the corresponding moment were 213.20 kips and 37,750 kips-in., respectively (Figure 3.16).

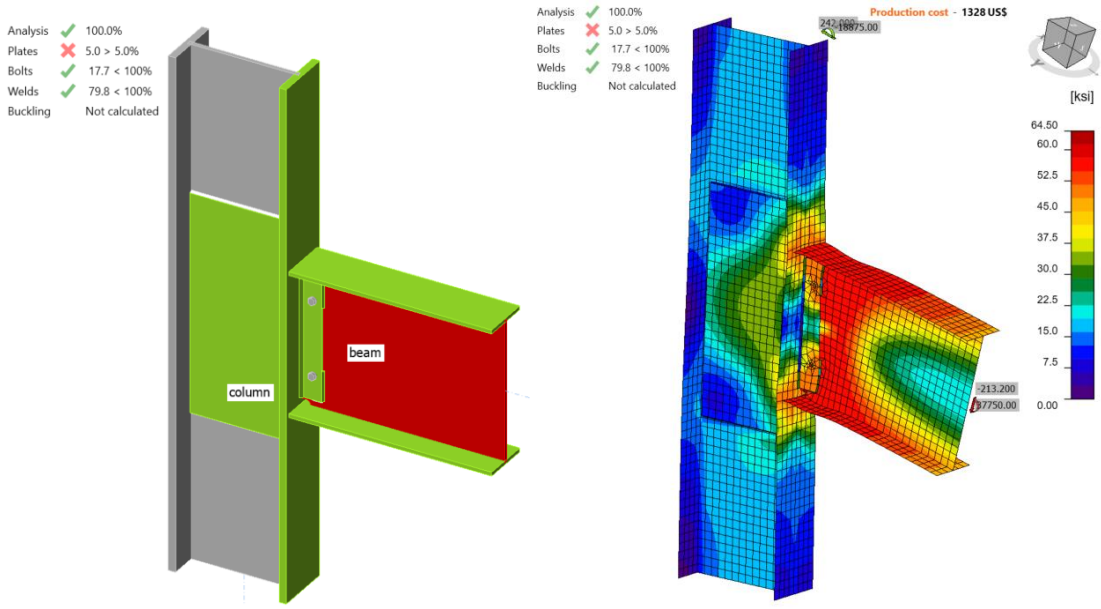

Figure 3.16: IDEA StatiCa model for Specimen C3

Following the same procedure, IDEA StatiCa analysis was conducted for specimen C4. It was observed that the beam web reached 5% plastic strain when the shear force and the corresponding moment were 213.60 kips and 37,820 kips-in., respectively (Figure 3.17).

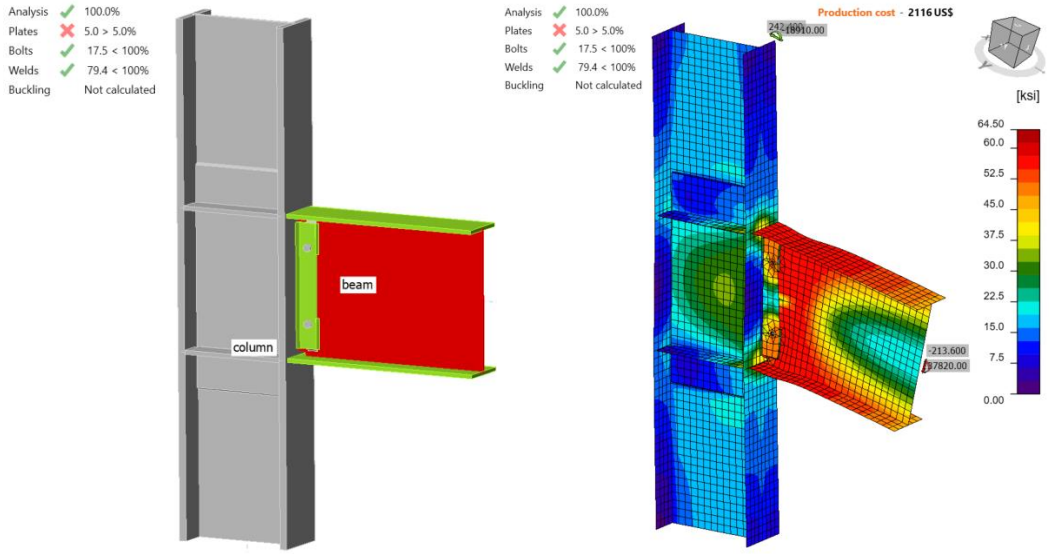

Figure 3.17: IDEA StatiCa model for Specimen C4

The six specimens were analyzed using IDEA StatiCa and their moment capacities at the column centerline were calculated by representing their test conditions. To compare the moment capacities with the ones calculated following the AISC 358 procedure, the moment capacities at the column face were calculated using Eq. 3.6 and presented in Table 3.5.

$$M_{y@foc} = M_{y@cc} - V\frac{d_c}{2} \quad (3.6)$$

where $M_{y@foc}$ is moment capacity at the column face, $M_{y@cc}$ is moment capacity at the column centerline, V is shear force, and d_c is depth of column.

Table 3.5: Moment capacity calculated by IDEA StatiCa

Specimen No	V (kips)	d_c (in.)	$M_{y@cc}$ (kips-in.)	$M_{y@foc}$ (kips-in.)
Baseline (T1)	167.70	17.1	29,700	28,266
T5	205.70	17.1	36,420	34,662
C1	212.60	18.3	37,650	35,705
C2	212.60	18.3	37,650	35,705
C3	213.20	29.0	37,750	34,659
C4	213.60	29.0	37,820	34,723

3.5. ABAQUS Analysis

In this section, the baseline model developed in Section 3.4.1 was constructed again using ABAQUS software (version 2022) for FE analysis and results were compared with IDEA StatiCa. The CAD model for the FE analysis was generated using the IDEA StatiCa's viewer platform. The two bolts and 5 weld lines (i.e., between the shear tab-beam web and shear tab-column flange) were then added manually to the assembly using the CAD interface in ABAQUS. The vertical load of 182.2 kips and the corresponding moment of 32,270 kips-in. (around Y axis) were applied to a defined reference point (i.e., RF_1) at the column centerline as shown in Figure 3.18. The analytical length of the column in IDEA StatiCa was 215.45 in. Therefore, to mimic the identical column length in ABAQUS, two other reference points (i.e., RF_2 and RF_3) were introduced 107.725 in. away from the center of the column along the Z axis in both directions (see Figure 3.18). These two reference points were fixed in all directions and were connected to the top and bottom faces of the column using the connector builder module in ABAQUS. In ABAQUS, the element size was chosen to be between 0.1–0.25 in. after mesh sensitivity analysis and a total of 240,417 elements were generated. The 3D stress, 8-node linear brick reduced integration (i.e., C3D8R) was selected as element type.

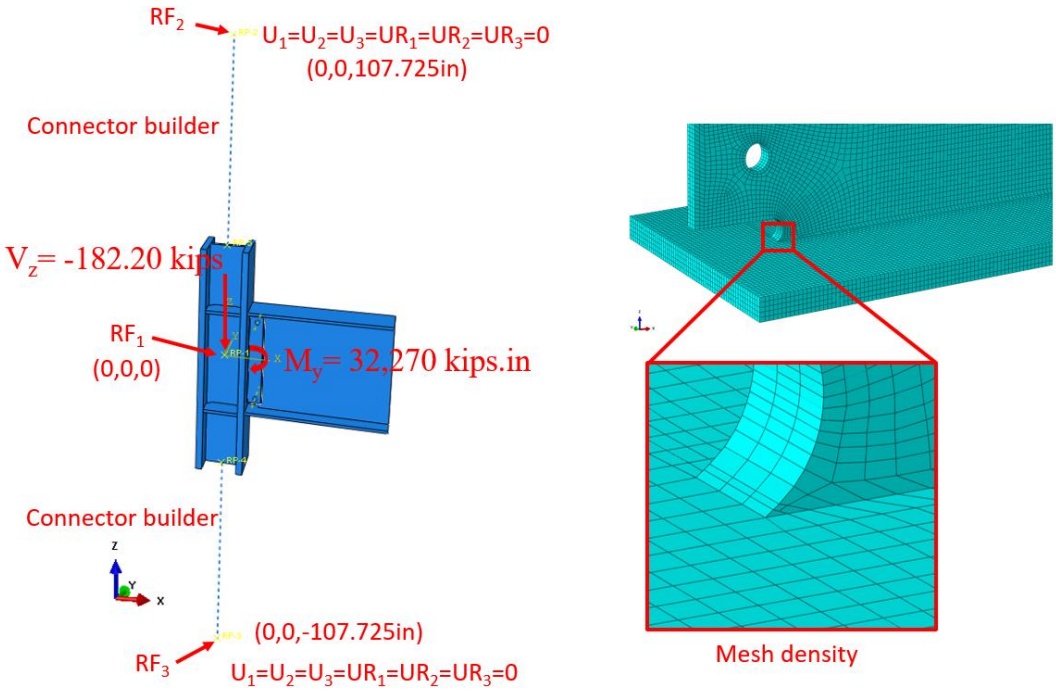

Figure 3.18: Model setup in ABAQUS

The tie constraint was applied between the weld lines and the attaching parts. The material behavior was modeled using bi-linear plasticity in ABAQUS. Other parameters, including density, elastic modulus, and Poisson's ratio were taken from the IDEA StatiCa materials library. The numerical simulation was carried out on four processors (Intel Xenon (R) CPU E5-2698 v4 @ 2.20GHz) and took approximately 155 minutes to finish. Figure 3.19 compares the predicted von-Mises stress between IDEA StatiCa and ABAQUS.

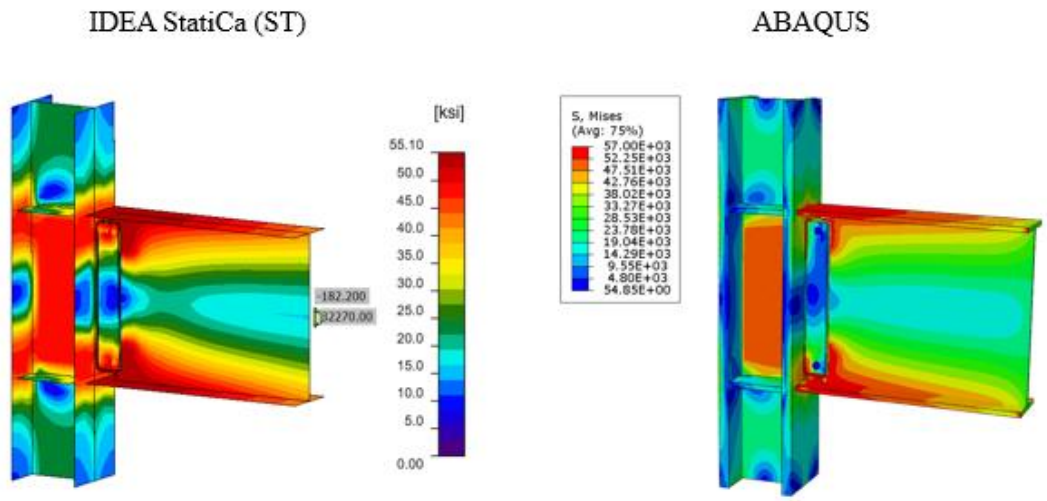

Figure 3.19: Comparison of the calculated von Mises stress between IDEA StatiCa and ABAQUS models

The maximum predicted stress in IDEA StatiCa was 55.90 ksi on the beam top flange (note that the IDEA StatiCa legend shows the design data) while the ABAQUS model shows a maximum stress of 56.5 ksi at the same location. The maximum stress of 57 ksi in the ABAQUS legend belongs to the front long weld line connecting the shear tab to the column. The slightly different stress distribution is likely due to the consideration of the length of the column in ABAQUS and the way that boundary conditions have been applied, utilization of finer mesh in the FE analysis, and the simplified CAD model in IDEA StatiCa. Note that the authors performed a routine mesh sensitivity analysis for the IDEA StatiCa model as well and some inconsistencies in the results were observed.

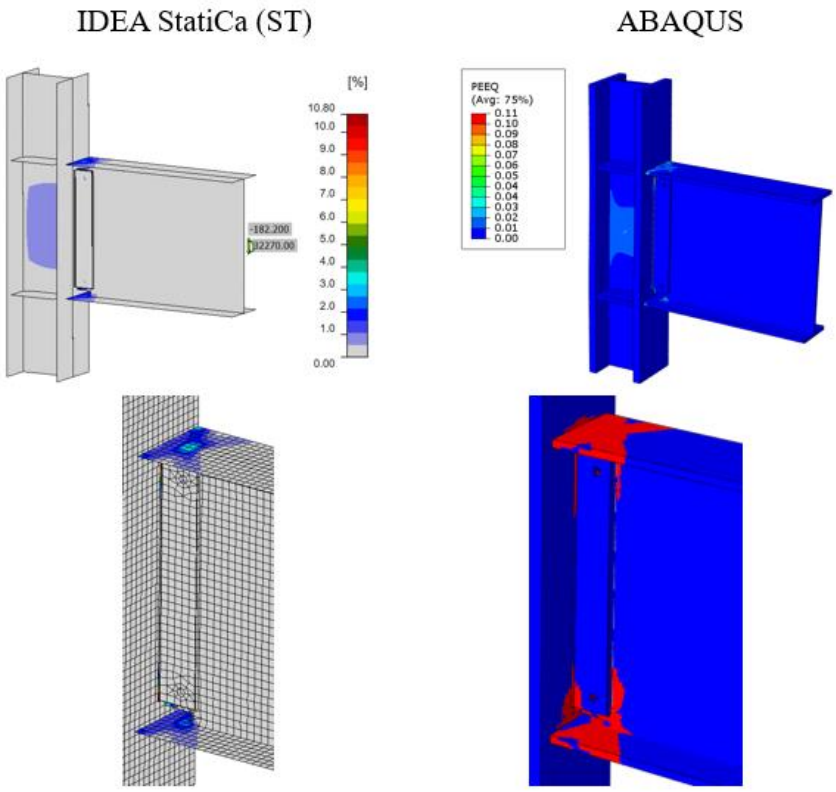

Figure 3.20: Comparison of the calculated plastic strain between IDEA StatiCa and ABAQUS models

The maximum calculated plastic strain in IDEA StatiCa and ABAQUS were 10.8% and 11%, respectively (both on the front weld line connecting the shear tab to the column). Also, the predicted plastic deformation region by IDEA StatiCa was consistent with the calculated yield map in ABAQUS (i.e., the bottom row in Figure 3.20). Figure 3.21 depicts the comparison of the moment-rotation curve between the two software with respect to the column centerline. Note that in Figure 3.21, to obtain the total rotation by IDEA StatiCa (shown by dashed orange line), the linear beam rotation at the column centerline was calculated using SAP2000 and then added to the default plastic rotation curve reported by IDEA StatiCa (shown by solid orange line). Both models offer comparable initial stiffness estimations. The minor discrepancy could be associated with the

difference in the element types (i.e., solid element in ABAQUS versus shell element in IDEA StatiCa) and the employment of the tie constraint in ABAQUS to represent the welds.

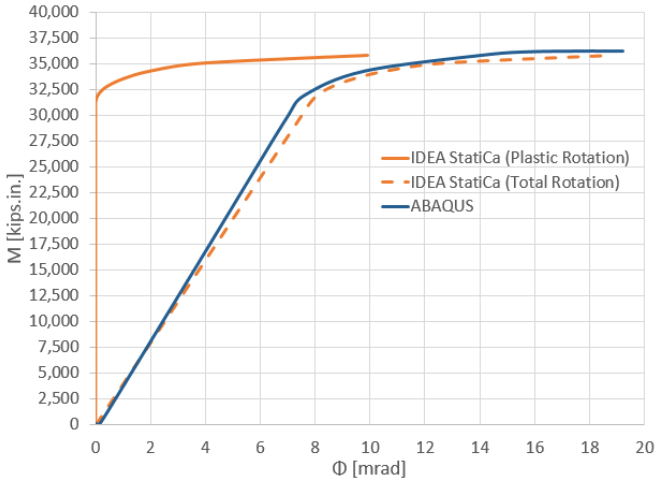

Figure 3.21: Moment-rotation comparison between IDEA StatiCa and ABAQUS

3.6 Summary and Comparison of Results

Experimental observations indicate that the baseline model failed due to the fracture occurred in the weld between the beam web and column flange. Similarly, IDEA StatiCa analysis indicated that the weld failed between the shear tab and column flange. Also, AISC design checks showed that this weld did not satisfy the beam web-to-column connection limitations outlined in Section 8.6 in AISC 358 (2016) (see Table 3.3). Moment-plastic rotation relationships measured during the experiment and computed using IDEA StatiCa analysis for the baseline model are compared in Figure 3.22. The moment capacity calculated following the AISC procedure at the column face was transferred to the column centerline using Eq. 3.6 since the moment-rotation comparison was performed at the column centerline, and it is shown in the same graph with the one calculated using IDEA StatiCa stress-strain analysis (Figure 3.5).

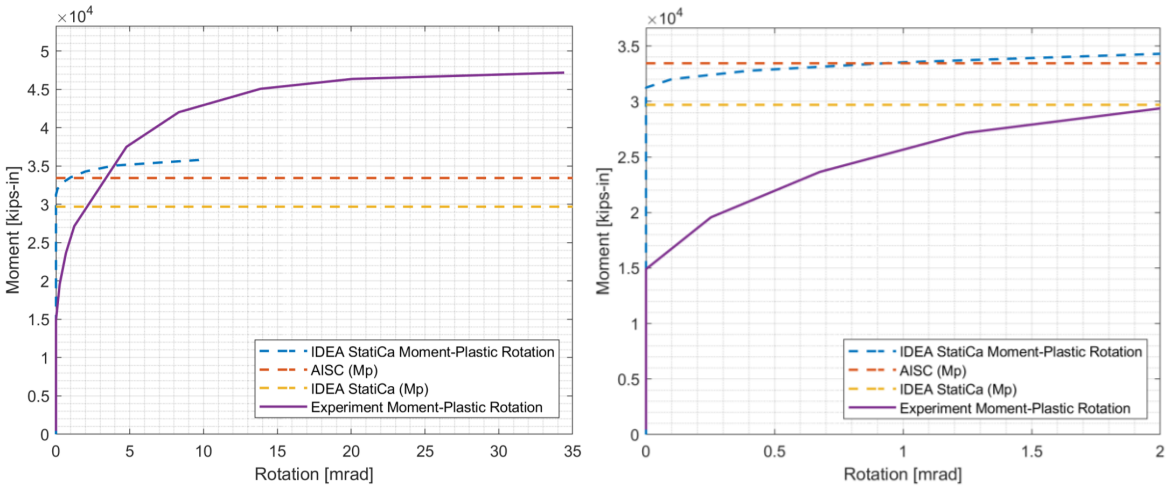

Figure 3.22: Moment-rotation comparison

Regarding the variation specimens (see Section 3.2), it was observed in the experimental study (Ricles et al., 2000) that the specimens failed due to severe local buckling and fracture in the beam flanges (Figures 3.6 through 3.10). Similarly, IDEA StatiCa analysis showed that specimens T5, C1, C2, C3, and C4 reached their capacities at beam web that reached 5% plastic strain limit (Figures 3.13 through 3.17). On the other hand, based on the AISC design checks, failure was expected to occur in the beam although some of the checks were not fully satisfied (e.g., continuity plate and weld access hole in Table 3.3). This is because of a slight difference in geometric requirements. The moment capacity of all specimens calculated using IDEA StatiCa (Table 3.5) and following AISC procedure (Table 3.4) are presented in Figure 3.23.

All moment strengths calculated from IDEA StatiCa (using actual or measured properties) are approximately 8% larger than those from AISC, except for the baseline model. This is reasonable because the AISC moment strength, M_p, are based on the design assumption that plastic hinge location is taken at the column face according to Section 8.7 in AISC 358 (2016). On the other hand, FEMA (2000) recommends plastic hinge location to be taken at half of the beam depth away from the column face for WUF-W moment connections. If the plastic hinge location was assumed to be a certain distance away from the column face, the additional moment due to the shear force on the plastic hinge to the column face should have been considered, thus larger moment capacities would have been calculated. The difference between the moment capacities calculated following AISC design procedure and using IDEA StatiCa can be attributed to the conservative assumption of AISC 358 for plastic hinge location of WUF-W moment connections.

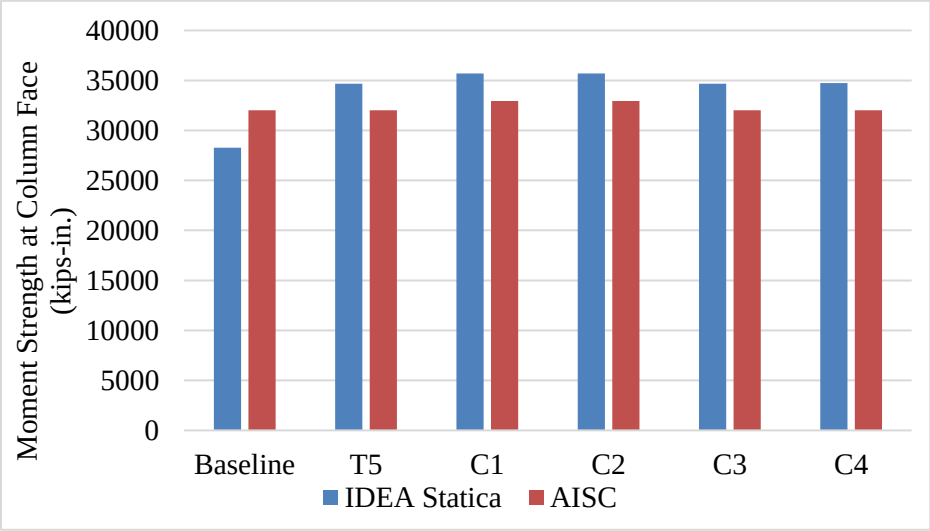

Figure 3.23: Moment capacity calculated by IDEA StatiCa and AISC procedure

References

AISC (2016), "Prequalified Connections for Special and Intermediate Steel Moment Frames for Seismic Applications, including Supplement No. 1," American Institute of Steel Construction ANSI/AISC 358-16, Chicago, Illinois.

Ricles, J.M., Mao, C., Lu, L.W. and Fisher, J.W. (2000), "Development and Evaluation of Improved Details for Ductile Welded Unreinforced Flange Connections," Report No. SAC/BD-00-24, SAC Joint Venture, Sacramento, CA.

FEMA (2000), Recommended Seismic Design Criteria for New Steel Moment-Frame Buildings, FEMA 350, Federal Emergency Management Agency, Washington, DC.

Chapter 4. Welded Unreinforced Flange-Bolted Web (WUF-B) Moment Connections

4.1. Introduction

Differently from the other moment connections covered in this study, welded unreinforced flange-bolted web (WUF-B) moment connection is permitted to be used only in ordinary moment frame (OMF) system. In this study, five tested and three developed WUF-B connections were investigated. Using IDEA StatiCa and following the AISC design procedure, flexural capacities of the eight connections were calculated, and the results were compared. One of the tested specimens was selected as a baseline model for the further investigation through Abaqus. Moment rotation curve was computed for the baseline model using both IDEA StatiCa and Abaqus, and the calculated curves were compared with the measured one presented in the test report. In addition, the effect of different bolt types was investigated in detail.

4.2 Experimental Study

Seven identical WUF-B moment connection pairs were assessed in accordance with the SAC Phase 2 Testing Protocol (SAC, 1997) by Lee et al. (1999) at Lehigh University as part of the SAC Phase II program. Five tested specimens were selected to be investigated in this study while one of them was chosen as a baseline model. The properties of the specimens are presented in Table 4.1. Baseline model consists of W24x68 beam and W14x120 column, six A325 slip critical (SC) bolts with a diameter of 7/8 in., 3/8-in.-thick shear plate, and 5/8-in.-thick continuity plate. Variation 1, variation 2, and variation 3 have identical beam W30x99, shear tab with a thickness of 1/2 in., continuity plate with a thickness of 3/4 in., and eight A325 slip critical (SC) bolts with a diameter of 1 in. whereas the sizes of columns are W14x145, W14x176, and W14x257, respectively. Variation 4 has W36x150 beam and W14x257 column, ten 1-in. diameter A325 bearing with threads excluded from shear planes, 5/8-in.-thick shear plate, and 1-in.-thick continuity plate.

Table 4.1: Properties of the WUF-B specimens (Lee et al., 1999)

Specimen no (Test ID)	Beam size	Column size	Shear tab	Bolts	Continuity plate thickness
Baseline (3.1)	W24x68	W14x120	18"x5"x3/8"	6×7/8-in. A325 SC	5/8 in.
Variation 1 (4.1)	W30x99	W14x145	24"x5"x1/2"	8×1-in. A325 SC	3/4 in.
Variation 2 (5.1)	W30x99	W14x176	24"x5"x1/2"	8×1-in. A325 SC	3/4 in.
Variation 3 (6.1)	W30x99	W14x257	24"x5"x1/2"	8×1-in. A325 SC	3/4 in.
Variation 4 (7.1)	W36x150	W14x257	30"x5"x5/8"	10-1-in. A325 X	1 in.

The length between the column supports is 144 in., and the distance from the column face to actuator is 134.9 in. The test setup and configurations of the five connections are presented in Figures 4.1 through 4.3.

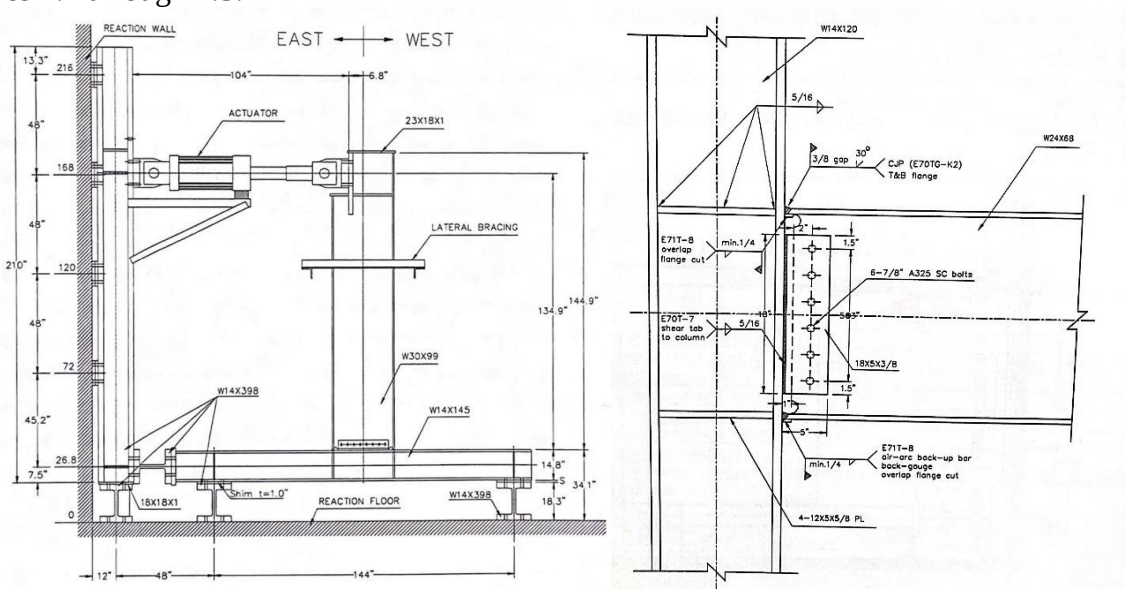

Figure 4.1: Left) Test setup; Right) configuration of baseline (Lee et al., 1999)

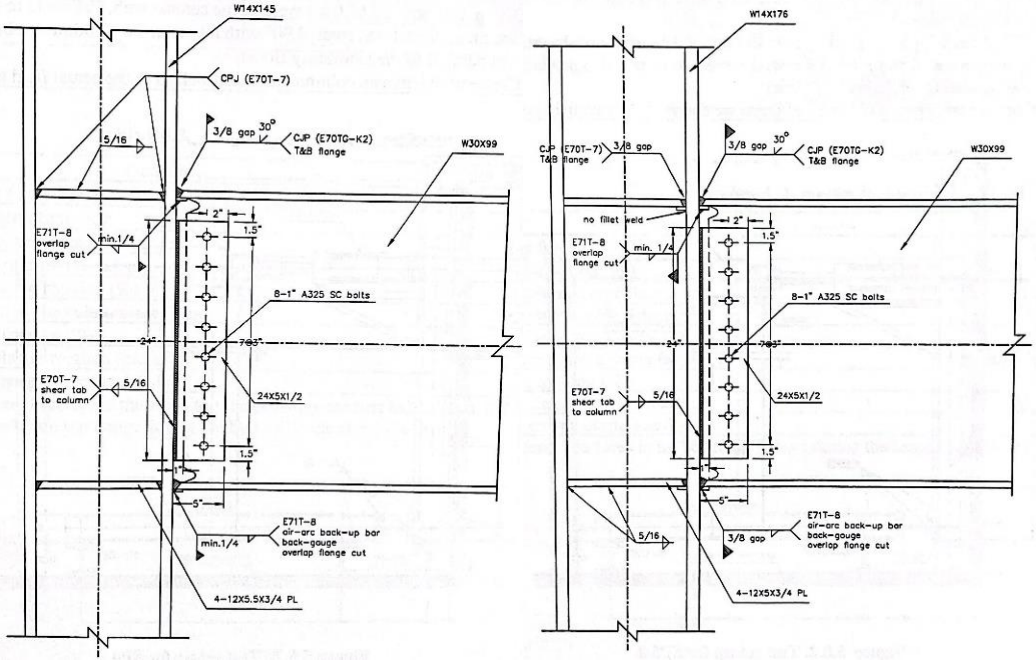

Figure 4.2: Left) Configuration of variation 1; Right) configuration of variation 2 (Lee et al., 1999)

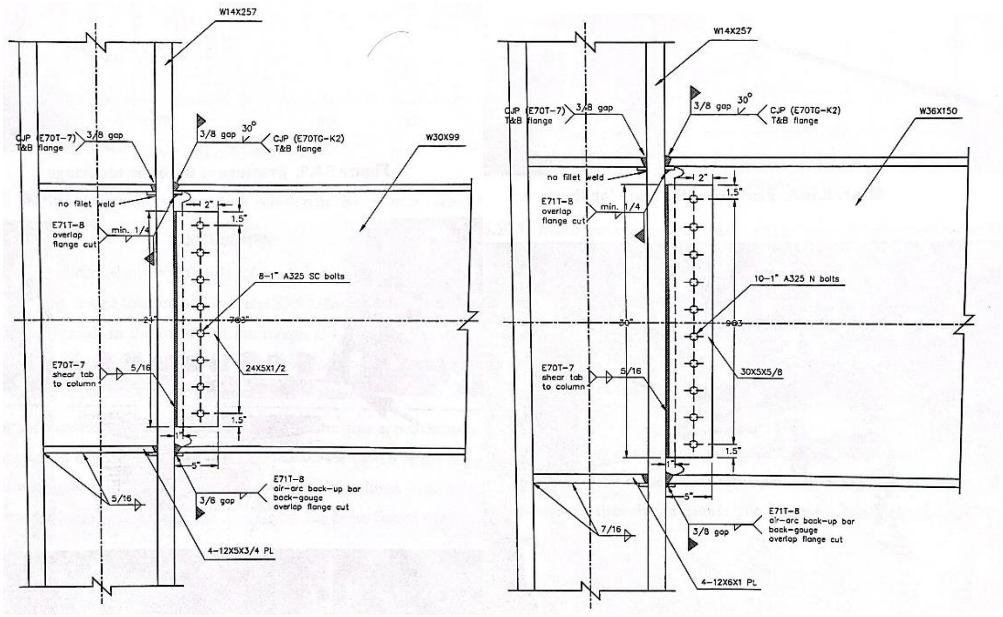

Figure 4.3: Left) Configuration of variation 3; Right) configuration of variation 4 (Lee et al., 1999)

The coupon test material properties for the beam flange, column flange, shear plate, and continuity plate are presented in Table 4.2.

Table 4.2: Measured material properties of selected WUF-B specimens (Lee et al., 1999)

Specimen no (Test ID)	Member	Yield stress (ksi)	Ultimate strength (ksi)
Baseline (3.1)	Beam	45.4	67.4
	Column	46.0	67.6
	Shear plate	46.6	70.4
	Continuity plate	51.6	73.4
Variation 1 (4.1)	Beam	51.2	69.8
	Column	47.7	69.0
	Shear plate	41.6	64.3
	Continuity plate	43.5	64.0
Variation 2 (5.1)	Beam	51.2	69.8
	Column	51.9	73.6
	Shear plate	41.6	64.3
	Continuity plate	43.5	64.0
Variation 3 (6.1)	Beam	49.8	68.9
	Column	48.8	72.9
	Shear plate	41.6	64.3
	Continuity plate	43.5	64.0
Variation 4 (7.1)	Beam	41.8	63.6
	Column	48.3	70.6
	Shear plate	51.6	73.4

	Continuity plate	44.7	68.5

According to the experimental tests, the panel zone of the baseline model started to yield at 0.75% drift cycles. Yielding in the beam flanges started at 1% drift cycles, and tearing out of the beam flange was observed at the second cycle at 3% drift (see Figure 4.4). Similarly, the first shear yielding was observed in the panel zone of variation 1 at 0.5 drift cycles. The yielding in the panel zone was spread out during 1.5 drift cycles. During 3% drift cycles, plastic hinge occurred in this zone and fracture in the column k-zone was observed (see Figure 4.5). Regarding variation 2, it was reported that the panel zone started to yield at 1% drift cycles, and it spread out during further cycles. During 2% drift cycles, the beam flanges yielded. Small crack occurred in the beam flanges at 3% drift cycles and fracture was observed in the beam top flange at the first cycle of 4% drift (see Figure 4.6).

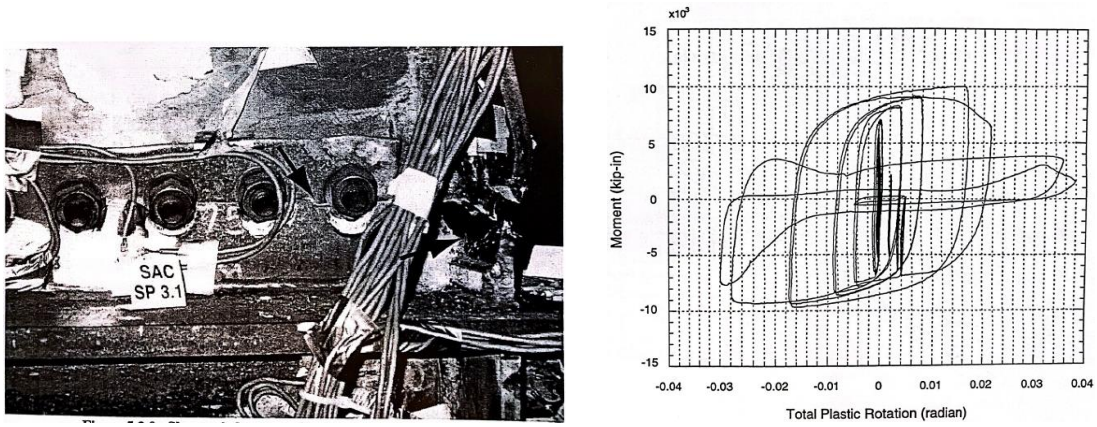

Figure 4.4: Left) Baseline model after testing; Right) moment-total plastic rotation relationship (Lee et al., 1999)

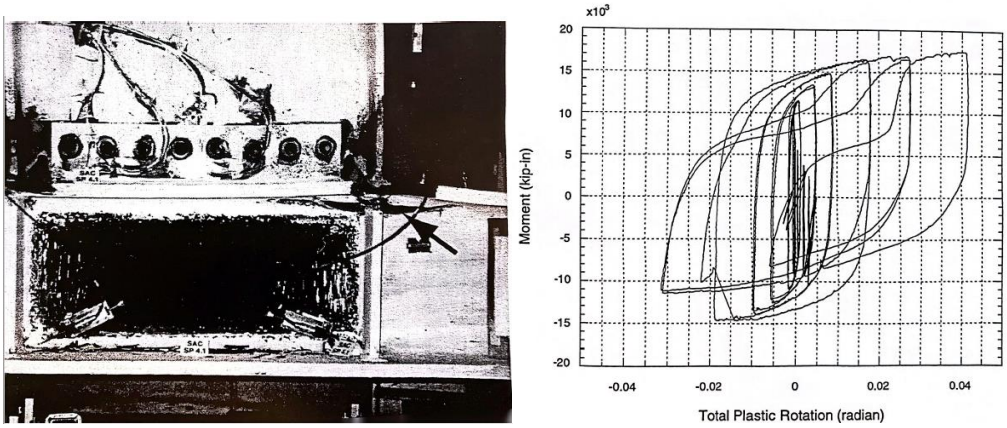

Figure 4.5: Left) Variation 1 after testing; Right) moment-total plastic rotation relationship (Lee et al., 1999)

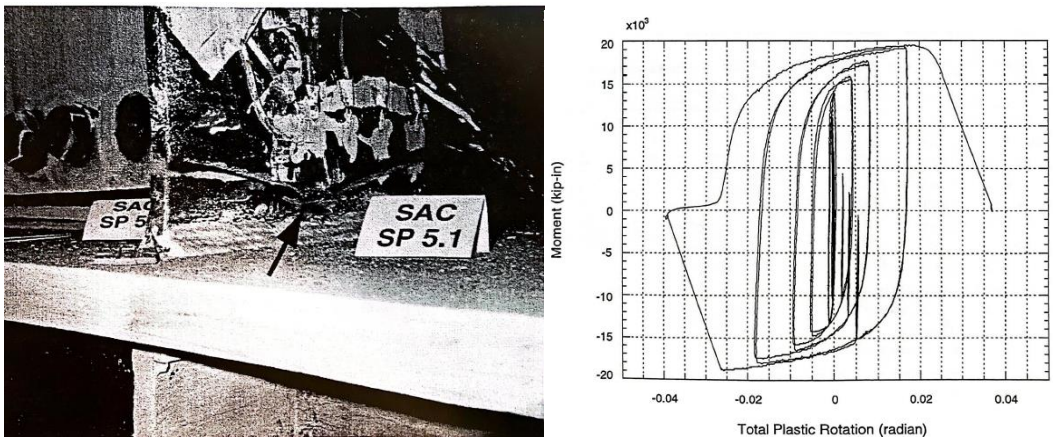

Figure 4.6: Left) Variation 2 after testing; Right) moment-total plastic rotation relationship (Lee et al., 1999)

Differently from the first three test specimens, the first yielding formed in the beam flanges during 1% drift cycles, and small cracks in this area were observed at 1.5 drift cycles during the test of variation 3. The panel zone started yielding during 2% drift cycles and ductile tearing was observed in the beam top flange at 2% drift cycles (see Figure 4.7).

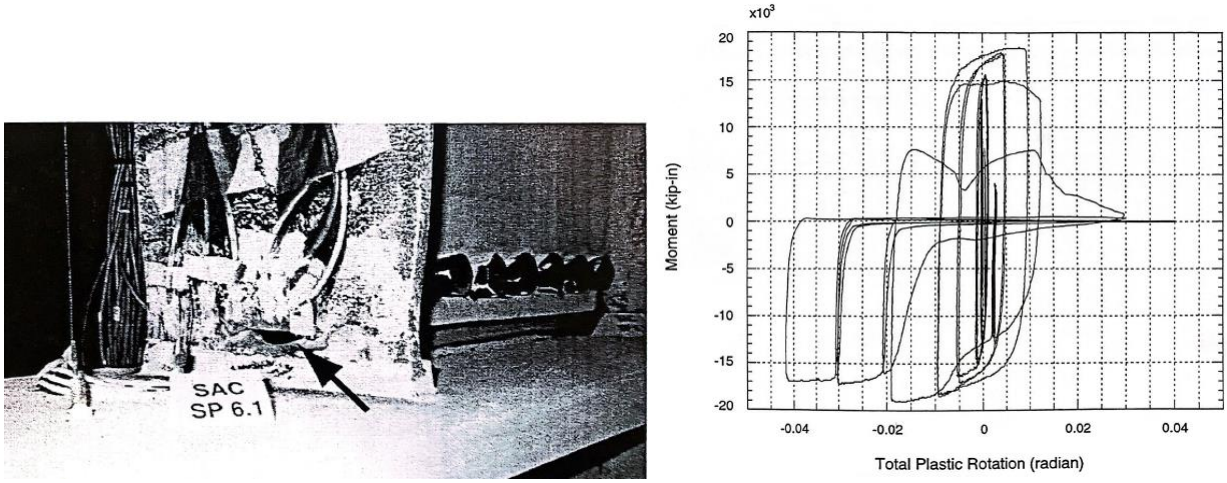

Figure 4.7: Left) Variation 3 after testing; Right) moment-total plastic rotation relationship (Lee et al., 1999)

For variation 4, it was stated in the test report that first yielding occurred in the panel zone at 0.75 drift cycles. The beam flanges yielded at 1% drift cycles, and small cracks were observed near the weld access hole of beam flanges at 2% drift cycles. Fracture in the beam flanges were observed during the 3% drift cycles (see Figure 4.8).

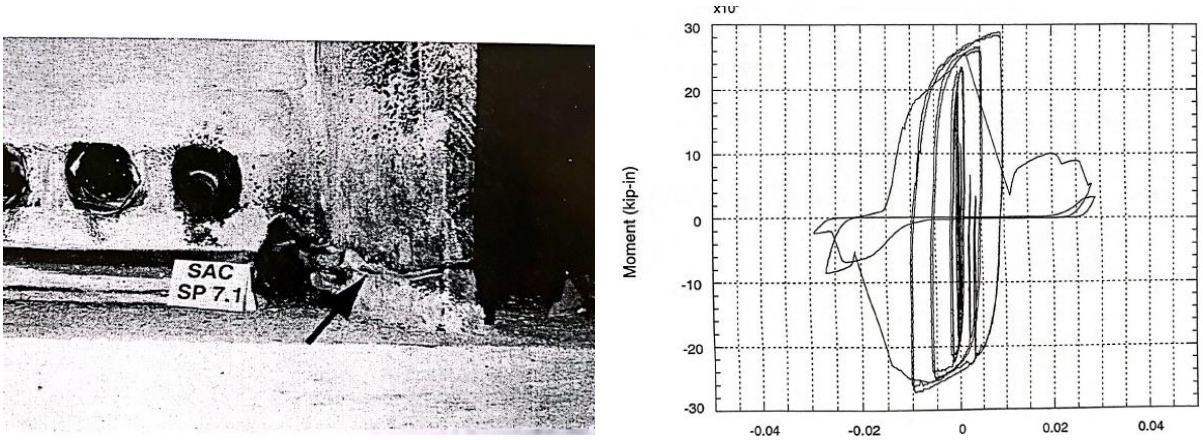

Figure 4.8: Left) Variation 4 after testing; Right) moment-total plastic rotation relationship (Lee et al., 1999)

4.3 Code Design Calculations

The code-based design checks were performed and failure modes were determined for WUF-W moment connections following the requirements of AISC 341 (2016) and AISC 360 (2016). According to Section D.2 in AISC 341, bolted connections with a minimum slip coefficient of 0.30 can be designed as pretensioned bearing joints. Since the pre-analysis of the tested specimens performed using IDEA StatiCa showed that the governing limit state is *bolt strength of slip critical joints* for the baseline model, variation 2, and variation 3, three additional variations were developed from those tested connections by switching the bolt types from slip critical (SC) to bearing type with threads excluded from the shear plane. The number of developed three specimens were named by adding ".X" to the initial names, which were presented in Table 4.2, (e.g., baseline model.X from baseline model) while the names of the tested three specimens were updated by adding ".SC" to their initial names (e.g., baseline model.SC from baseline model, see Table 4.3 for the updated names).

The following design checks were identified for WUF-B moment connections from AISC 341 (2016) and AISC 360 (2016).

- Check beam flexural strength (AISC 360 (2016), Eq. F2-1)
- Check column flexural strength (AISC 360 (2016), Eq. F2-1)
- Check panel zone shear strength (AISC 341 (2016), J10-11)
- Check continuity plate requirements (AISC 341 (2016), Sec. E3.6f)
- Check shear yielding on beam (AISC 360 (2016), Eq. J4-3)
- Check weld strength between shear tab and column (AISC 360 (2016), Eq. J4-2)
- Check bolt shear strength (AISC 360 (2016), Eq. J3-6a)
- Check beam flange to column flange (AISC 341 (2016), Sec E1.6)
- Weld access hole (AWS (2016) D1.8/D1.8M)

Since bolt strength of the test specimens was not measured and provided in the report, A325 slip critical bolts were assumed to have class A surfaces with slip coefficient of 0.3, and the nominal values given by AISC Table J3 were used for the nominal tensile strength (f_{nt} = 90 ksi) and shear strength (f_{nv} = 68 ksi) for A325 bearing type bolts. The summary of design checks is presented in Table 4.3.

Table 4.3: Design checks for WUF-W moment connections

AISC Design Checks	Baseline Model.SC	Variation 1	Variation 2.SC	Variation 3.SC	Variation 4	Baseline Model.X	Variation 2.X	Variation 3.X
Beam flexural strength	OK	OK	OK	OK	OK	OK	OK	OK
Column flexural strength	OK	OK	OK	OK	OK	OK	OK	OK
Bolt shear strength	Not OK	Not OK	Not OK	Not OK	OK	OK	OK	OK
Panel zone shear strength	Not OK	Not OK	OK	OK	OK	Not OK	OK	OK
Beam shear strength	OK	OK	OK	OK	OK	OK	OK	OK
Weld strength between shear tab and column	OK	OK	OK	OK	OK	OK	OK	OK
Beam flange to column flange connection	OK	OK	OK	OK	OK	OK	OK	OK
Continuity plate requirements	Not OK	Not OK	Not OK	Not OK	Not OK	Not OK	Not OK	Not OK
Access hole requirements	Not OK	Not OK	Not OK	Not OK	Not OK	Not OK	Not OK	Not OK

Failure mode of the specimens can be predicted by calculating strength of the following limit states and determining the controlling one by comparing them with the required strength calculated from structural analysis that represents test setup condition:

5- Plastic flexural strength of column
6- Plastic flexural strength of beam
7- Flexural strength corresponding to inelastic shear strength capacity of panel zone

Plastic moment strength of beam and column at plastic hinge location ($M_{by@ph}$ and $M_{cy@ph}$) are calculated as follows:

$$M_{b@ph} = F_{yb} Z_{bx} \quad (4.1)$$

$$M_{c@ph} = F_{yc}Z_{cx} \tag{4.2}$$

where F_{yb} is yield stress of beam, Z_{bx} is plastic section modulus of beam, F_{yc} is yield stress of column, and Z_{cx} is plastic section modulus of column. Inelastic panel zone shear strength, R_{npz}, is calculated with an assumption that required axial strength of column is less than or equal to 75% of its axial yield strength in accordance with Section J10 in AISC 360 (2016) as follows:

$$R_{npz} = (1.0)(0.6)F_{yc}d_c t_{cw}\left(1 + \frac{3b_{cf}{t_{cf}}^2}{d_c d_b t_{cw}}\right) \tag{4.3}$$

where d_c is column depth, t_{cw} is thickness of column web, b_{cf} is width of column flange, t_{cf} is thickness of column flange, d_b is beam depth.

Flexural strength capacity of panel zone at column centerline, M_{npz}, can be calculated by considering story shear of column acting in opposite direction as shown in Figure 4.9 as follows:

$$M_{npz} = (R_{npz} + V_c)(d_b - t_{bf}) \tag{4.4}$$

where V_c is shear force of column, d_b is beam depth, t_{bf} is thickness of beam flange. Flexural strength capacity of panel zone at column face, $M_{npz@foc}$, can be calculated by subtracting additional moment due to gravity load from column face to column centerline as follows:

$$M_{npz@foc} = M_{npz} - V_{grav}\frac{d_c}{2}$$

where V_{grav} is gravity force at the plastic hinge location of beam.

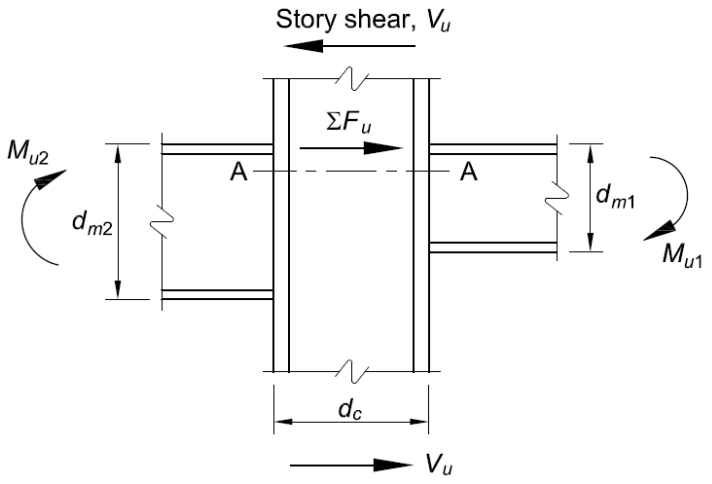

Figure 4.9: Forces in panel zone (AISC 360, 2016)

To calculate the response of specimens, SAP2000 model representing the test setup was developed. It is assumed that column supports are pin connections. For the baseline model, developed

SAP2000 model and the calculated moment diagram corresponding to 10 kips vertical load at the beam end are illustrated in Figure 4.10.

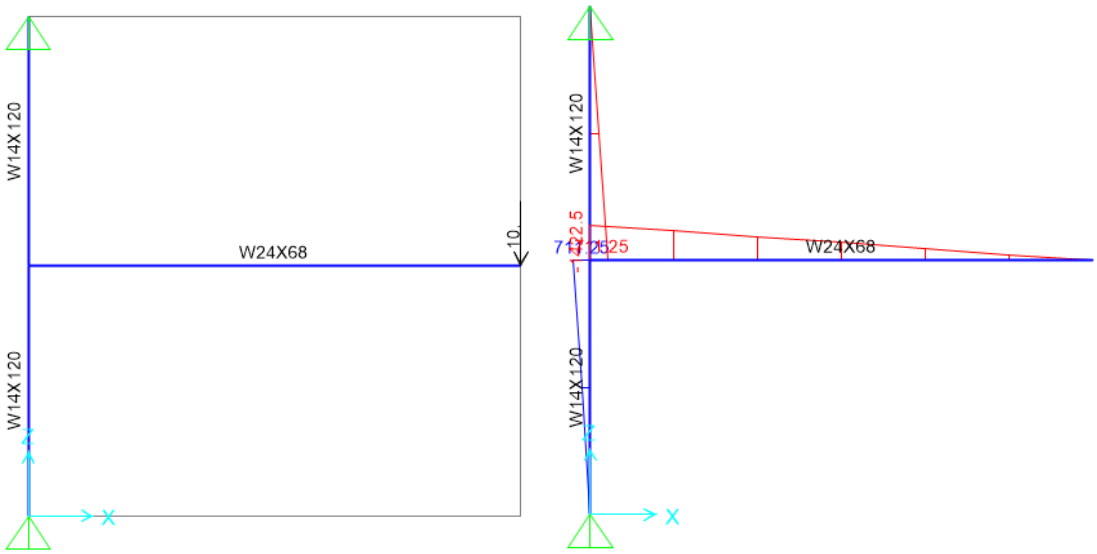

Figure 4.10: Left) SAP2000 model; Right) Moment diagram

Moment responses of the beam and column at their centerlines ($M_{bu@cc}$ and $M_{cu@cc}$) were obtained from SAP2000 model, and the corresponding moment values at the member faces (i.e., $M_{bu@foc}$ and $M_{cu@foc}$) were calculated as follows:

$$M_{bu@foc} = M_{bu@cc} - V_{ub}\frac{d_b}{2} \tag{4.5}$$

$$M_{cu@foc} = M_{cu@cc} - V_{uc}\frac{d_c}{2} \tag{4.6}$$

where V_{ub} is calculated shear force of the beam and V_{uc} is calculated shear force of the column. It is assumed that the plastic hinge in the beam forms at the column face, and the plastic hinge in the column occurs in the beam face. Calculated flexural strength capacities of the panel zone and beam at the column face (i.e., $M_{npz@foc}$ and $M_{b@ph}$), and the flexural strength capacity of the column at the beam face ($M_{c@ph}$) are presented in Table 4.4. Also, SAP2000 analysis was performed for each connection in a way that beam reaches its plastic moment strength capacity due to the applied shear force at the end of the beam which represents actuator. Calculated moment responses of the column and beam at the member faces (i.e., $M_{cu@foc}$, $M_{bu@foc}$) are also presented in Table 4.4. These values were compared with each other and the controlling limit state was determined.

Table 4.4: Summary of capacity calculations

Specimen No	$M_{b@ph}$ [kip-in]	$M_{c@ph}$ [kip-in]	$M_{npz@foc}$ [kip-in]	$M_{bu@foc}$ [kip-in]	$M_{cu@foc}$ [kip-in]	Controlling limit state [kip-in]

Baseline.SC	8,036	9,752	**7,410**	8,036	3,537	7,410
Variation 1	15,974	12,402	**11,831**	15,974	6,687	11,831
Variation 2.SC	**15,974**	16,608	16,676	15,974	6,697	15,974
Variation 3.SC	**15,538**	23,766	25,934	15,538	6,541	15,538
Variation 4	**24,286**	23,522	30,938	24,286	9,670	24,286
Baseline.X	8,036	9,752	**7,410**	8,036	3,537	7,410
Variation 2.X	**15,974**	16,608	16,676	15,974	6,697	15,974
Variation 3.X	**15,538**	23,766	25,934	15,538	6,541	15,538

Failure modes of the baseline model.SC, variation 1, and baseline model.X are panel zone strength while plastic flexural strength of beam are governing limits for the rest of the specimens.

4.4 IDEA StatiCa Analysis

The eight WUF-B moment connections described in the previous section were modelled in IDEA StatiCa with the purpose of simulating the behavior of the experiments. The measured coupon test material properties provided in Lee et al. (1999) were used in the IDEA StatiCa software and the resistance factors were set to 1.0. Using the stress-strain analysis type in IDEA StatiCa (i.e., EPS), the moment capacities and failure modes of the connections were identified. For the baseline model, the moment-rotation relationship was calculated using the connection stiffness analysis type (i.e., ST) in IDEA StatiCa software.

4.4.1 Analysis of Baseline.SC Model

The IDEA StatiCa model was developed for the baseline.SC model using measured material properties (Table 4.2). The overstrength coefficients, R_y and R_t, and all LRFD resistance factors were set to 1.0. To obtain the loads at the column centerline, a beam-column frame model was created in SAP2000 with the lengths of the column and beam in the test setup (See Figure 4.10). Pinned connections were assigned at both ends of column, and a shear force of 10 kips was applied at a distance of 134.9 in. away from the face of the column. The calculated nodal loads were applied to the IDEA StatiCa model at the beam position equal to zero (column centerline) by switching on the "loads in equilibrium" option. For the capacity calculation, the loads were gradually increased until any of the following is achieved:

7) 5% plastic strain in plates (beam, column, shear tab, continuity plate)
8) 100% strength capacity in bolts
9) 100% strength capacity in welds

When the shear force and the corresponding moment values reached 47.60 kips and 6,770 kips-in., respectively, bolt strength capacity was achieved and the calculated average plastic strain in beam flanges is 3.2% (Figure 4.11). Using "ST" analysis, moment-rotation relationship was

calculated and is shown in Figure 4.12. Note that in “ST” analysis, column is fixed at both ends, which may lead to differences between the bending resistance obtained by “EPS” analysis with loads in equilibrium.

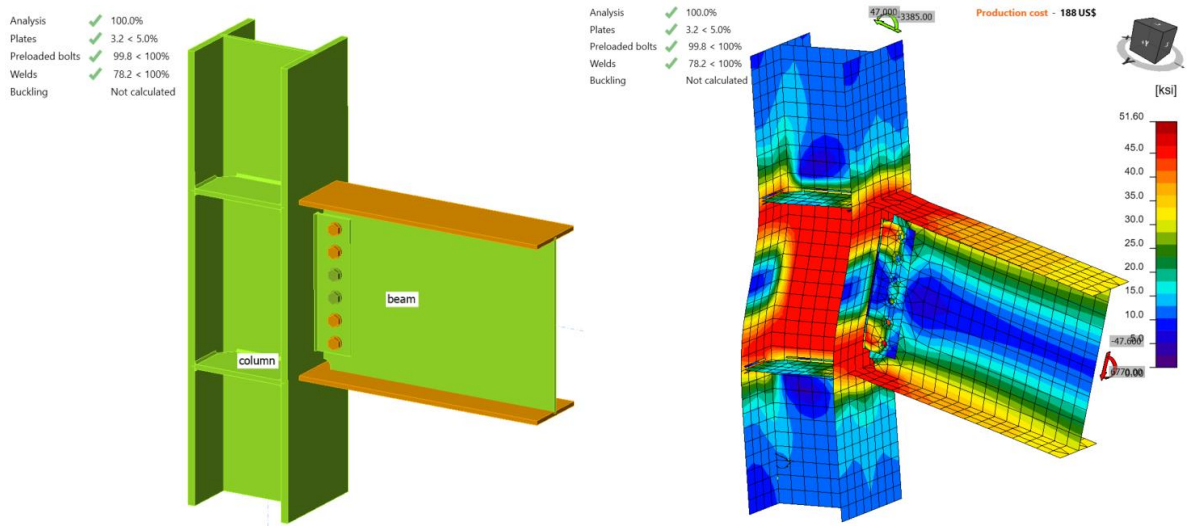

Figure 4.11: IDEA StatiCa model for Baseline.SC model under the moment of 6,770 kips-in.

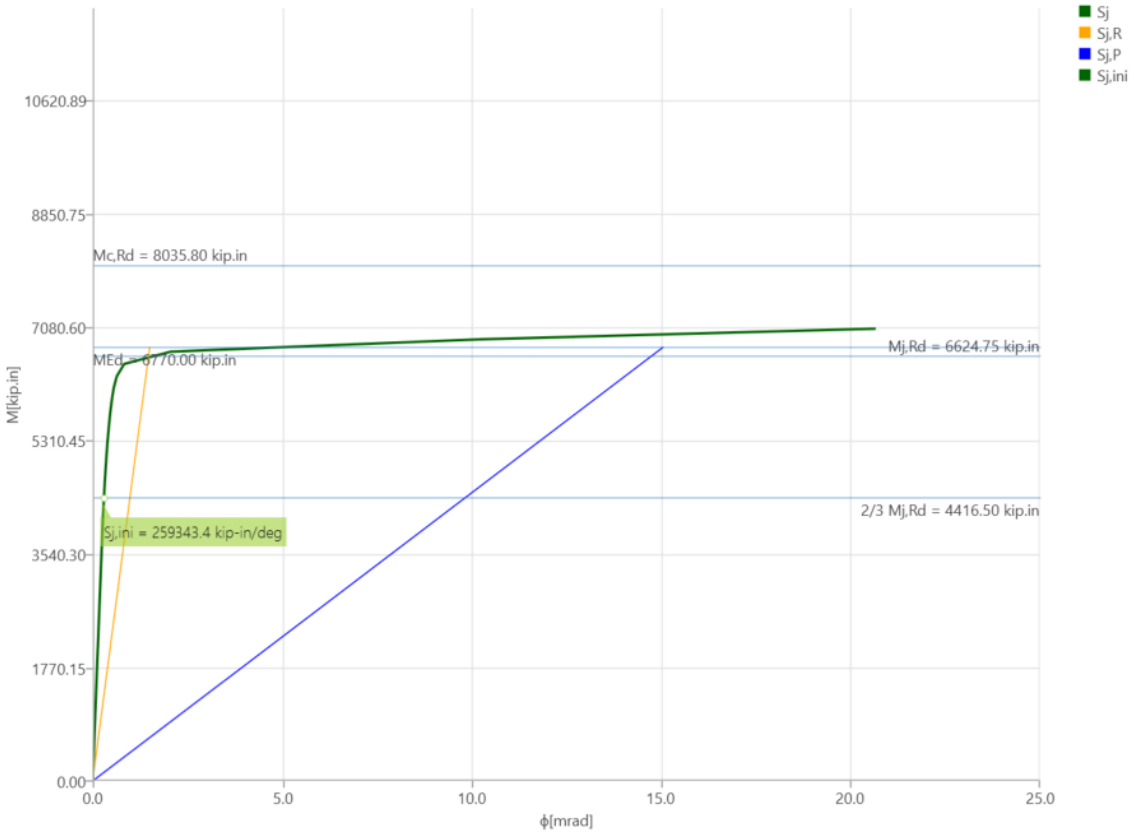

Figure 4.12: Moment-rotation relationship for baseline.SC model

4.4.2 Analysis of Variation 1

Following the same procedure described for the baseline.SC model, IDEA StatiCa model was developed for the variation 1 with slip-critical bolts. It was observed from the incremental loading that when the shear force and the corresponding moment were 82.20 kips and 11,700 kips-in., respectively, the beam web reached 5% plastic strain limit while 4.6% and 4.0% plastic strains were achieved in the beam flanges and column web, respectively (Figure 4.13).

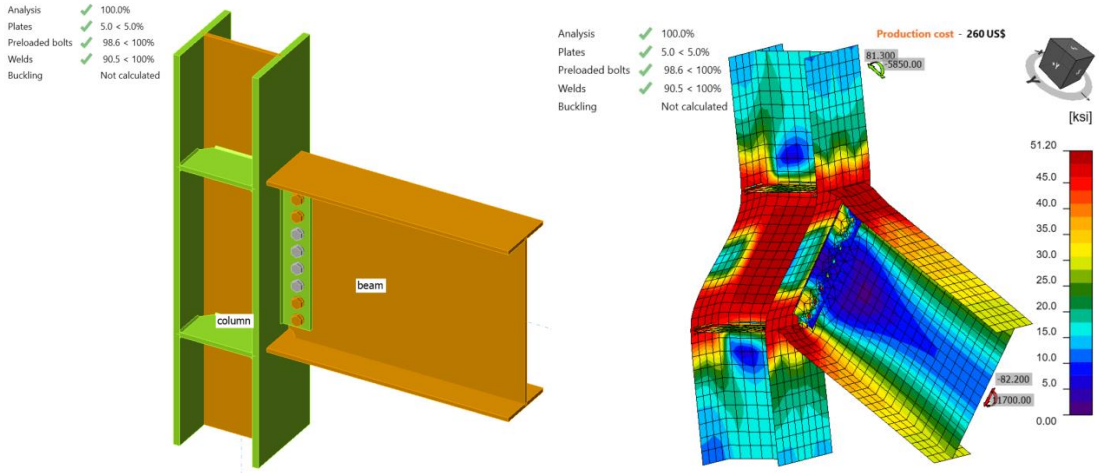

Figure 4.13: IDEA StatiCa model for variation 1 under the moment of 11,700 kips-in.

4.4.3 Analysis of Variation 2.SC

Following the same procedure described in the previous two sections, IDEA StatiCa analysis was performed for variation 2.SC. It was observed that strength capacity of bolts was reached when the shear force and the corresponding moment were 90.0 kips and 12,800 kips-in., respectively (Figure 4.14).

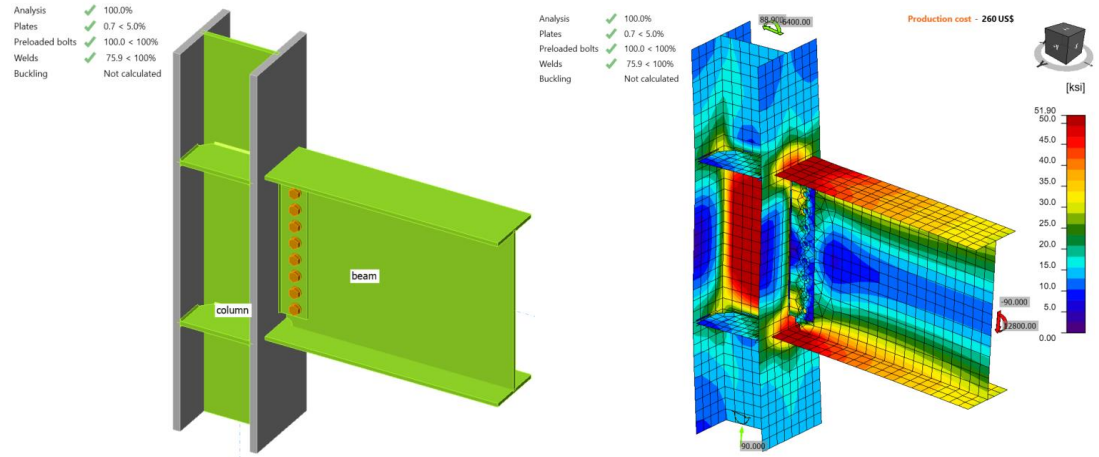

Figure 4.14: IDEA StatiCa model for variation 2 under the moment of 12,800 kips-in.

4.4.4 Analysis of Variation 3.SC

Following the same procedure, the flexural strength capacity of variation 3.SC was obtained using IDEA StatiCa. When the shear force and the corresponding moment reached 87.90 kips and 12,500 kip-in., respectively, strength capacity of the slip critical bolts was achieved (Figure 4.15).

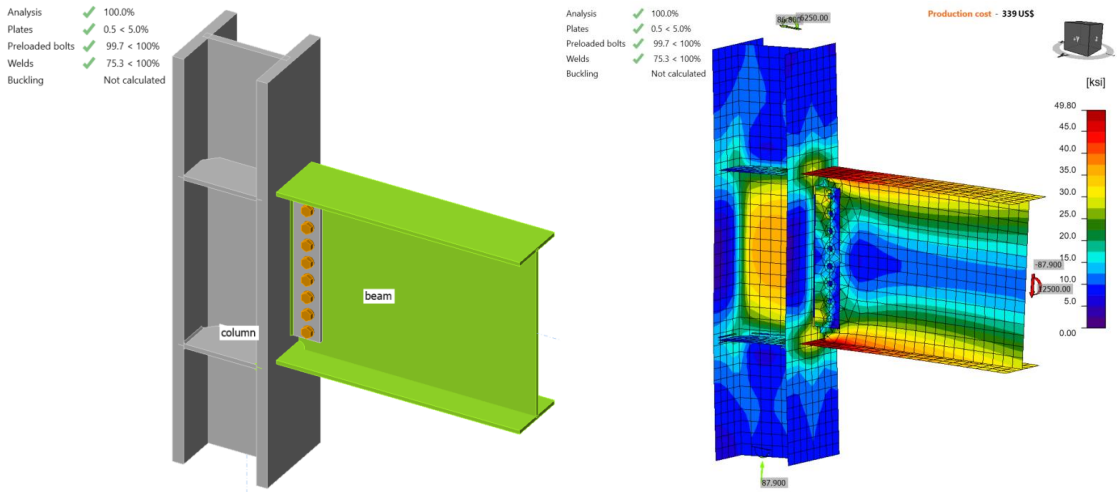

Figure 4.15: IDEA StatiCa model for variation 3 under the moment of 12,500 kips-in.

4.4.5 Analysis of Variation 4

IDEA StatiCa analysis was performed for variation 4 following the same procedure. IDEA StatiCa analysis showed that 5% plastic strain limit was reached in the beam web and 3.8% plastic strain was calculated in the top flange of beam when the shear force of 156.60 kips and the corresponding moment of 22,270 kips-in. were reached (Figure 4.16).

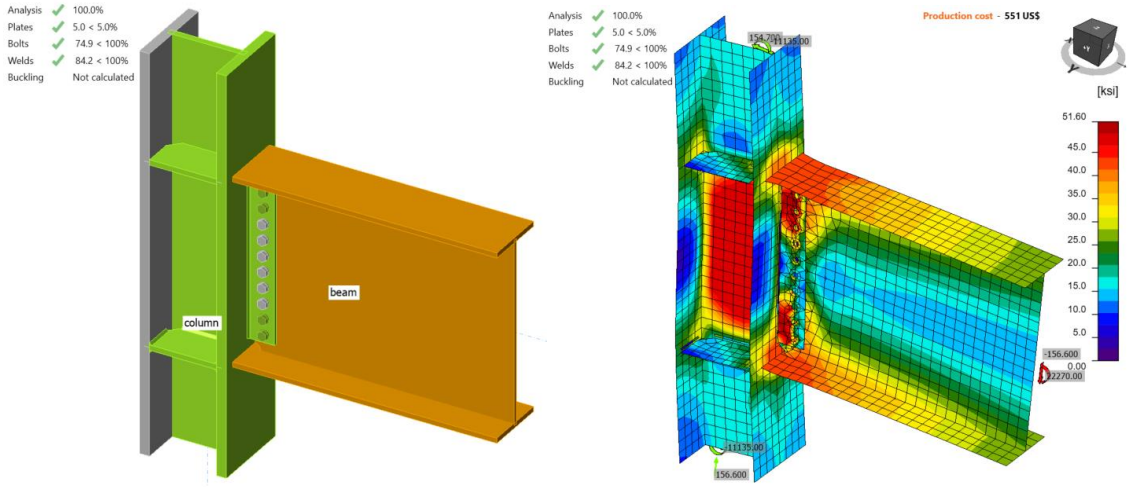

Figure 4.16: IDEA StatiCa model for variation 4 under the moment of 22,270 kips-in.

4.4.6 Analysis of Baseline.X Model

IDEA StatiCa model for baseline model.X was developed from the baseline model.SC by changing the bolt types from slip critical to bearing bolts. The same procedure is followed, and the flexural capacity of the specimen was calculated. It was observed that 5% plastic strain was calculated in top flange of beam when shear force of 48.00 kips and the corresponding moment of 6,830 kip-in. were reached (see Figure 4.17). This is XX% higher than for Baseline.SC model.

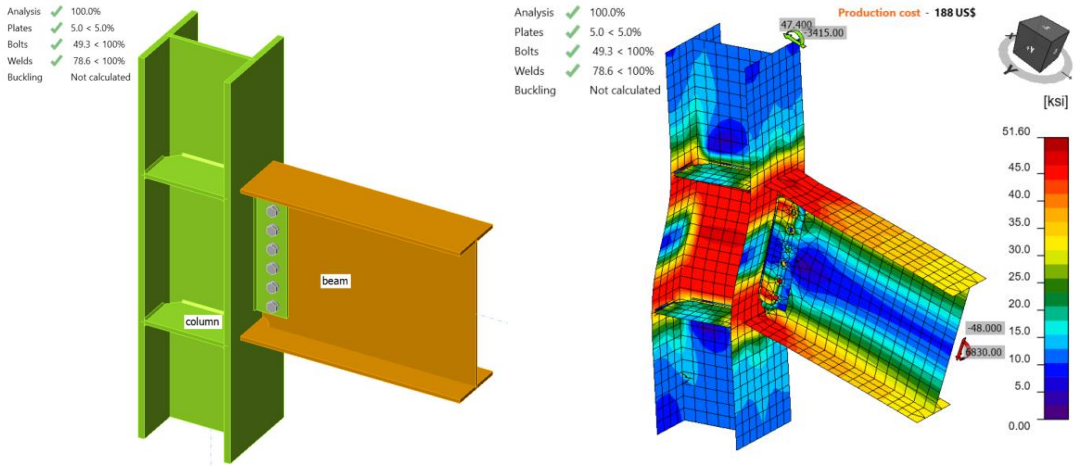

Figure 4.17: IDEA StatiCa model for baseline.X model under the moment of 6,830 kips-in.

4.4.7 Analysis of Variation 2.X

IDEA StatiCa model for variation 2.X was developed from variation 2.SC by switching the bolt type. It was observed that 5% plastic strain was achieved in top beam web when the shear force of 97.00 kips and the corresponding moment of 13,800 kip-in. were applied (see Figure 4.18). Also, 4.8% plastic strain was calculated in the top flange of beam. This is XX% higher than for 2.SC model.

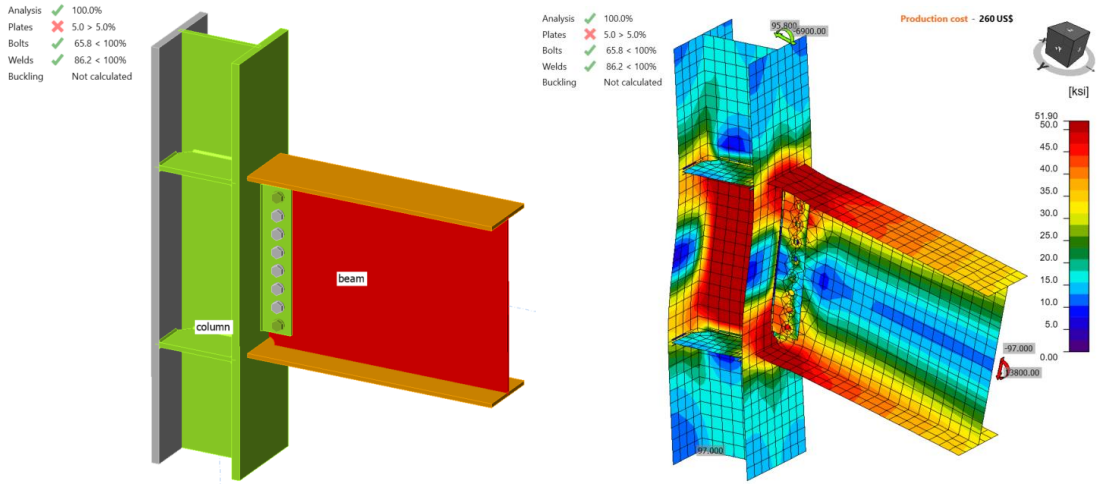

Figure 4.18: IDEA StatiCa model for variation 2.X model under the moment of 13,800 kips-in.

4.4.8 Analysis of Variation 3.X

IDEA StatiCa model for variation 3.X was developed from variation 3.SC by following the same steps explained in the previous two sections. It was observed that 5% plastic strain limit was achieved in the beam web while 4.9% plastic strain was calculated in the top flange of the beam when the shear force and the corresponding moment reached 98.20 kips and 13,970 kip-in., respectively (see Figure 4.19). This is XX% higher than for 3.SC model.

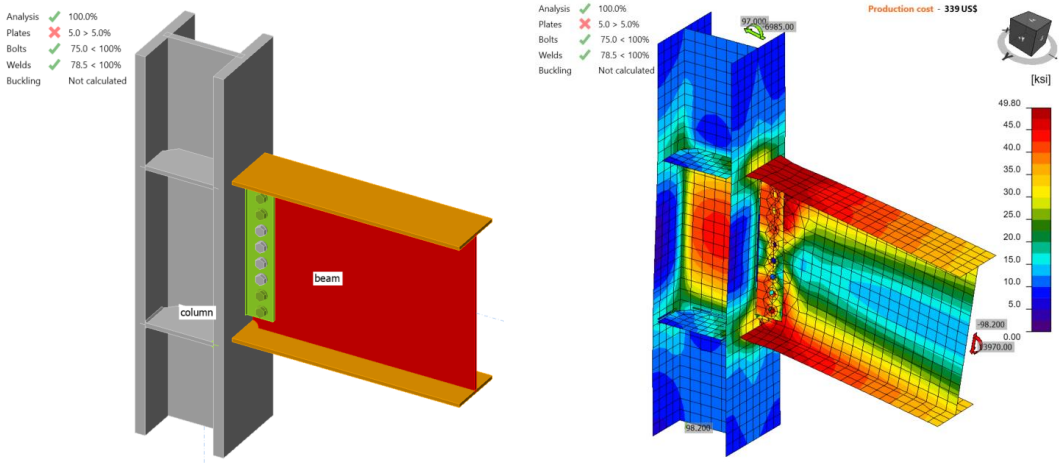

Figure 4.19: IDEA StatiCa model for variation 3.X under the moment of 13,970 kips-in.

Eight WUF-W moment connections were analyzed using IDEA StatiCa and their moment capacities at the column centerline were calculated. Moment capacities at the column face were calculated using Eq. 4.7 and are presented in Table 4.5.

$$M_{y@foc} = M_{y@cc} - V\frac{d_c}{2} \tag{4.7}$$

where $M_{y@foc}$ is moment capacity at the column face, $M_{y@cc}$ is moment capacity at the column centerline, V is shear force, and d_c is depth of column.

Table 4.5: Moment capacities calculated by IDEA StatiCa

Specimen No	$M_{y@cc}$ (kips-in.)	$M_{y@foc}$ (kips-in.)
Baseline.SC	6,770	6,425
Variation 1	11,700	11,091
Variation 2.SC	12,800	12,116
Variation 3.SC	12,500	11,779
Variation 4	22,270	20,986
Baseline.X	6,830	6,482
Variation 2.X	13,800	13,063
Variation 3.X	13,970	13,165

4.5. ABAQUS Analysis

In this section, the baseline model developed in Section 4.4.1 was constructed again using ABAQUS software (version 2022) for FE analysis and results were compared with IDEA StatiCa. The CAD model for the FE analysis was generated using the IDEA StatiCa's viewer platform. The six bolts and 28 weld lines that connected the entire assembly were then added manually using the CAD interface in ABAQUS. The vertical load of 47.6 kips and the corresponding moment of 6,770 kips-in. (around Y axis) were applied to a defined reference point (i.e., RF_1) at the column centerline as shown in Figure 4.20. The analytical length of the column in IDEA StatiCa is 175.95 in. Therefore, to mimic the identical column length in ABAQUS, two other reference points (i.e., RF_2 and RF_3) were introduced 87.975 in. away from the center of the column along the Z axis in both directions (see Figure 4.20). These two reference points were fixed in all directions and were connected to the top and bottom faces of the column using the connector builder module in ABAQUS. To replicate the friction type shear force transfer in bolts in IDEA StatiCa, pretention load was applied in ABAQUS along the axis of each bolt shank. In ABAQUS, the element size was chosen to be between 0.1-0.4 in. after routine mesh sensitivity analysis, and a total of 310,451 elements were generated in the model. The 3D stress, 8-node linear brick reduced integration (i.e., C3D8R) was selected as element type.

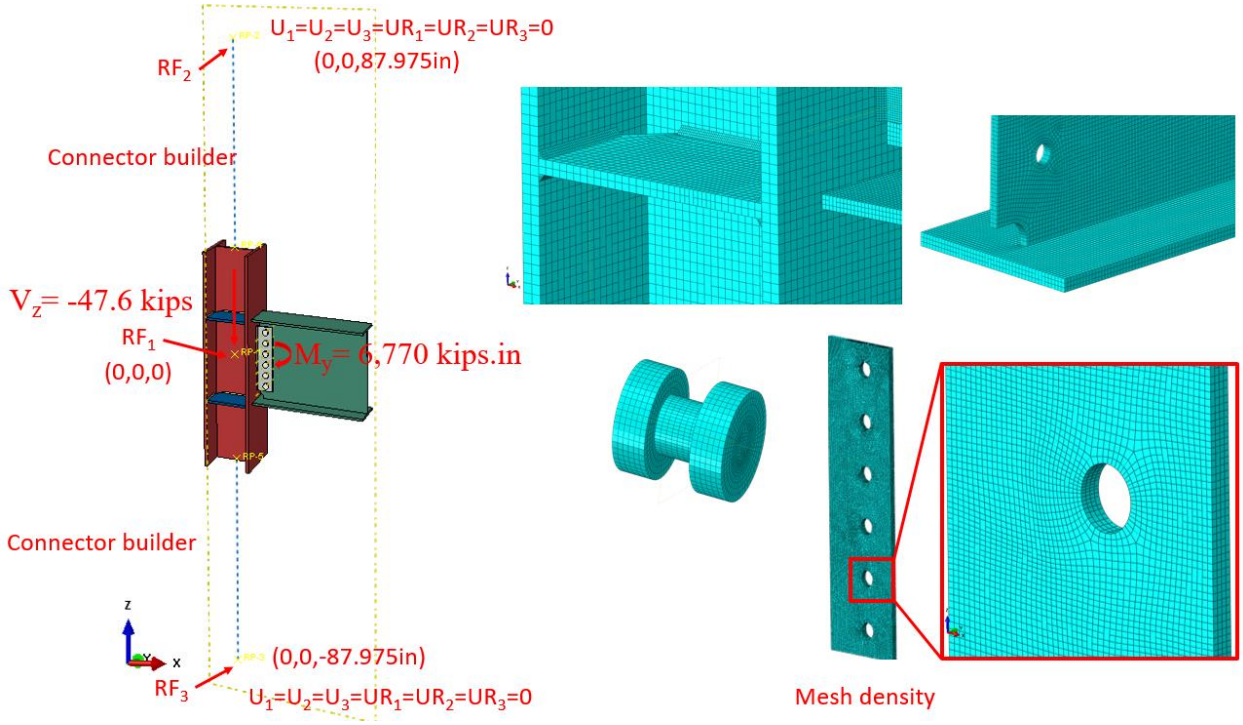

Figure 4.20: Model setup and mesh density in ABAQUS

The tie constraint was applied between the weld lines and the attaching parts. The material behavior was modeled using bi-linear plasticity in ABAQUS. Other parameters, including density, elastic modulus, and Poisson's ratio were taken from the IDEA StatiCa materials library. The numerical simulation was carried out on four processors (Intel Xenon ® CPU E5-2698 v4 @ 2.20GHz) and took approximately 270 minutes to finish. Figure 4.21 compares the predicted von-Mises stress between IDEA StatiCa and ABAQUS.

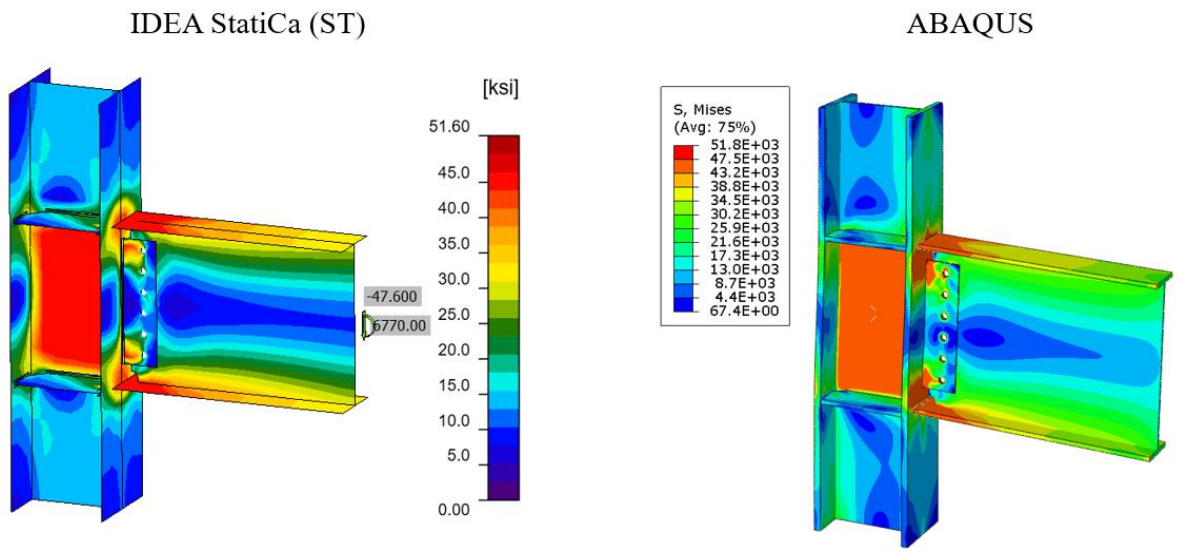

Figure 4.21: Comparison of the calculated von Mises stress between IDEA StatiCa and ABAQUS models

The maximum predicted stress in IDEA StatiCa was 46.2 ksi on the column web (note that the IDEA StatiCa legend shows the design data) while the ABAQUS model shows a maximum stress of 46.8 ksi at the same location. The maximum stress of 51.8 ksi in the ABAQUS legend belongs to the front weld line connecting the shear tab to the column. The slightly different stress distribution is likely due to the consideration of the length of the column in ABAQUS and the way that boundary conditions were applied, utilization of finer mesh in the FE analysis, and the simplified CAD model in IDEA StatiCa. Note that the authors performed a routine mesh sensitivity analysis for the IDEA StatiCa model and some inconsistencies in the results were observed.

The maximum calculated plastic strain in IDEA StatiCa and ABAQUS were 2.3% and 2.9%, respectively (both on the top beam flange). Also, the predicted plastic deformation region by IDEA StatiCa was consistent with the calculated yield map in ABAQUS (i.e., the bottom row in Figure 4.22). In addition, the ABAQUS results show that bolts were also experiencing plastic deformation.

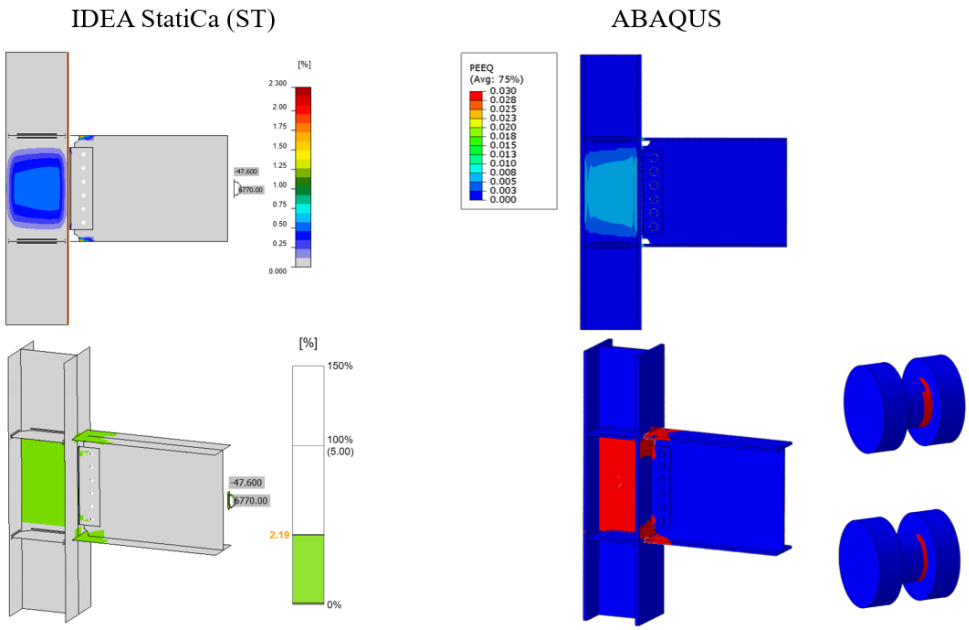

Figure 4.22: Top row) Comparison of the calculated plastic strain between IDEA StatiCa and ABAQUS models; bottom row) Comparison of the yield map between IDEA StatiCa and ABAQUS

Figure 4.23 depicts the comparison of the moment-rotation curve between the two software with respect to the column centerline. Note that in Figure 4.23, to obtain the total rotation by IDEA StatiCa (shown by dashed orange line), the linear beam rotation at the column centerline was calculated using SAP2000 and then added to the default plastic rotation curve reported by IDEA StatiCa (shown by solid orange line). Both models offer comparable initial stiffness estimations. The minor discrepancy could be associated with the difference in the element types (i.e., solid element in ABAQUS versus shell element in IDEA StatiCa) and the employment of the tie constraint in ABAQUS to represent the welds.

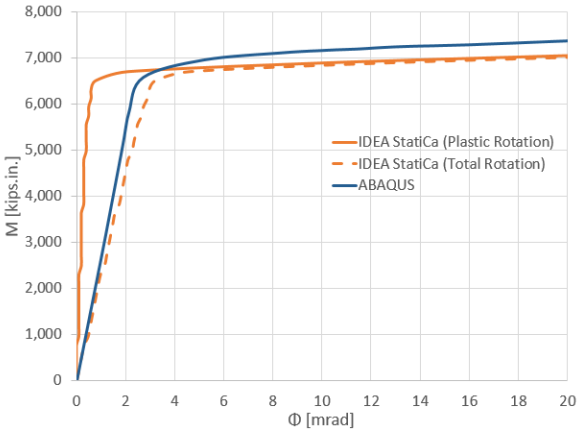

Figure 4.23: Moment-rotation comparison between IDEA StatiCa and ABAQUS

4.6 Summary and Comparison of Results

The eight WUF-B moment connections were investigated using IDEA StatiCa and following the AISC design procedure. Also, the results from IDEA StatiCa baseline model (i.e., SC) were compared with those from the equivalent ABAQUS model.

During the test of the baseline model.SC, the specimen failed due to tearing out of beam flange while the controlling limit state calculated from AISC procedure is panel zone strength which is 8% less than beam strength. IDEA StatiCa analysis for the baseline model.SC calculated the failure mode as bolt slip strength. On the other hand, IDEA StatiCa model of the baseline model.X failed due to the beam flange since the bolt type was changed to the bearing type from the slip critical as AISC 341 allows for the moment connections. Also, the calculated moment-plastic rotation relationship using IDEA StatiCa was compared with the curve provided in the test report as illustrated in Figure 4.24.

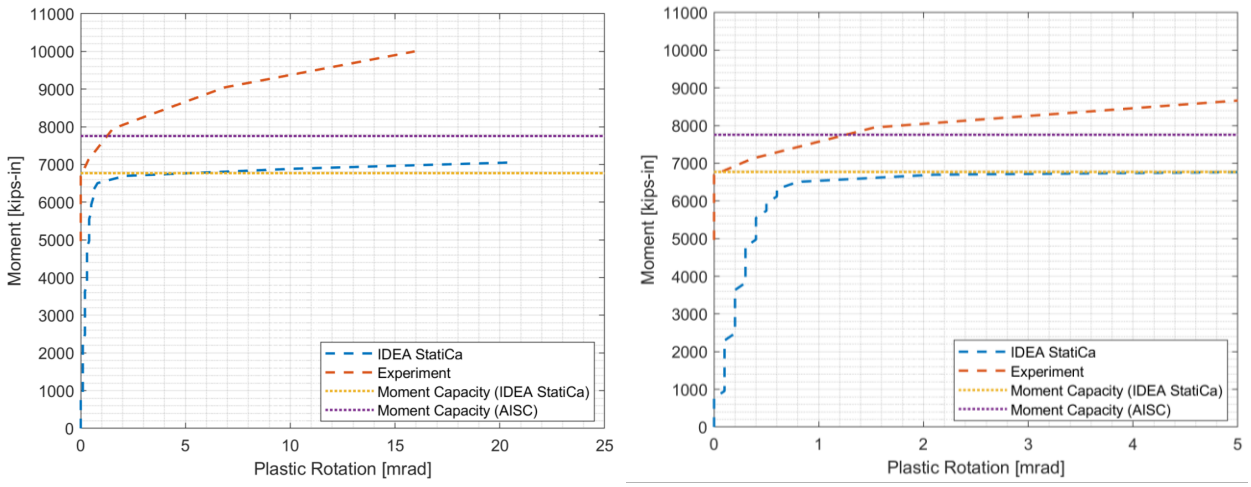

Figure 4.24: Moment rotation comparison for the baseline model.SC with a zoomed view on the right

For variation 1, it is indicated in the test report that plastic hinge occurred in the panel zone. The same failure mode was calculated from AISC procedure. On the other hand, IDEA StatiCa analysis showed that the specimen reached its capacity due to beam web with 5% plastic strain while 4% plastic strain was calculated in the panel zone.

Regarding variation 2.SC, fracture of the beam flange was reported as a failure mode of the specimen. Similarly, AISC procedure calculated the same failure mode. IDEA StatiCa model for variation 2.SC showed that the failure mode is bolt slip strength while IDEA StatiCa analysis performed for variation 2.X calculated the same failure mode with the test and AISC procedure.

For variation 3.SC, ductile tearing is reported during the experiment. The same failure mode was calculated following the AISC procedure. IDEA StatiCa model for variation 3.SC showed that the

bolt slip strength was achieved while the one developed for variation 3.X showed that the specimen reached its capacity due to the flexural beam strength as observed by AISC procedure and during the experiment.

Regarding variation 4, the test observation, AISC procedure and IDEA StatiCa analysis calculated the same failure modes. The flexural moment capacity following IDEA StatiCa was computed as 20,656 kips-in. while it is calculated as 24,286 kips-in. using AISC procedure. The calculated flexural moment capacities of the eight specimens IDEA StatiCa and following AISC procedure are presented in Figure 4.25.

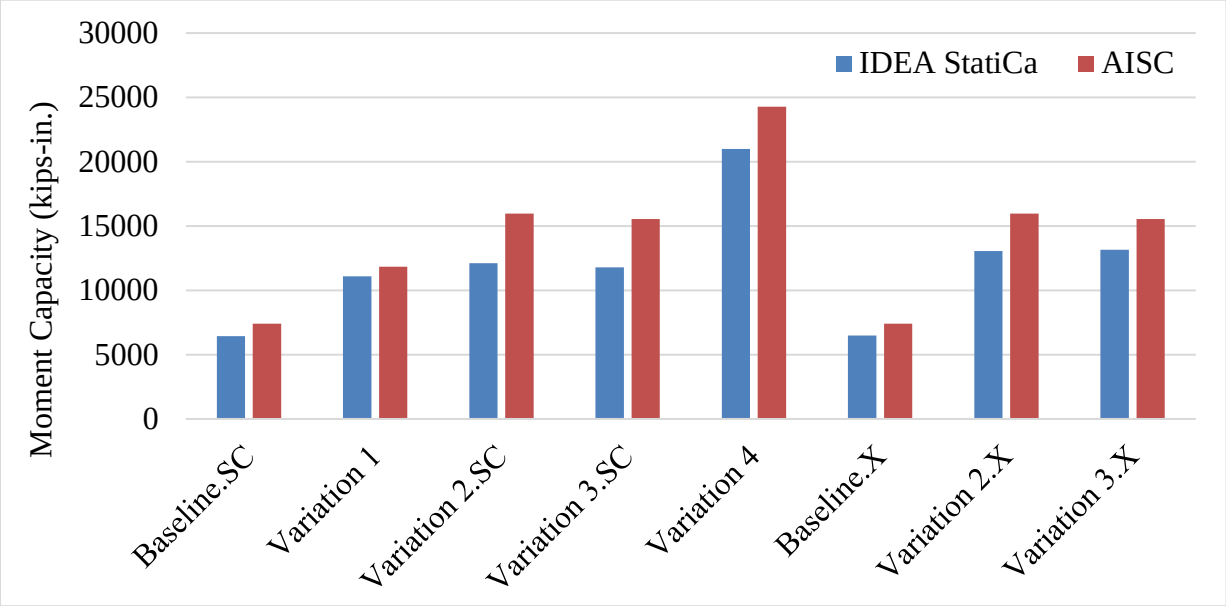

Figure 4.25: Moment capacities calculated by IDEA StatiCa and AISC procedure

Please add some comments at the end – e.g. IDEA StatiCa shows consistently safe results compared to experimental results and AISC procedures. Although slip-critical bolts are designed, they may be checked using bearing bolts in IDEA StatiCa, utilizing their post-slip bearing strength.

References

Lee, K. H., Stojadinovic, B., Goel, S. C., Margarian, A. G., Choi, J., Wongkaew, A., Reyher, B. P., and Lee, D. Y. (2002). *Parametric Tests on Unreinforced Connections, Volume I-Final Report*. SAC/BD-00/01.

AISC 360 (2016), "Specification for Structural Steel Buildings," American Institute of Steel Construction ANSI/AISC 360-16, Chicago, Illinois.

AISC 341 (2016), "Seismic Provisions for Structural Steel Buildings," American Institute of Steel Construction ANSI/AISC 341-16, Chicago, Illinois.

AWS D1.8/D1.8M (2016) *Structural Welding Code—Seismic Supplement* AWS B4.0:2007 *Standard Methods for Mechanical Testing of Welds*

Chapter 5. Double-Tee Moment Connections

5.1. Introduction

The last steel connection type studied in this research is double-tee moment connection (see Figure 5.1). Double-tee is a prequalified connection to be used in the seismic region as part of IMF and SMF system if the requirements outlined in AISC 358 are satisfied. For the scope of this study, an experimental study conducted for a double-tee connection and its variations was chosen from the literature and their flexural capacities were examined following AISC design procedure as well as using IDEA StatiCa. Also, the baseline model was analyzed using ABAQUS software, and the results were compared.

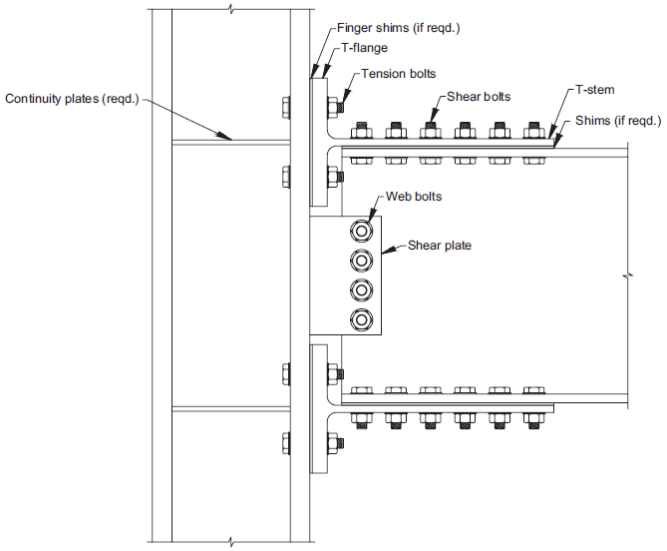

Figure 5.1: Typical double-tee moment connection (AISC 358)

In the following sections, the experimental test is described, AISC design checks conducted for those specimens are summarized, and the numerical analysis results obtained from IDEA StatiCa and ABAQUS are discussed. At the end, the results obtained from three sources (i.e., tests, AISC design procedures, and numerical analyses) are compared.

5.2 Experimental Study

Six full-scale double-tee connections and 48 individual T-stubs were tested at Georgia Institute of Technology by Leon (1999) as part of the SAC Task 7.03 project. The primary purpose of this study was to have a better understanding of the behavior of bolted connections under cyclic loads and verify whether the results of small-scale component tests can be extrapolated to full-scale connections. In the scope of this study, only the details and results of six full-scale tests are summarized. For further details of the experiments, readers are referred to Swanson (1999) and Smallidge (1999) in addition to the test report by Leon (1999).

All specimens consist of a W14×145 column whereas beam varies from W21×44 to W24×55. All fasteners were high strength A490 tension-controlled bolts with a diameter of either 7/8 in. or 1 in. T-stubs were cut from three different wide flange steel sizes (W16×45, W16×100 and W21×93). A 3/8-in. thick shear tab was used for all the specimens with a length of either 9 in. or 12 in. depending on the number of bolts. Among the six specimens, one of them was chosen as a baseline model (Test ID: FS-06), and the rest were studied as variation models (see Table 5.1).

Table 5.1: Properties of the double-tee specimens (Leon, 1999)

Specimen no (Test ID)	Beam	Column	T-stub	Bolts
Baseline (FS-06)	W24×55	W14×145	W16×100	1 in. A490
Variation 1 (FS-03)	W21×44	W14×145	W16×45	7/8 in. A490
Variation 2 (FS-04)	W21×44	W14×145	W16×45	1 in. A490
Variation 3 (FS-05)	W24×55	W14×145	W16×100	7/8 in. A490
Variation 4 (FS-07)	W24×55	W14×145	W21×93	7/8 in. A490
Variation 5 (FS-08)	W24×55	W14×145	W21×93	1 in. A490

The test setup consists of a 152 in. long column (from pinned top to pinned bottom locations) and a beam connected to column flange at 82 in. above from the bottom support of column. The length of the beam from column face to actuator was 176 in., and a lateral bracing was provided at 5 ft from the connection. The test setup is shown in Figure 5.2.

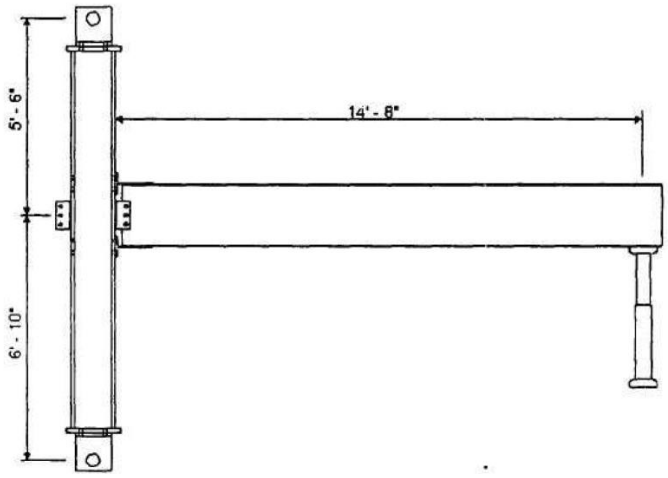

Figure 5.2: Test setup (Leon, 1999)

The baseline model consists of a W14×145 column, a W24×55 beam, and two T-stubs cut from W16×100. Eight 1 in. diameter A490 shear and eight 1 in. diameter A490 tension bolts are used in the T-stub flanges. Four 1 in. diameter A490 bolts are used to fasten the shear tab to the beam web while the shear tab is welded to the column flange with 5/16 in. double fillet weld. Also, four ½ in. thick continuity plate and ½ in. thick one-sided doubler plate are used as depicted in Figure 5.3.

Variation 1 consists of a W14×145 column, a W21×44 beam, two T-stubs cut from a W16×45 which are used to fasten the beam flanges and the column flanges with eight 7/8 in. diameter A490 shear and eight 7/8 in. diameter A490 tension bolts. Three 7/8 in. diameter A490 bolts are used between the shear tab and the beam web, and 5/16 in. double fillet weld is used between the column face and shear tab as shown in Figure 5.3.

Variation 2 consists of 1 in. diameter A490 bolts differently from variation 1. All other details are identical to variation 1. The configuration of the variation 2 is illustrated in Figure 5.4. Variation 3 consists of a W14×145 column, a W24×55 beam and T-stubs cut from a W16×100. Ten 7/8 in. diameter A490 shear bolts and eight 7/8 in. diameter A490 tension bolts are used in both T-stubs. Four 7/8 in. diameter A490 bolts are used to fasten the shear tab and beam web while 5/16 in. double fillet weld is used between the column flange and the shear tab. Four ½ in. thick continuity plate and ½ in. thick one-sided doubler plate is used to reinforced the column panel zone. The differences between the baseline model and variation 3 are the diameter of the bolts and the number of shear bolts used to fasten the T-stub flanges and the beam flanges (see Figure 5.4).

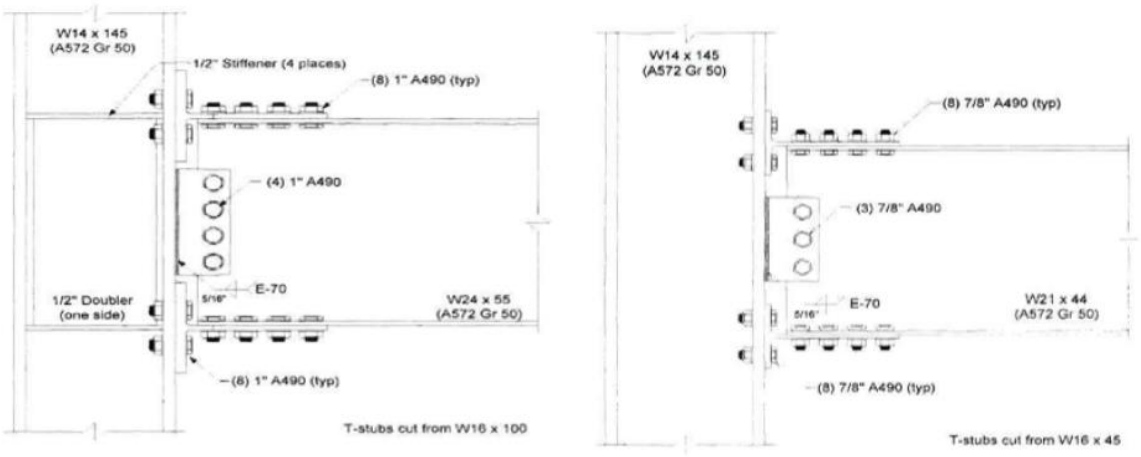

Figure 5.3: Left) Configuration of baseline model; Right) configuration of variation 1 (Leon, 1999)

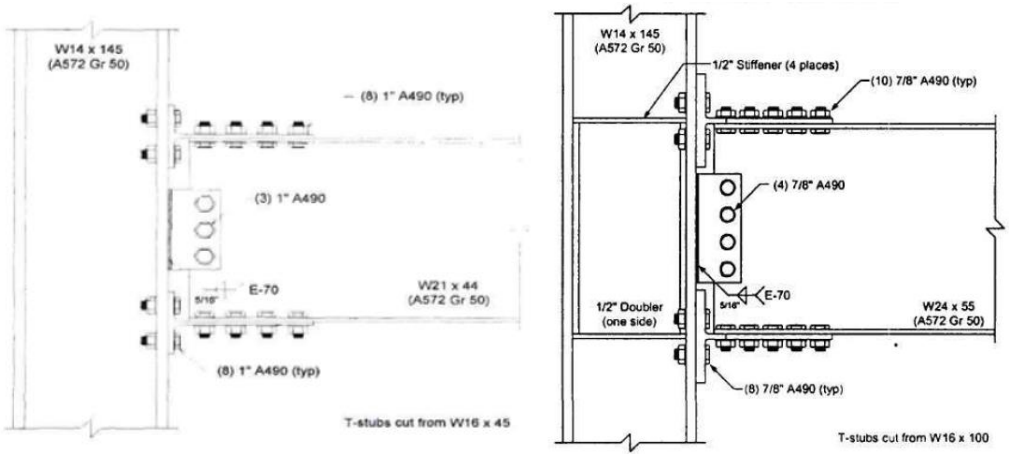

Figure 5.4: Left) Configuration of variation 2; Right) configuration of variation 3 (Leon, 1999)

Variation 4 consists of a W24×55 beam, T-stubs cut from a W21×93, and four bolted shear tab. Ten shear bolts are used to fasten T-stub flanges to the beam flanges and eight tension bolts on at each T-stub to be attached to the column face. The column panel zone is reinforced with four ½ in. thick continuity plate and ½ in. thick one-sided doubler plate. A490 bolts with 7/8 in. diameter are used for all fasteners. Variation 5, differently from variation 4, has a larger bolts with 1 in. diameter. Rather than this, all other geometrical properties are identical as illustrated in Figure 5.5. The average coupon test and mill certificate material properties for beam, column and T-stubs are presented in Table 5.2.

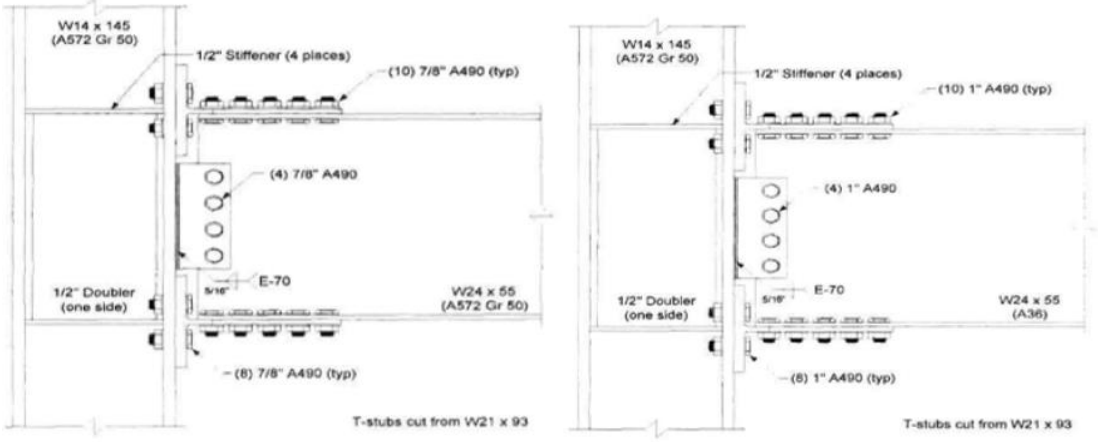

Figure 5.5: Left) Configuration of variation 4; Right) configuration of variation 5 (Leon, 1999)

Table 5.2: Measured material properties of the tested double-tee specimens (Leon, 1999)

Specimen No	Component	Yield stress [ksi]		Ultimate stress [ksi]	
		Mill	Coupon	Mill	Coupon
Baseline model and variation 3	Beam	61.0	-	76.0	-
	Column	56.0	-	74.0	-
	T-stub	53	46.1 (flange)	70	66.7 (flange)
			51.1 (web)		68 (web)
Variation 1 and variation 2	Beam	58.0	-	71.0	-
	Column	56.0	-	74.0	-
	T-stub	50.0	57.4 (flange)	65.0	80.8 (flange)
			61.9 (web)		82.6 (web)
Variation 4	Beam	61.0	-	76.0	-
	Column	56.0	-	74.0	-
	T-stub	55	52.5 (flange)	69.5	72.3 (flange)

			54.9 (web)		72.6 (web)
Variation 5	Beam	53.8	-	70.7	-
	Column	56.0	-	74.0	-
	T-stub	55	52.5 (flange)	69.5	72.3 (flange)
			54.9 (web)		72.6 (web)

From the test of baseline model, the local buckling of the beam was identified as the failure mode. The experiment was discontinued after extensive local buckling was observed on the beam web and flanges when the peak moment reached approximately 9,003 kips-in. at the connection. At this point, the corresponding force in T-stub was 381.1 kips. After test photo and measured moment plastic rotation are presented in Figure 5.6.

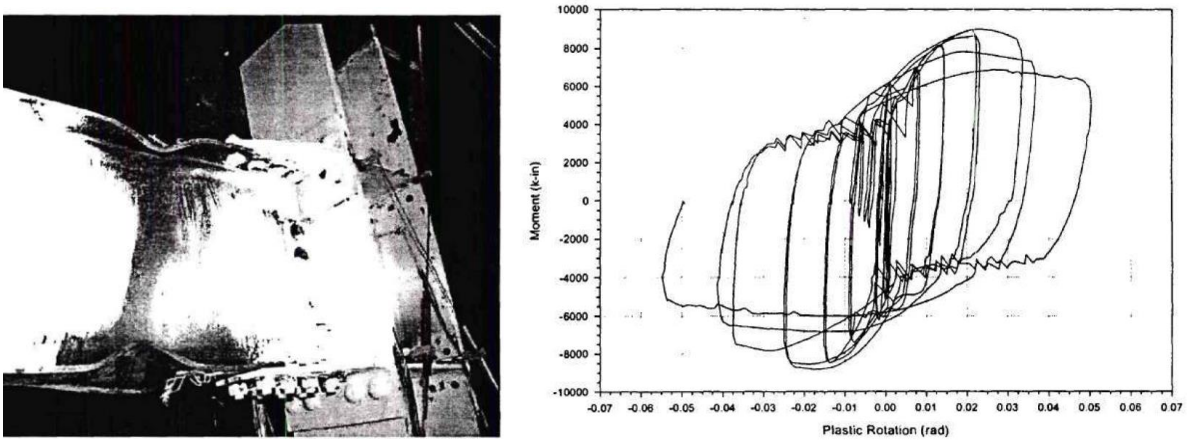

Figure 5.6: Left) Baseline model after testing; Right) moment-total plastic rotation relationship (Leon, 1999)

In variation 1, the maximum actuator load and the maximum moment at the connection were reported as 32.8 kips and 6,011 kips-in., respectively. Initial yielding of T-stub was observed when the force in T-stub and the moment at the connection were approximately 185 kips and 3,800 kips-in., respectively. The first yielding of beam was reported when the moment at the connection was around 5,000 kips-in. During further cycles, the specimen failed due to the T-stub fracture along the first row of shear bolts. After the test photo and measured moment plastic rotation are presented in Figure 5.7.

In variation 2, the first yielding in T-stub and beam flange was noticed when the force in the T-stub and moment at the connection were approximately 245 kips and 5,000 kips-in., respectively. Flange buckling was observed during the further loads, and the specimen failed due to the net section fracture. The reported maximum moment at the connection was approximately 6,183 kips-in. After the test photo and measured moment plastic rotation are presented in Figure 5.8.

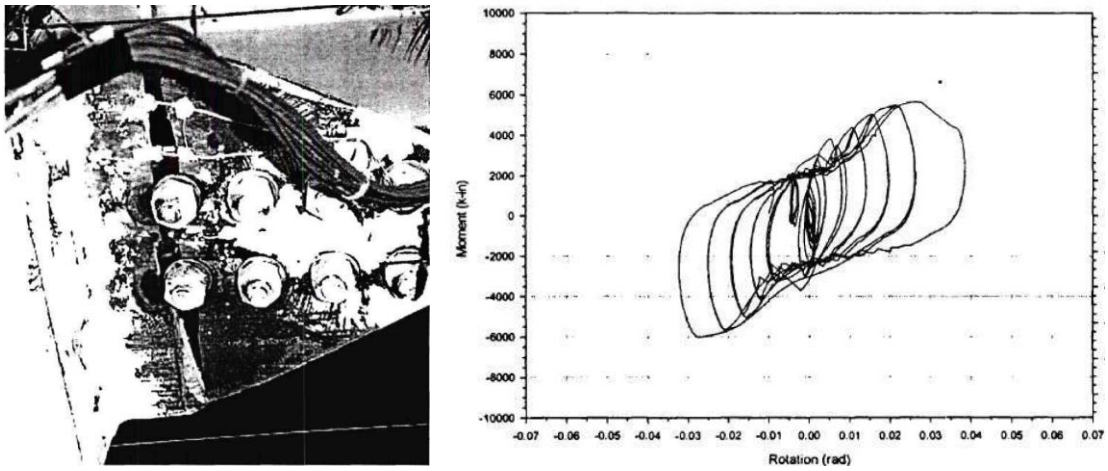

Figure 5.7: Left) Variation 1 after testing; Right) moment-total plastic rotation relationship (Lee et al., 1999)

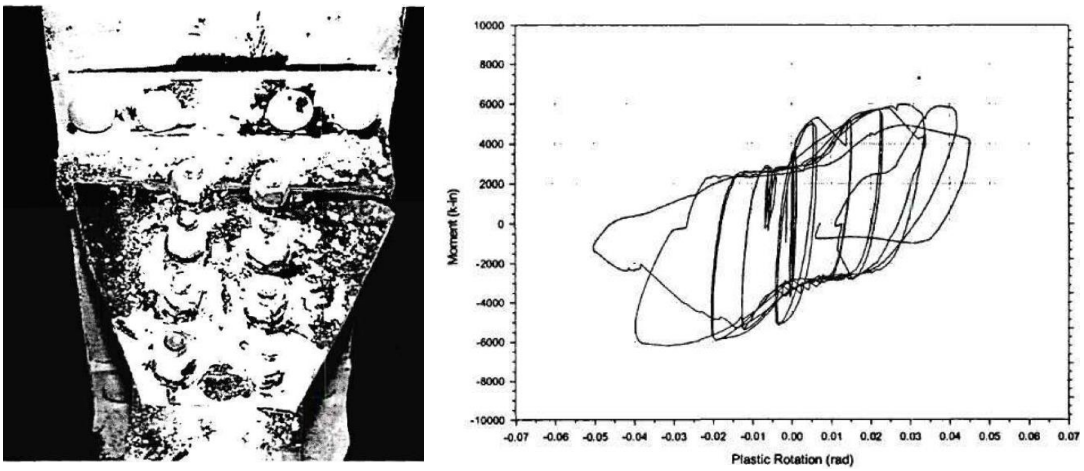

Figure 5.8: Left) Variation 2 after testing; Right) moment-total plastic rotation relationship (Leon, 1999)

Regarding the test of variation 3, the failure mode was reported as beam local buckling. After that the extensive local buckling was observed on the beam flanges, the test was stopped. The maximum moment at the connection was approximately 9,739 kips-in. After the test photo and measured moment plastic rotation are presented in Figure 5.9.

It was observed from the test of variation 4 that the specimen underwent local buckling in the flange. When the tip displacement was approximately 12.8 in., fracture occurred on the beam flange along the bolt line farthest to the column flange. The peak moment at the connection was approximately 9,580 kips-in. with a corresponding T-stub force of 405.5 kips. After the test photo and measured moment plastic rotation are presented in Figure 5.10.

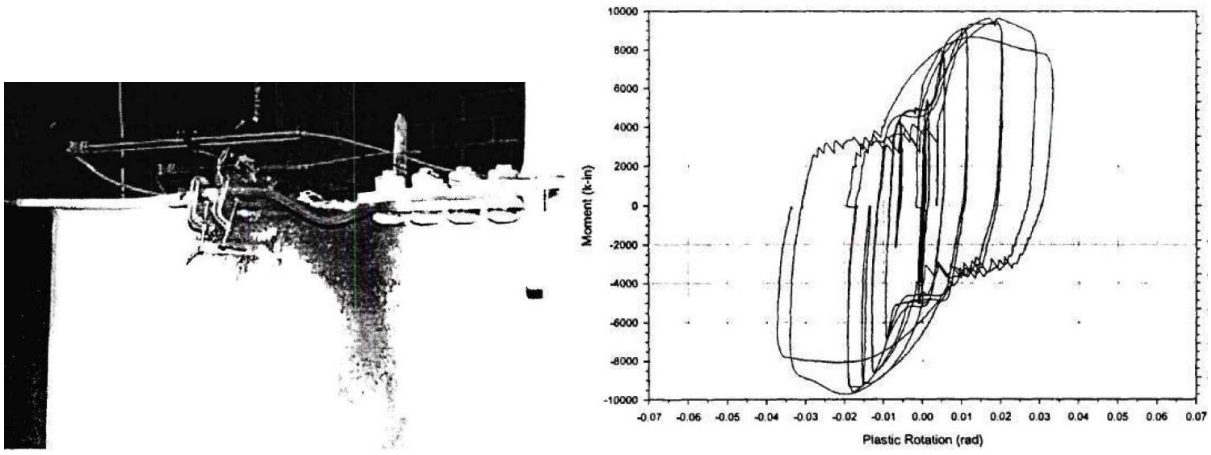

Figure 5.9: Left) Variation 3 after testing; Right) moment-total plastic rotation relationship (Leon, 1999)

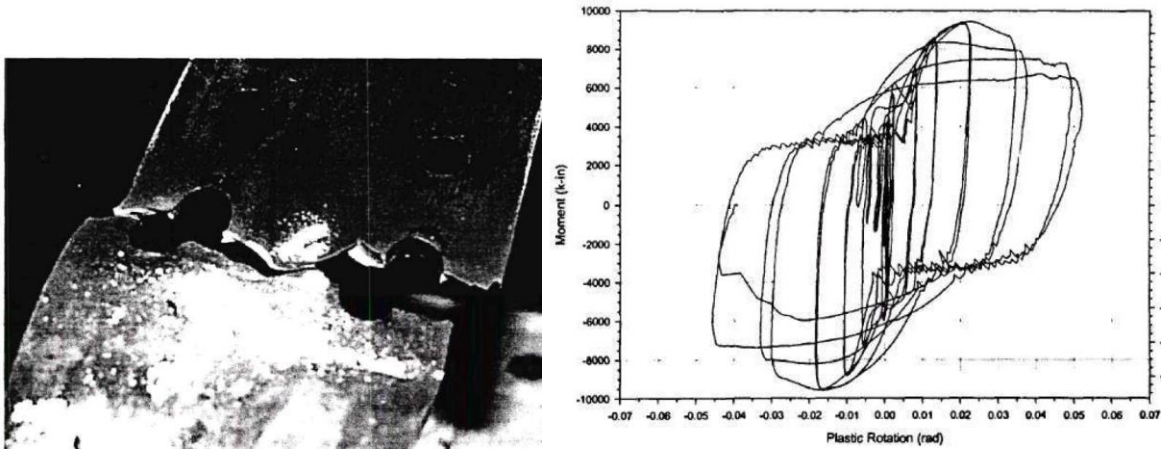

Figure 5.10: Left) Variation 4 after testing; Right) moment-total plastic rotation relationship (Leon, 1999)

The observations from the test of variation 5 were similar to those of the baseline model and variation 3. The specimen experienced extensive beam local buckling during the test. The test was discontinued when the maximum moment at the connection was approximately 8,586 kips-in. At this point, the corresponding force in T-stub was 363,4 kips. After the test photo and measured moment plastic rotation are presented in Figure 5.11.

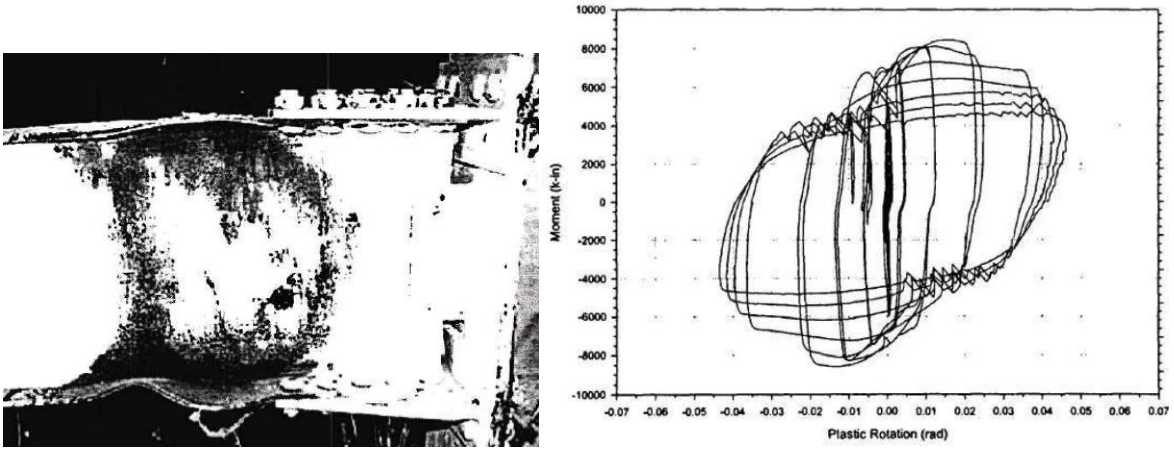

Figure 5.11: Left) Variation 5 after testing; Right) moment-total plastic rotation relationship (Leon, 1999)

5.3 Code Design Calculations

Prequalification limits and design procedure for double-tee moment connections are outlined in Chapter 13 of AISC 358 (2016). The following design checks were identified and performed for the tested specimens:

- T-stem strength (AISC 358, Eq. 13.6-45)
- Shear bolt diameter (AISC 358, Eq. 13.6-4)
- Tension bolt diameter (AISC 358, Eq. 13.6-16)
- Minimum T-flange thickness (AISC 358, Eq. 13.6-27)
- Rotational stiffness of connection (AISC 358, Eq. 13.6-28)
- T-stub strength (AISC 358, Eq. 13.6-46)
- Bearing/tearout strength of beam flange (AISC 360, Eq. J3-6)
- Bearing/tearout strength of T-stem (AISC 360, Eq. J3-6)
- Block shear strength of beam flange (AISC 360-16, Eq. J4-5)
- Block shear strength of T-stem (AISC 360-16, Eq. J4-5)
- Flexural yielding strength of column (AISC 358, Eq. 13.6-61)
- Continuity plate requirements (AISC 341, Sec. E3.6f.1(a))
- Column-beam relationships (AISC 341, Eq. E3-1)
- Panel zone strength (AISC 360, Eq. J10-11)
- Beam flexural strength (AISC 360, Eq. F1-1)
- Check bolt strength of shear plate (AISC 360, Eq. J3-6a)
- Check weld strength of shear tab (AISC 360, Eq. J4-2)
- Check shear yielding, rupture, block shear strength of shear plate (AISC 360, Eq. J3-J4)

It was assumed that shear tab, doubler plate and continuity plate had identical measured material properties with T-stub. The nominal tensile strength (f_{nt} = 90 ksi) and shear strength (f_{nv} = 68 ksi) values provided in AISC Table J3 were used for A490 bolts. Five models were developed using

mill certificate material test reports for each specimen. Two additional models were developed for variation 1 and variation 2 using coupon material test properties measured for T-stub. Design checks were performed for the selected specimens, and the summary is presented in Table 5.3.

Table 5.3: Design checks for double-tee moment connections

AISC Design Checks	Baseline	Var-1		Var-2		Var-3	Var-4	Var-5
	Mill	Mill	Coupon	Mill	Coupon	Mill	Mill	Mill
T-stem strength	Not OK	Not OK	Not OK	Not OK	Not OK	OK	OK	OK
Shear bolt diameter	OK	Not OK	OK	Not OK	OK	OK	OK	OK
Tension bolt diameter	OK	OK	OK	OK	OK	OK	OK	OK
Minimum T-flange thickness	OK	OK	OK	OK	OK	OK	OK	OK
Rotational stiffness of connection	OK	OK	OK	OK	OK	OK	OK	OK
T-stub strength	OK	OK	OK	OK	OK	OK	OK	OK
Bearing/tearout strength of beam flange	OK	Not OK	Not OK	OK	OK	OK	OK	OK
Bearing/tearout strength of T-stem	OK	Not OK	Not OK	Not OK	Not OK	OK	OK	OK
Block shear strength of beam flange	Not OK	Not OK	Not OK	Not OK	Not OK	Not OK	OK	OK
Block shear strength of T-stem	Not OK	Not OK	Not OK	Not OK	Not OK	OK	OK	OK
Flexural yielding strength of column	OK	OK	OK	OK	OK	OK	OK	OK
Continuity plate requirements	Not OK	Not OK	Not OK	Not OK	Not OK	Not OK	Not OK	Not OK
Column-beam relationships	OK	OK	OK	OK	OK	OK	OK	OK
Panel zone strength	OK	OK	OK	OK	OK	OK	OK	OK
Beam flexural strength	OK	OK	OK	OK	OK	OK	OK	OK
Bolt strength of shear plate	OK	OK	OK	OK	OK	OK	OK	OK

Weld strength of shear tab	OK	OK	OK	OK	OK	OK	OK	OK
Shear yielding, shear rupture, block shear strength of shear plate	Not OK	OK	OK	OK	OK	Not OK	Not OK	Not OK

Failure mode of a double-tee moment connection can be estimated if the governing limit state of the followings are known:

- Strength of stem gross section yielding
- Strength of stem net section fracture
- Strength of stem flexural buckling
- Strength of shear bolt
- Strength of bearing/tearout of beam
- Strength of bearing/tearout of T-stem
- Strength of block shear of beam
- Strength of block shear of T-stem
- Beam plastic moment strength

For each limit state, moment strengths at column face of the specimens were calculated (see Appendices I and J), and the results are presented in Table 5.4. The controlling moment strength (i.e., the lowest strength) are identified and shown with bolded font.

Table 5.4: Moment strength of the specimens

Moment Strength	Baseline [kips-in.]	Var-1 [kips-in.]		Var-2 [kips-in.]		Var-3 [kips-in.]	Var-4 [kips-in.]	Var-5 [kips-in.]
	Mill	Mill	Coupon	Mill	Coupon	Mill	Mill	Mill
Stem gross section yielding	10,412	4,570	**5,246**	5,041	**5,787**	11,623	11,956	11,956
Stem net section fracture	11,400	4,996	6,211	5,432	6,753	13,369	13,157	12,793
Stem flexural buckling	10,412	4,570	5,246	5,041	5,787	11,623	11,956	11,956
Shear bolt	12,758	7,928	9,856	9,061	11,264	12,189	12,187	15,944
Bearing/tearout of beam	14,619	9,524	9,524	10,590	10,590	16,906	16,903	17,482
Bearing/tearout of T-stem	16,681	7,222	8,667	7,956	9,608	19,299	19,012	20,945
Block shear of beam	9,213	6,266	6,266	6,673	6,673	10,460	10,922	10,878
Block shear of T-stem	9,829	**4,398**	5,467	**4,684**	5,823	11,160	11,471	12,281

Beam plastic moment	**8,749**	8,071	8,108	8,108	8,162	**8,802**	**8,802**	**7,880**

Based on the AISC design calculations, beam plastic moment was the estimated failure mode for the baseline model, variation 3, variation 4, and variation 5. Regarding variation 1 and variation 2, block shear of T-stem was the governing limit state when coupon test properties are used for T-stubs. When the mill certificate material properties are used for all members, their failure modes were switched to the stem gross section yielding.

5.4 IDEA StatiCa Analysis

IDEA StatiCa models were developed for the specimens to evaluate their moment strength capacities. Since the purpose was to simulate the experimental tests, SAP2000 model was developed for the test setup condition, and the forces at the column centerline were calculated. The measured material properties were used, and the resistance factors were set to 1.0. Using the stress-strain analysis type in IDEA StatiCa (i.e., EPS), the moment capacities were calculated, and the failure modes of the specimens were estimated. For the baseline model, the moment-rotation relationship was calculated using the connection stiffness analysis type (i.e., ST) in IDEA StatiCa software. Moreover, capacity design analysis (i.e., CD) was used to ensure that the connection has enough deformation capacity.

5.4.1 Analysis of Baseline Model

To estimate the behavior of tension-controlled bolts on capacity and rotational stiffness of the connection, two different IDEA StatiCa models were developed for the baseline model using two different bolt types: 1) bearing, and 2) friction. Mill certificate material properties (See Table 5.2) were introduced in the software, and the overstrength coefficients, R_y and R_t, and all LRFD resistance factors were set to 1.0. A beam-column frame model was developed using SAP2000 with the lengths of the column and beam in the test setup, and the forces at column centerline were obtained. Using "Loads in equilibrium option", stress-strain analysis (EPS) was performed to calculate the capacity of the baseline model. The loads were gradually increased until any of the following is achieved:

10) 5% of plastic strain in plates (beam, column, shear tab, continuity plate)
11) 100% strength capacity in bolts
12) 100% strength capacity in welds

From the IDEA StatiCa analysis of the model created with friction type bolts, it was observed that the bolt strength capacity was achieved when the applied shear force and moment reached 26.70 kips and 4,900 kips-in., respectively (Figure 5.12). The second model was developed by switching "shear force transfer" option from "friction" to "bearing - tension/shear interaction" for T-stubs and shear tab. Also, "deformation at bolt hole at service load is a design consideration" option (under code setup) was turned off. An incremental loading was applied to the connection

(proportionally with all loads being in equilibrium), it was observed that 5% of plastic limit strain was achieved on the beam flange when the shear force and the corresponding moment values reached 46.00 kips and 8,430, respectively (Figure 5.13). Analysis type was switched to stiffness analysis (e.g., “ST”), and moment-rotation relationship was computed for each model as shown in Figure 5.14.

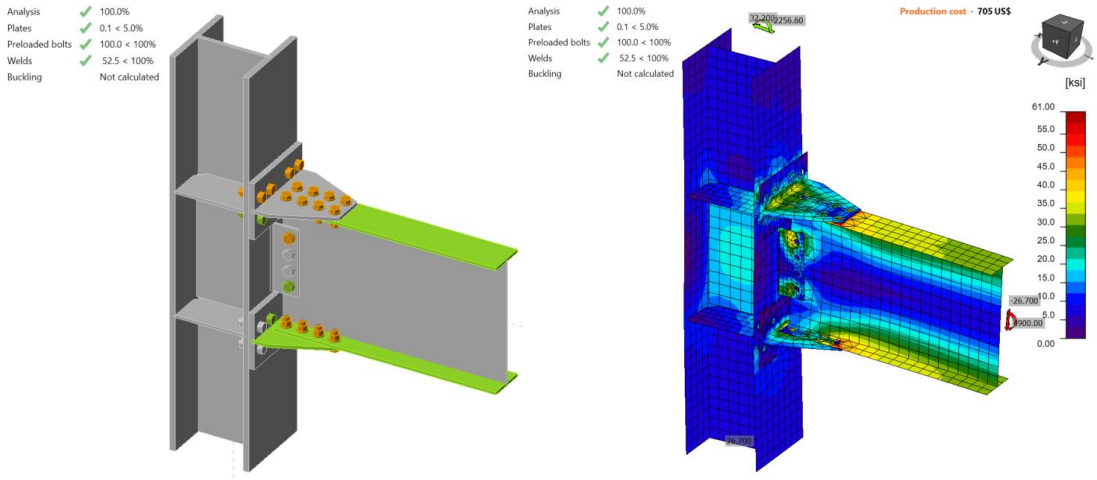

Figure 5.12: IDEA StatiCa model for Baseline model (with friction bolts) under the moment of 4,900 kips-in.

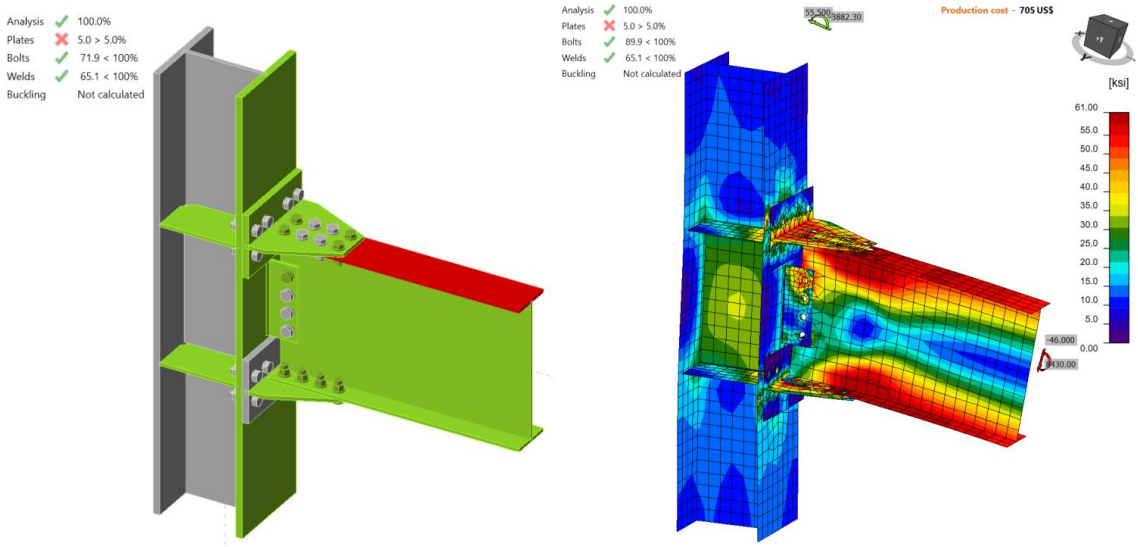

Figure 5.13: IDEA StatiCa model for Baseline model (with bearing bolts) under the moment of 8,430 kips-in.

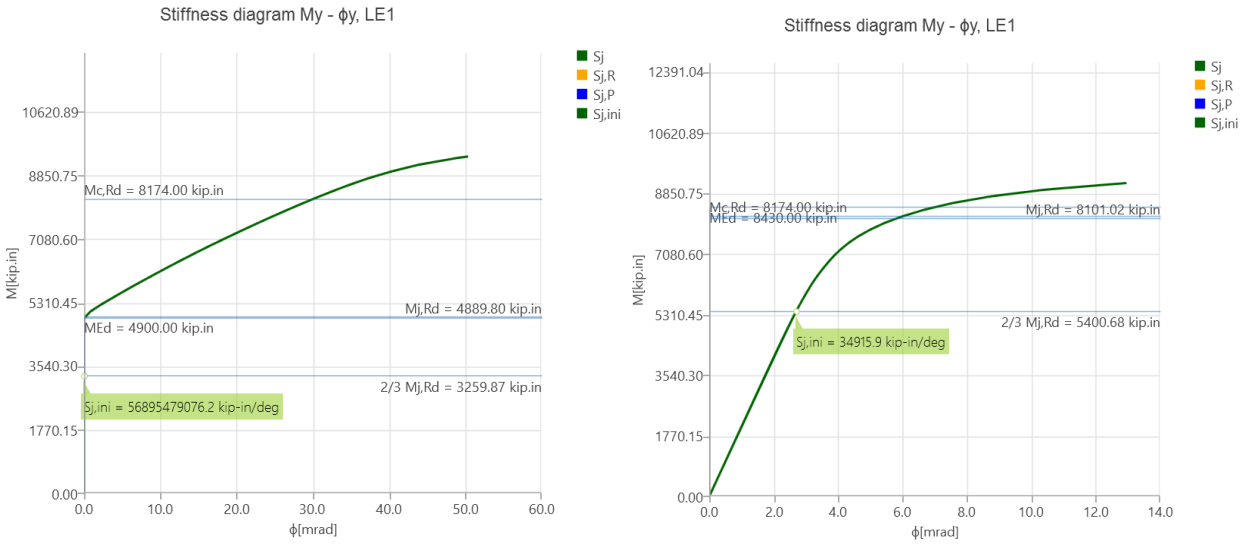

Figure 5.14: Left) Moment-rotation relationship for baseline model with friction bolts; right) moment-rotation relationship for baseline model with bearing bolts

Analysis type was switched to capacity design (e.g., "CD") to check whether the connection has enough ductility when the plastic moment strength of the beam is achieved. To be able to perform this analysis, plastic moment of beam, location of plastic hinge and shear force at plastic hinge location are required to be calculated. According to Eq. 2.4-1 in AISC 341 (2016), the probable maximum moment of beam at plastic hinge location, M_p, is calculated as:

$$M_p = C_{pr} F_y R_y Z_x \tag{5.1}$$

where Z_x is plastic section modulus of beam, F_y is yield stress of beam, R_y is ratio of the expected yield stress to the specified minimum yield stress, and C_{pr} is a factor to account for peak connection strength which is given by Eq. 2.4-2 in AISC 341 (2016) as:

$$C_{pr} = \left(F_y + F_u\right)/\left(2F_y\right) \tag{5.2}$$

F_u is ultimate stress of beam. It is assumed that R_y is equal to 1.0 when using measured material properties. Using the mill certificate material properties and plastic section modulus of beam (134 in.^{3}) given in Table 1.1 in AISC Manual (2017), C_{pr} and M_p were calculated using the properties given below as 1.12 and 9,154.88 kips-in. respectively. The distance of plastic hinge location from column centerline and the shear force at the plastic hinge location were calculated as 19.9 in. and 103 kips, respectively (see Appendix I) with an assumption that the distance between the column centerlines is equal to 30 ft. The calculated loads were applied at the beam position equal to 19.9 in. by setting loads as percentage of members in a way that are equal to the calculated plastic moment and shear force values as shown in Figure 5.15. The connection is inadequate, the T-stems are too weak (22.1% of plastic strain was reached in the top T-stem).

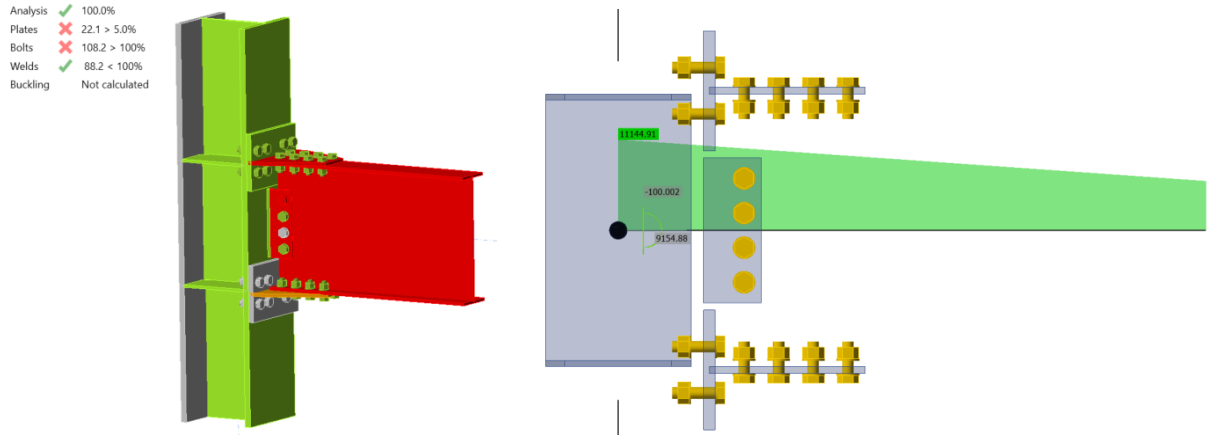

Figure 5.15: Capacity design analysis of baseline model

5.4.2 Analysis of Variation 1

Two IDEA StatiCa models were developed for variation 1 for different measured material properties of T-stub. For the first model, mill certificate material properties were used for all members of the specimens whereas the second model was created using the coupon test material properties of T-stub flange. Following the same procedure described in the previous section, an incremental loading was applied. The first model reached its capacity with 5% of plastic strain in the T-stubs when the shear force and the corresponding moment values were 26.70 kips and 4,900 kips-in., respectively (Figure 5.16). The material properties of T-stubs were updated using coupon test properties and the same incremental loading procedure was followed. The same failure mode was observed when the shear force and the corresponding moment values reached 30,00 kips and 5,500 kips-in., respectively (Figure 5.17).

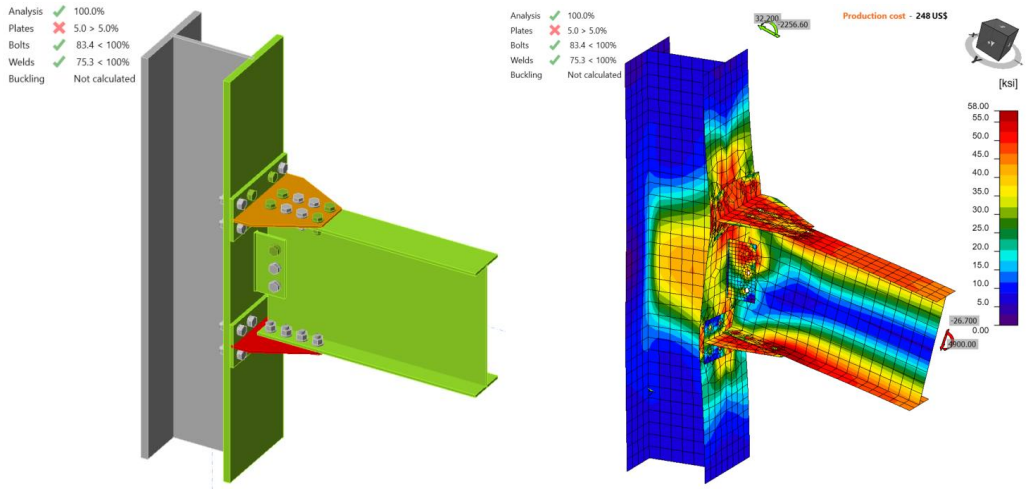

Figure 5.16: IDEA StatiCa model for variation 1 (Mill) under the moment of 4,900 kips-in.

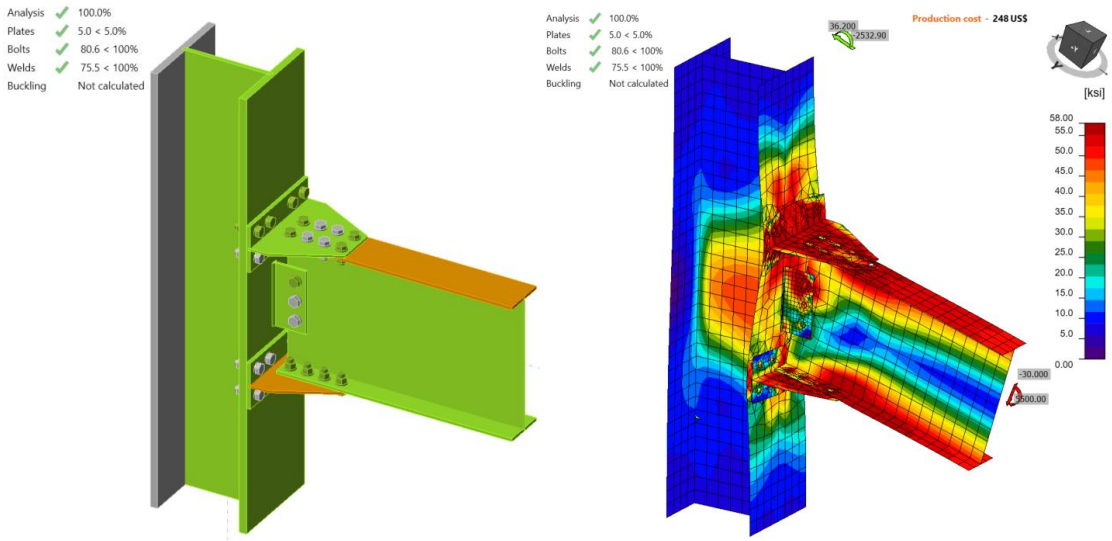

Figure 5.17: IDEA StatiCa model for variation 1 (Coupon) under the moment of 5,500 kips-in.

5.4.3 Analysis of Variation 2

Following the same procedure, two IDEA StatiCa models were developed for variation 2. From the model developed with the mill certificate properties, it was observed that T-stub reached the plastic strain limit (i.e., 5.0%) when the applied shear force and moment were 26.90 kips and 4,940 kips-in., respectively (Figure 5.18). After the material properties of T-stub were switched to coupon test properties, a higher flexural moment capacity was calculated as 5,730 kips-in. with the corresponding 31.20 kips shear force (Figure 5.19). The failure mode remained the same.

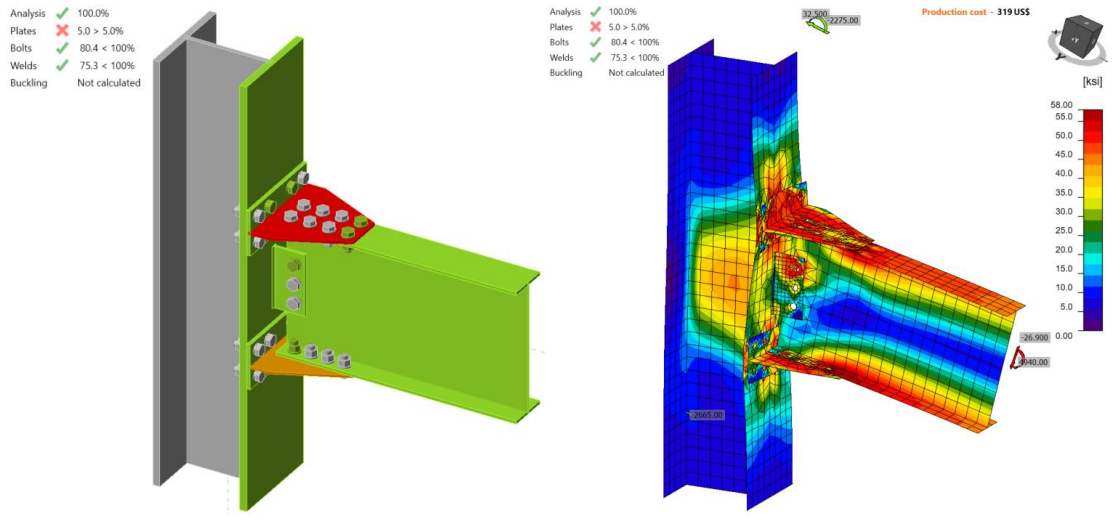

Figure 5.18: IDEA StatiCa model for variation 2 (Mill) under the moment of 4,940 kips-in.

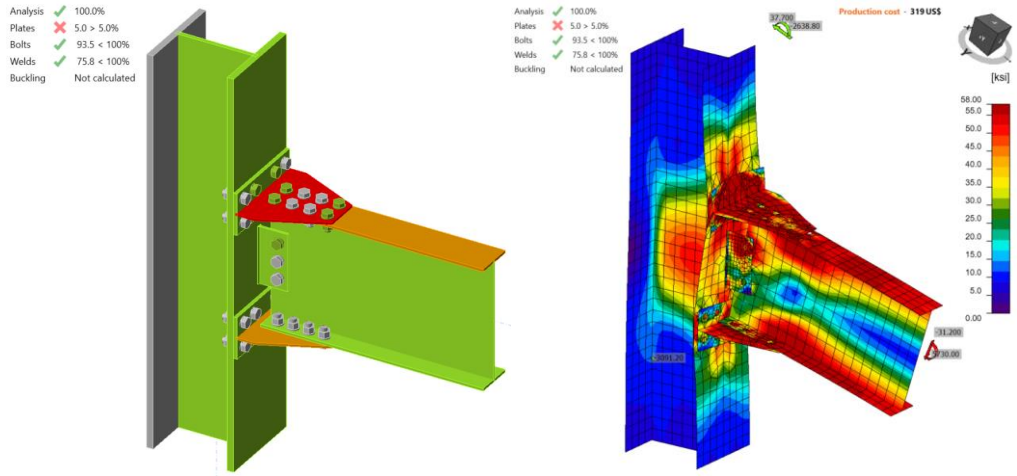

Figure 5.19: IDEA StatiCa model for variation 2 (Coupon) under the moment of 5,730 kips-in.

5.4.4 Analysis of Variation 3

For variation 3, the IDEA StatiCa model was developed using mill certificate material properties. When the shear force and the corresponding moment reached 45.50 kips and 8,350 kips-in., respectively, 5% of plastic strain was achieved on the beam flange (Figure 5.20).

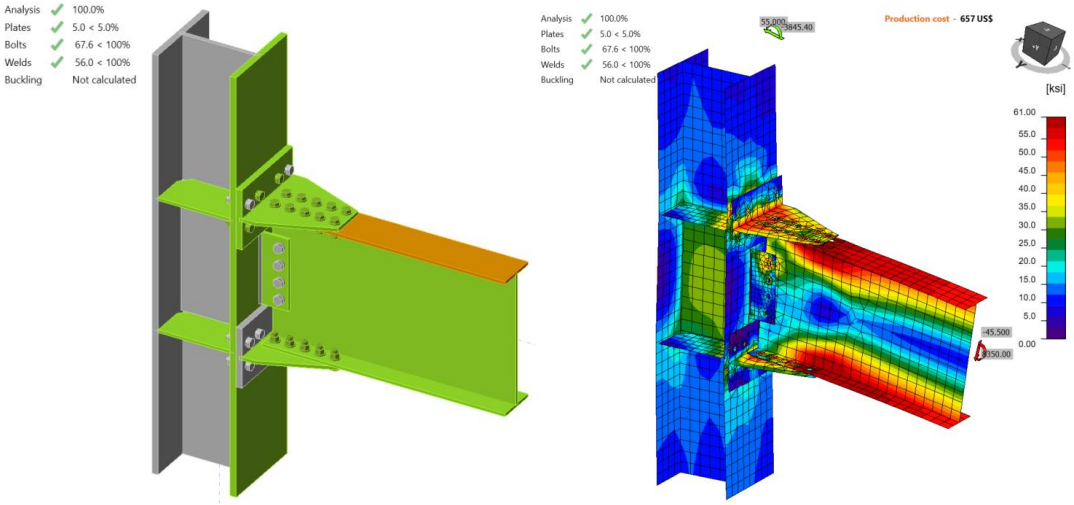

Figure 5.20: IDEA StatiCa model for variation 3 under the moment of 8,350 kips-in.

5.4.5 Analysis of Variation 4

The IDEA StatiCa model was created for variation 4 using mill certificate material properties. 5% of plastic strain was captured on the beam flange when the shear force and the corresponding moment were 45.50 kips and 8,350 kips-in., respectively (Figure 5.21).

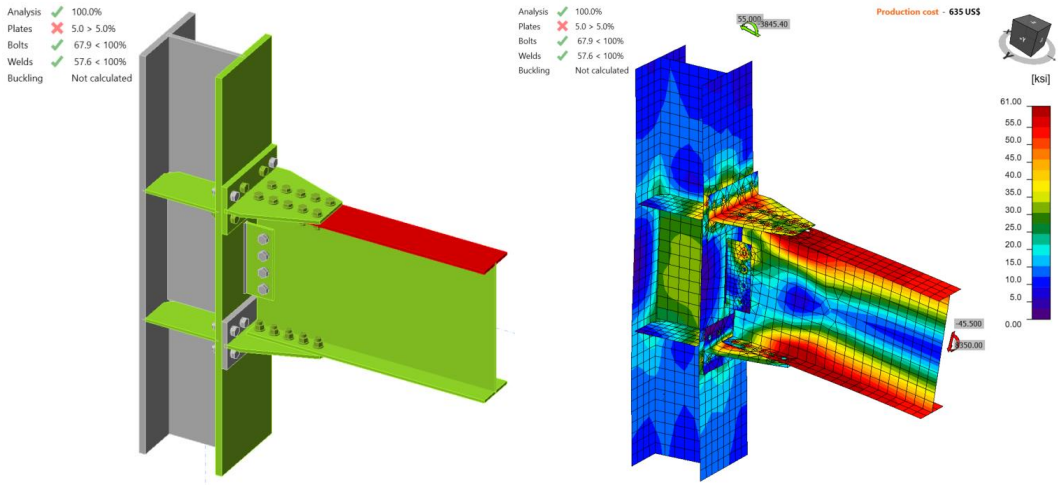

Figure 5.21: IDEA StatiCa model for variation 4 under the moment of 8,350 kips-in.

5.4.6 Analysis of Variation 5

Following the same procedure, IDEA StatiCa analysis was performed for variation 5. Mill certificate material properties were used for all members of the connection. 5% of plastic strain was achieved on the beam flange when the shear force and the corresponding reached 48.40 kips and 7,950 kips-in., respectively (Figure 5.22).

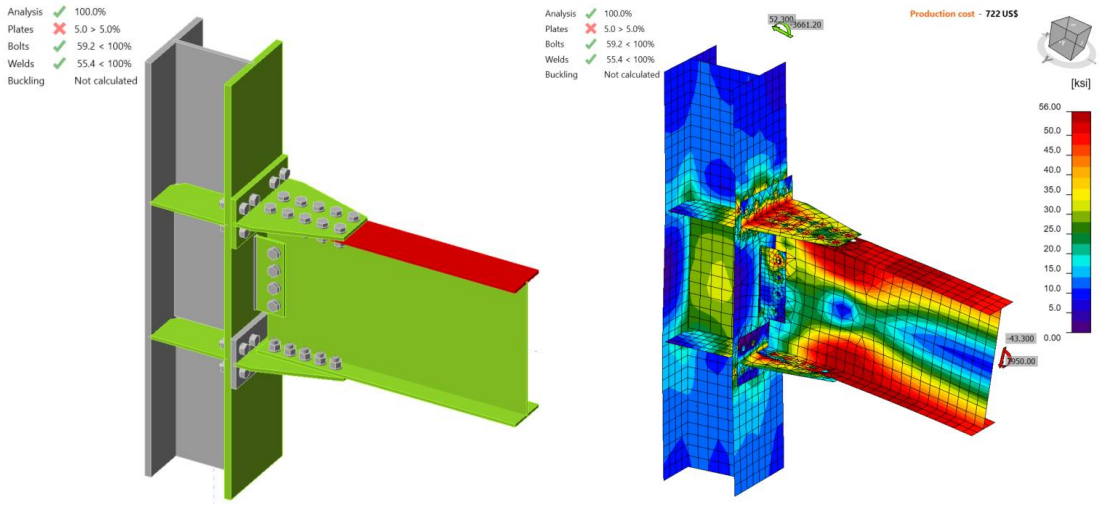

Figure 5.22: IDEA StatiCa model for variation 5 under the moment of 7,950 kips-in.

The moment capacities of double-tee moment connections with respect to column centerline, $M_{y@cc}$, were obtained with IDEA StatiCa analysis. Moment capacities at the column face, $M_{y@foc}$, were calculated using Eq. 5.3 and are presented in Table 5.5.

$$M_{y@foc} = M_{y@cc} - V_g \frac{d_c}{2} \tag{5.3}$$

where V_g is shear force, and d_c is depth of column.

Table 5.5: Moment capacities calculated by IDEA StatiCa

Specimen No	$M_{y@cc}$ [kips-in.]	V_g [kips]	$M_{y@foc}$ [kips-in.]
Baseline (Bearing)	8,430	46.0	8,090
Baseline (Friction)	4,900	26.7	4,702
Variation 1 (Mill)	4,900	26.7	4,702
Variation 1 (Coupon)	5,500	30.0	5,278
Variation 2 (Mill)	4,940	26.9	4,741
Variation 2 (Coupon)	5,730	31.2	5,499
Variation 3	8,350	45.5	8,013
Variation 4	8,350	45.5	8,013
Variation 5	7,950	43.3	7,630

5.5. ABAQUS Analysis

In this section, the baseline model developed in Section 5.4.1 was rebuilt using ABAQUS software (version 2022) for generic FE analysis and results were compared with IDEA StatiCa. The initial CAD model for the FE analysis was generated using the IDEA StatiCa's viewer platform. The 36 bolts and two weld lines that connected the entire assembly were then added manually using the CAD interface in ABAQUS. Two bolt types were investigated in this section as described in Section 5.4.1. For the bearing type bolt, the vertical load of 46 kips and the corresponding moment of 8,430 kips-in. (around Y axis) were applied to a defined reference point (i.e., RF_1) at the column centerline as shown in Figure 5.23. For the friction type bolt, the vertical load of 26.7 kips and the corresponding moment of 4,900 kips-in. (around Y axis) were applied to the same reference point (i.e., RF_1). The analytical length of the column in IDEA StatiCa is 190 in. Therefore, to mimic the identical column length in ABAQUS, two other reference points (i.e., RF_2 and RF_3) were introduced 95 in. away from the center of the column along the Z axis in both directions (see Figure 5.23). These two reference points were fixed in all directions and were connected to the top and bottom faces of the column using the connector builder module in ABAQUS. Note that to simulate the friction bolt in IDEA StatiCa, pretention load was applied in ABAQUS model along the axis of each bolt's shank. In ABAQUS, the element size was chosen to be between 0.1-0.3 in. after routine mesh sensitivity analysis, and a total of 387,893 elements were generated in the model. The 3D stress, 8-node linear brick reduced integration (i.e., C3D8R) was selected as element type. The tie constraint was applied between the two weld lines and the attaching parts. The material behavior was modeled using bi-linear plasticity in ABAQUS. Other parameters, including density, elastic modulus, and Poisson's ratio were taken from the IDEA StatiCa materials library which was updated according to the mill certificates (see Table 5.2). The numerical simulation was carried out on 16 processors (16vCP & 64GB RAM) and took approximately 210 minutes to finish. Figure 5.24 compares the predicted von-Mises stress between IDEA StatiCa and ABAQUS for both bolt type scenarios.

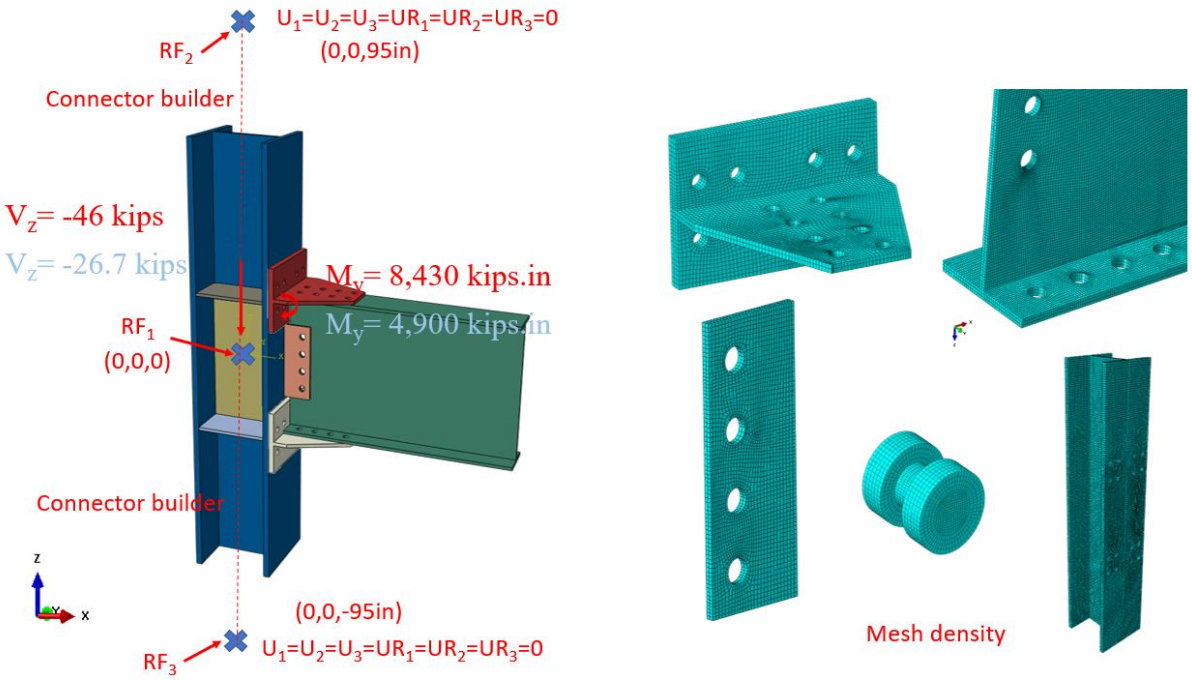

Figure 5.23: Model setup and mesh density in ABAQUS

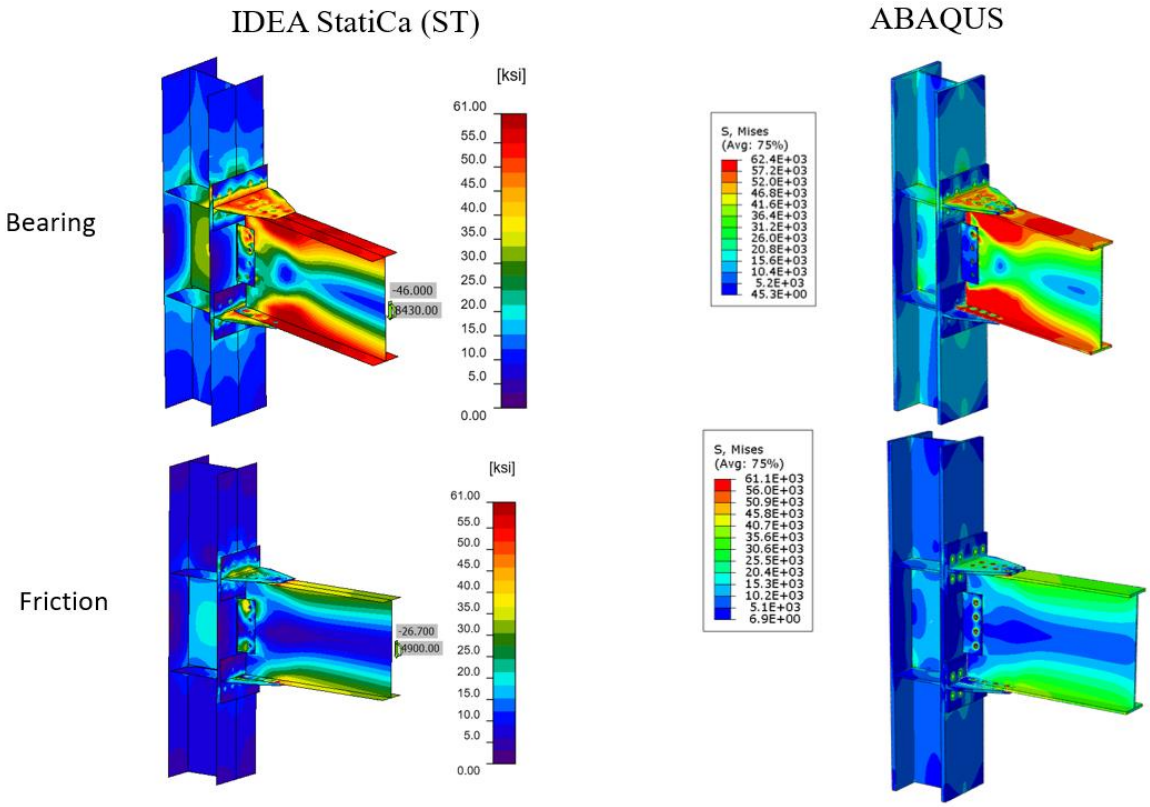

Figure 5.24: Comparison of the calculated von Mises stress between IDEA StatiCa and ABAQUS models*;* top row) bearing bolts assumption, bottom row) friction bolts assumption

The maximum predicted stress in IDEA StatiCa for the bearing type bolts was 62.4 ksi on the beam top flange (note that the IDEA StatiCa legend shows the design data) while the ABAQUS model shows similar stress at the same location. The maximum predicted stress in IDEA StatiCa for the friction type bolts was 61 ksi on the beam top flange while the ABAQUS model shows the stress of 61.1 ksi at the same location. The slightly different stress distribution is likely due to the consideration of the length of the column in ABAQUS and the way that boundary conditions were applied, utilization of finer mesh in the FE analysis, and the simplified CAD model in IDEA StatiCa. Note that the authors also investigated the potential effect of frictional behavior of the bolts on the results in the ABAQUS model by changing the friction coefficient from 0.3 to frictionless, however, the results were not sensitive to that parameter.

The maximum calculated plastic strain in IDEA StatiCa and ABAQUS for the bearing type bolt was 6.3% for both models (i.e., on the beam top flange as shown in Figure 5.25). Also, the predicted plastic deformation region by IDEA StatiCa was consistent with the calculated yield map in ABAQUS (i.e., the bottom row in Figure 5.25).

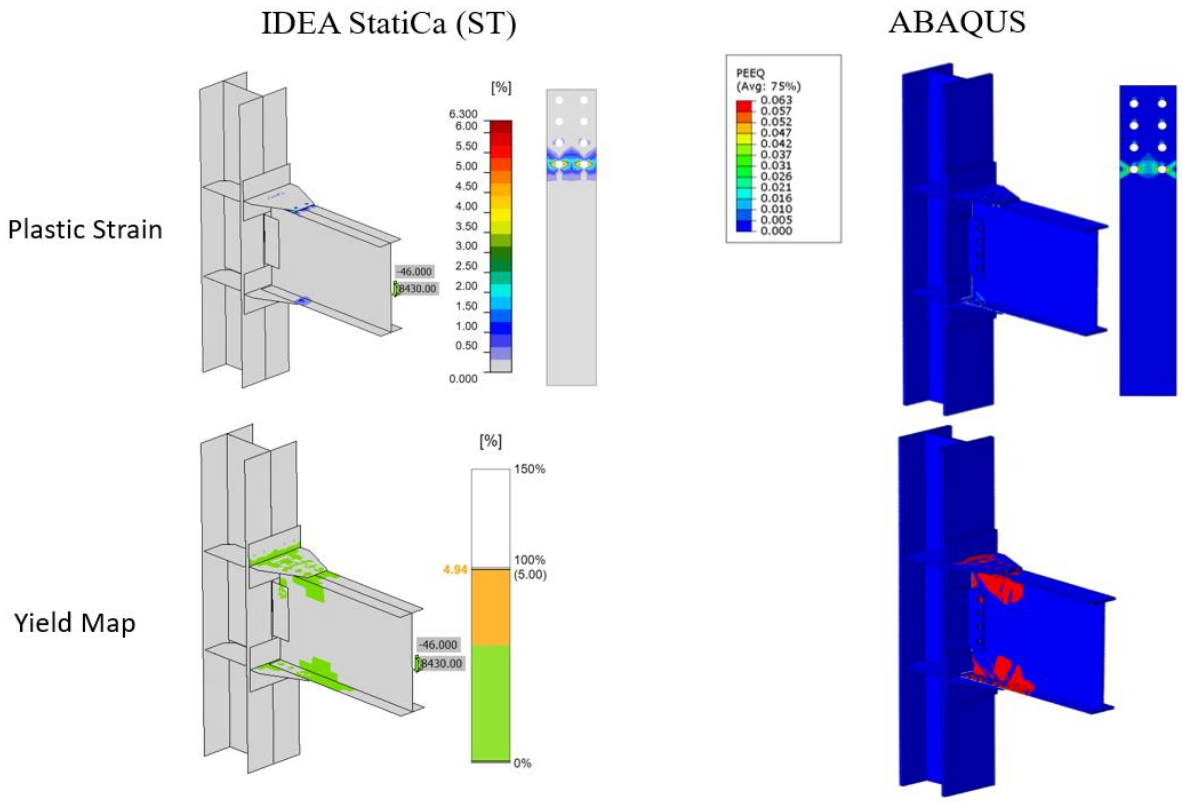

Figure 5.25: Bearing type bolts: Top row) Comparison of the calculated plastic strain between IDEA StatiCa and ABAQUS model; bottom row) comparison of the yield map between IDEA StatiCa and ABAQUS model

The maximum calculated plastic strain in IDEA StatiCa and ABAQUS for the friction type bolts were 0.1% and 0.17%, respectively (i.e., both on the beam top flange around the front bolt holes as indicated in Figure 5.26). Also, the predicted plastic deformation region by IDEA StatiCa was consistent with the calculated yield map in ABAQUS (i.e., the bottom row in Figure 5.26).

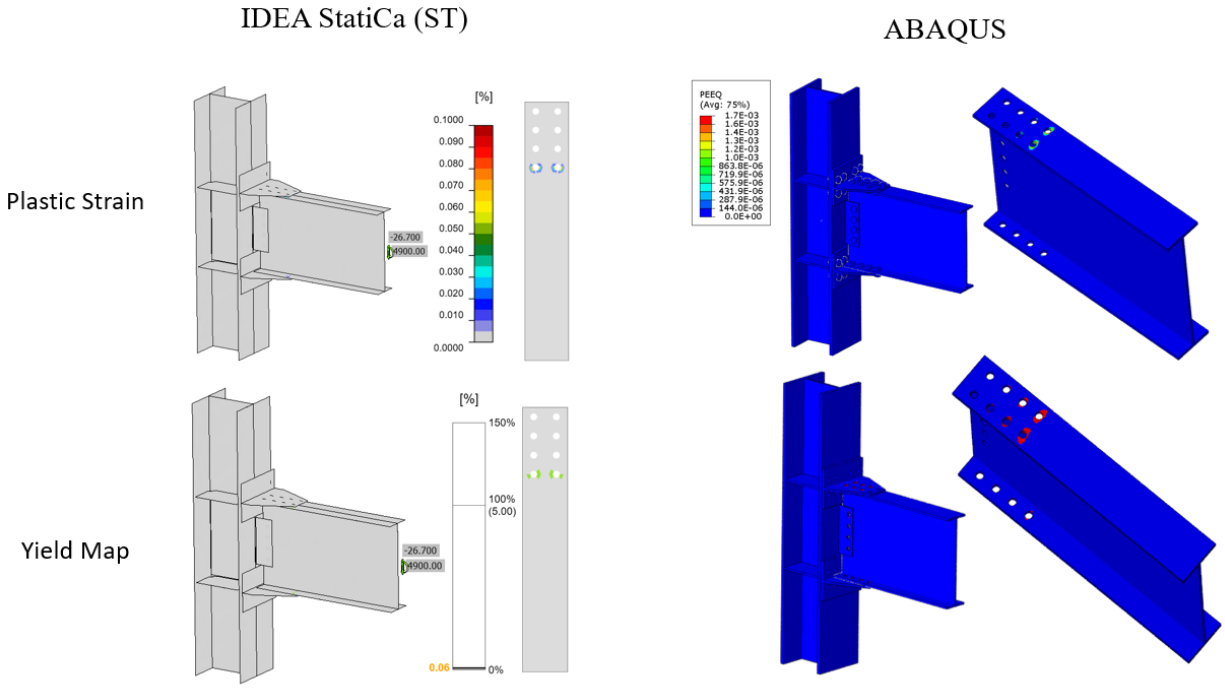

Figure 5.26: Friction type bolts: Top row) Comparison of the calculated plastic strain between IDEA StatiCa and ABAQUS model; Bottom row) Comparison of the yield map between IDEA StatiCa and ABAQUS model

Figure 5.27 depicts the comparison of the moment-rotation curve between the two software with respect to the column centerline for both bolt types investigated in this section. Note that in Figure 5.27, to obtain the total rotation by IDEA StatiCa (shown by dashed orange line), the linear beam rotation at the column centerline was calculated using SAP2000 and then added to the default plastic rotation curve reported by IDEA StatiCa (shown by solid orange line). Both models offer comparable initial stiffness estimations. The minor discrepancy could be associated with the difference in the element types (i.e., solid element in ABAQUS versus shell element in IDEA StatiCa) and the employment of the tie constraint in ABAQUS to represent the welds.

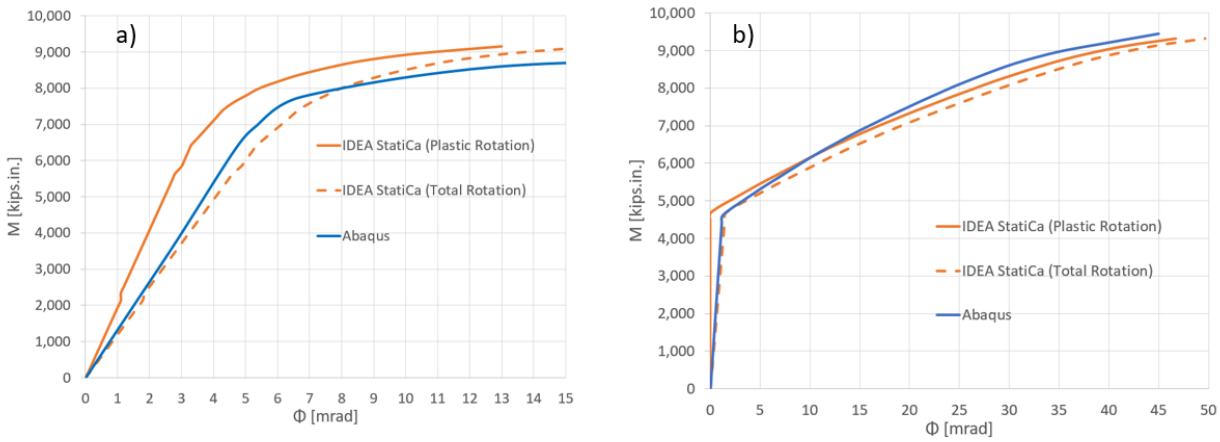

Figure 5.27: Moment-rotation comparison between IDEA StatiCa and ABAQUS for a) bearing type bolts, b) friction type bolts

5.6 Summary and Comparison of Results

Six double-tee moment connections from experimental campaign were studied using IDEA StatiCa and following the AISC design procedure. Two different models were created for the baseline model to investigate the effects of using bearing and friction type bolts on moment capacity and moment rotation curve. Since the difference between the mill certificate and coupon test material properties was relatively high for variation 1 and variation 2, two different IDEA StatiCa models were developed for each of them. Mill certificate material properties were used for the rest of the specimens. In addition, for the baseline model, the moment rotation relationships calculated using IDEA StatiCa for each bolt type were compared with those from the equivalent ABAQUS models.

For the test of the baseline model, the failure mode was reported as local buckling of the beam. From the incremental loading of IDEA StatiCa analysis, it was observed that the model using friction bolts failed due to insufficient bolt slip strength while the failure occurred on the beam flange from the model that consists of bearing bolts. AISC design calculations show that plastic moment strength of beam was the controlling limit state. Since AISC 341 allows to design moment connections including tension-controlled based on their bearing strength capacity, it can be concluded that there is a good agreement on failure mode of the baseline model between observations from test, IDEA StatiCa analysis and AISC design procedure. In addition, the moment rotation curves obtained from both IDEA StatiCa models and the one provided in the test report are compared in Figure 5.28. It can be seen that the moment rotation relationship of the double-tee specimen having tension-controlled high strength A490 bolts fall within the curves calculated from IDEA StatiCa models developed with bearing bolts and friction bolts separately. Also, the capacity design analysis performed for the baseline model showed that T-stub and shear tab did not have sufficient strength. Similarly, both members did not satisfy the AISC design checks.

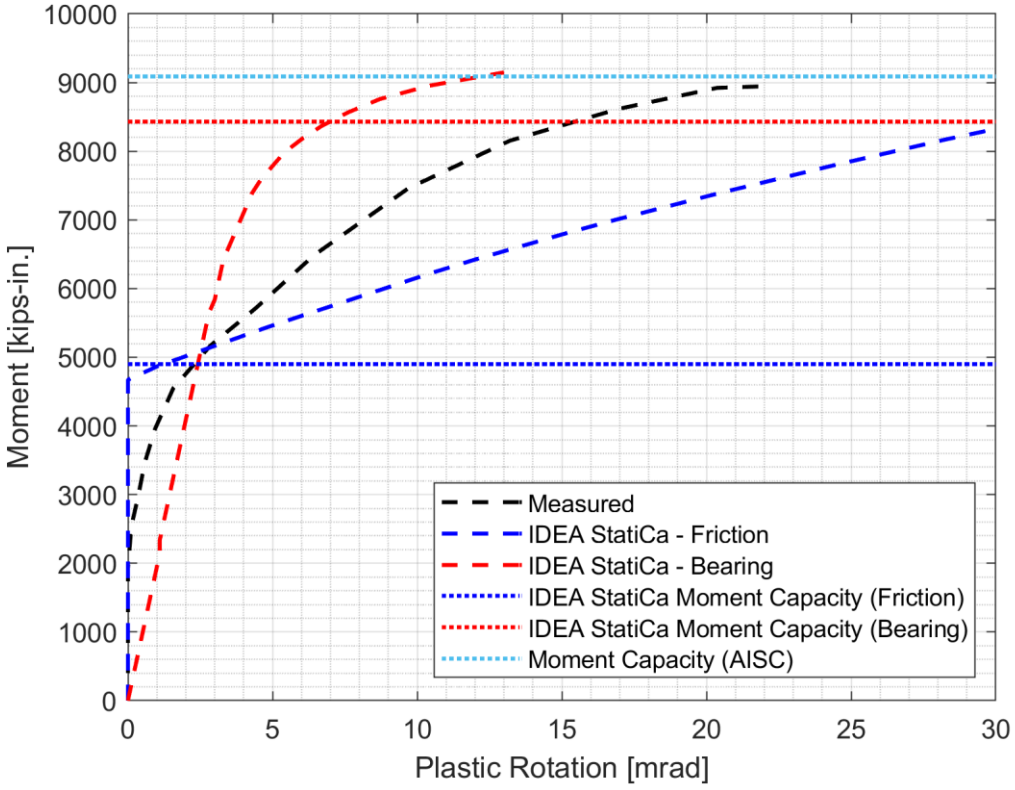

Figure 5.28: Moment rotation comparison

Variation 1 failed due to the net-section fracture of T-stub during the test. It was observed from the AISC design calculations that the controlling limit state was block shear of T-stem when mill certificate material properties were used while the controlling limit state became stem gross section yielding when coupon test material properties were used for T-stubs. Similarly, IDEA StatiCa analysis performed for both cases showed that insufficient T-stub strength was the failure mode of the specimen.

The experimental observations of variation 2 were similar to those of variation 1. The failure mode was reported as a net-section fracture of T-stub. Following the AISC design procedure, the controlling limit state was identified as block shear strength of T-stub when mill certificate material properties were introduced to all members. For the case that coupon test material properties were used for T-stub, stem gross section yielding was calculated as the controlling limit state. From both IDEA StatiCa analyses, it was observed that failure occurred in T-stub with 5.0% of plastic strain.

For variation 3, variation 4 and variation 5, the failure mode observed from the tests, AISC design procedure, and IDEA StatiCa analyses was the beam failure. Since the local buckling occurred during the cycle loads, no clear strength capacity was captured from the experiment. Although the

specimens satisfied the buckling requirements (see Appendices I and J), the reason local buckling occurred during the experiments can be attributed to the inaccurate measured material properties provided in the test report. The calculated moment capacities using IDEA StatiCa and following AISC design procedure and the maximum reached moment values during the experiments are shown in Figure 5.29.

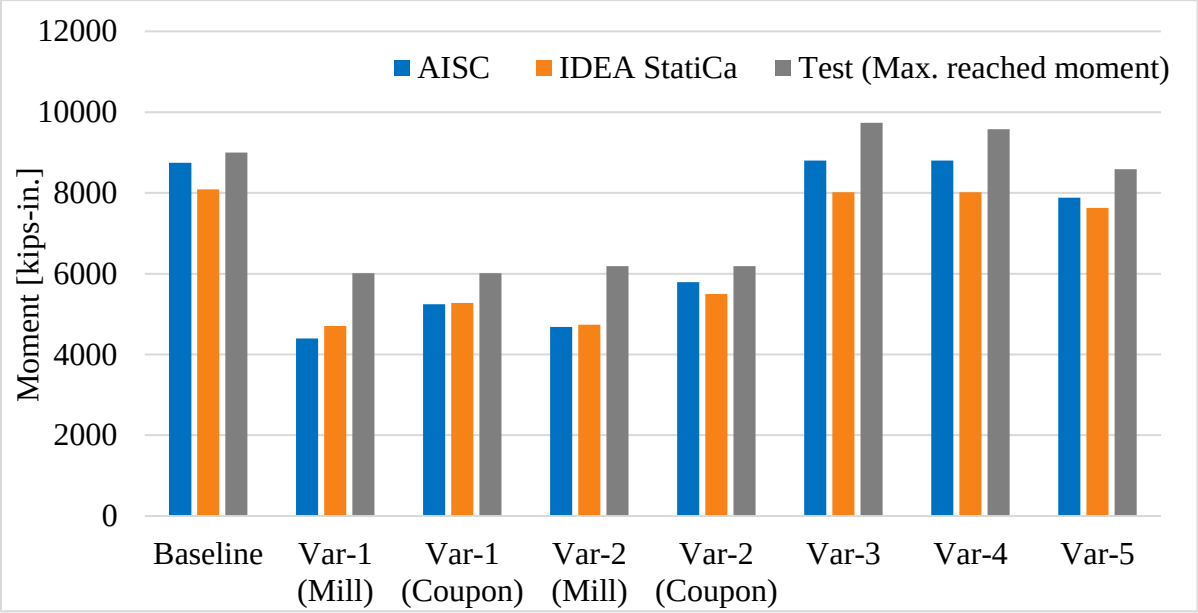

Figure 5.29: Moment capacity calculated by IDEA StatiCa and AISC procedure

References

Leon, R. T. (1999). *Tests on T-stub connections-SAC phase II-Subtask 7.03*. Georgia Institute of Technology.

Smallidge, J. M. (1999). *Behavior of bolted beam-to-column T-stub connections under cyclic loading*, Ph.D. Thesis, Georgia Institute of Technology, Atlanta, GA.

Swanson, J.A. (1999). *Characterization of the Strength, Stiffness, and Ductility Behavior of T-stub Connections*, Ph.D. Thesis, Georgia Institute of Technology, Atlanta, GA.

AISC 358 (2016), "Prequalified Connections for Special and Intermediate Steel Moment Frames for Seismic Applications, including Supplement No. 1," American Institute of Steel Construction ANSI/AISC 358-16, Chicago, Illinois.

AISC 360 (2016), "Specification for Structural Steel Buildings," American Institute of Steel Construction ANSI/AISC 360-16, Chicago, Illinois.

AISC 341 (2016), "Seismic Provisions for Structural Steel Buildings," American Institute of Steel Construction ANSI/AISC 341-16, Chicago, Illinois.

AISC Manual (2017), "Steel Construction Manual," American Institute of Steel Construction, Chicago, Illinois.

Chapter 6 Summary, Conclusion, and Recommendations

In chapter 1, one tested RBS moment connection was chosen from an experimental study (Uang et al., 2000) and five additional variations were created. The moment strength capacities of six specimens with failure modes were estimated following the AISC procedure and using IDEA StatiCa. Differences between the calculated capacities (1- moment capacity by IDEA StatiCa/moment capacity calculated by AISC procedure) vary from -3% to +7% while the average difference is approximately 4% (Table 6.1). Also, the moment rotation relationship calculated by IDEA StatiCa using stiffness analysis was compared with the one provided in the test report (Figure 6.1). It can be seen that IDEA StatiCa is capable of identifying the failure mode, calculating the moment strength capacity and moment rotation curve of RBS moment connections.

Table 6.1: Flexural moment strength of RBS moment connections calculated by IDEA StatiCa and AISC procedure (with respect to column face)

Specimen No	AISC Flexural moment capacity (kips-in.)	IDEA StatiCa Flexural moment capacity (kips-in.)	IDEA/AISC
Baseline	13,422	13,874	1.03
Var-1	11,162	10,800	0.97
Var-2	6,847	7,345	1.07
Var-3	11,983	12,157	1.01
Var-4	6,844	7,338	1.07
Var-5	6,842	7,337	1.07

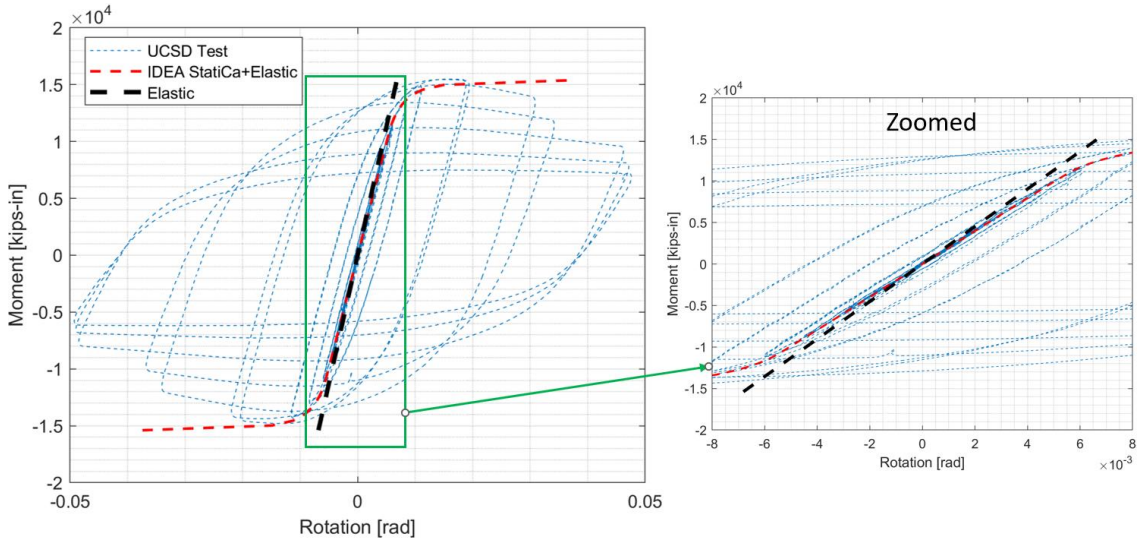

Figure 6.1: Moment (with respect to column centerline) plastic rotation comparison of RBS moment connection (baseline model)

In chapter 2, six tested EPM connections were assessed following the AISC design procedure and using IDEA StatiCa. Their moment capacities and failure modes were calculated and compared with the observations from the experiment (Sumner et al., 2000). Differences between the results vary from -7% to +11% while the average difference is approximately 2% (Table 6.2). It should be noted that the end plate yielding is controlling limit state for variation 3 where 11% difference is calculated while the insufficient weld strength between end plate and beam web is the failure mode observed from IDEA StatiCa analysis. When the weld reaches its strength limit, 1.9% of plastic strain is calculated in the end plate which is less than 5% of plastic strain limit for plates. From this example, it can be interpreted that the procedure outlined in AISC 358 for end plate yielding limit state provides a more conservative result than IDEA StatiCa. For the baseline model, the moment rotation curve obtained using IDEA StatiCa was compared with the experimentally measured one. IDEA StatiCa shows its capability in estimating the bolt rupture capacity including the effects of prying on strength capacity of bolts and the contribution of end plate stiffener on the flexural strength of EPM specimens. The difference between slopes after yielding and the gap between the reached peak moment values can be attributed to the stiffness degradation that the test specimen experienced and the bilinear material model used by IDEA StatiCa, respectively.

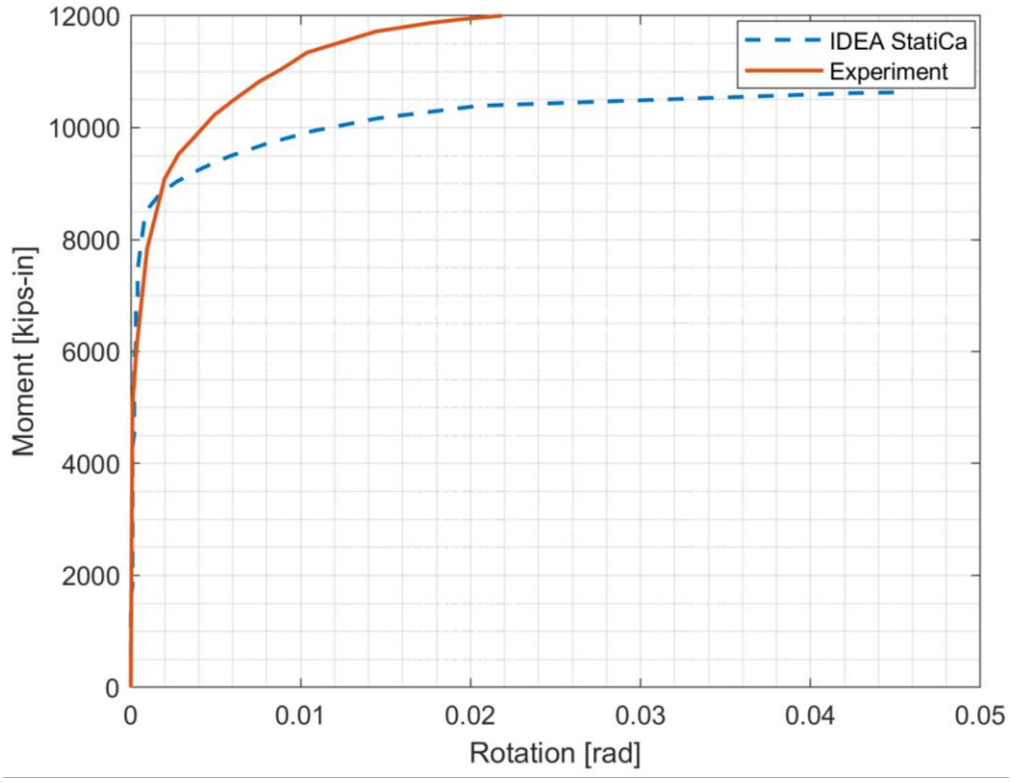

Figure 6.2: Moment (with respect to column centerline) plastic rotation comparison of EPM connection (baseline model)

Table 6.2: Flexural moment strength of EPM connections calculated by IDEA StatiCa and AISC procedure (with respect to column face)

Specimen No	AISC Flexural moment capacity (kips-in.)	IDEA StatiCa Flexural moment capacity (kips-in.)	IDEA/AISC
Baseline	10,216	9,969	0.98
Var-1	8,669	8,856	1.02
Var-2	34,323	36,298	1.06
Var-3	17,327	19,310	1.11
Var-4	18,338	19,275	1.05
Var-5	30,890	28,595	0.93

In chapter 3, the moment capacities and failure modes of six tested WUF-W specimens were calculated using IDEA StatiCa and following the AISC design procedure, and the observations were compared with the results of the tests performed by Ricles et al. (2000). The failure modes obtained from three sources are similar in all connections while the moment capacities calculated using IDEA StatiCa are approximately 8% larger than those obtained from AISC design procedure except the baseline model (Table 6.3). The reason that IDEA StatiCa calculates larger moment capacities than AISC procedure for variations can be associated with the assumption of plastic hinge location. It is recommended to be taken at column face by AISC 358 for WUF-W moment connections which leads to a lesser additional moment due to the shear force at the plastic hinge location compared to the case that it occurs a distance away from the column face. For the baseline model, IDEA StatiCa analysis shows that the specimen reaches its capacity when the weld between column face and shear tab fails. Similarly, hand calculations performed following AISC design procedure indicate that the weld does not satisfy the required strength limit. However, there is no procedure outlined by AISC to calculate moment capacity of these type of connections controlled by the weld between the column and beam or shear tab. It should be noted that the calculated moment capacity following AISC procedure is based on plastic moment strength of the beam though this connection is not permitted to be designed by AISC since the strength requirement for the weld is not satisfied. Overall, the average difference between the moment capacities calculated by IDEA StatiCa and AISC procedure is approximately 5%. In addition, moment rotation analysis was performed using IDEA StatiCa and ABAQUS for the baseline model and the results were compared. The moment plastic rotation curve calculated by IDEA StatiCa was compared with the measured one provided by test researchers (Figure 6.3). The difference between the slopes of the curves can be attributed to the stiffness degradation that the tested specimen underwent during the cyclic loading. Another comment that can be made is that since IDEA StatiCa employes bilinear material model, the strain hardening behavior could not be captured completely.

Table 6.3: Flexural moment strength of WUF-W moment connections calculated by IDEA StatiCa and AISC procedure (with respect to column face)

Specimen No	AISC Flexural moment capacity (kips-in.)	IDEA StatiCa Flexural moment capacity (kips-in.)	IDEA/AISC
Baseline	32,013	28,266	0.88
Var-1	32,013	34,662	1.08
Var-2	32,943	35,705	1.08
Var-3	32,943	35,705	1.08
Var-4	32,013	34,659	1.08
Var-5	32,013	34,723	1.08

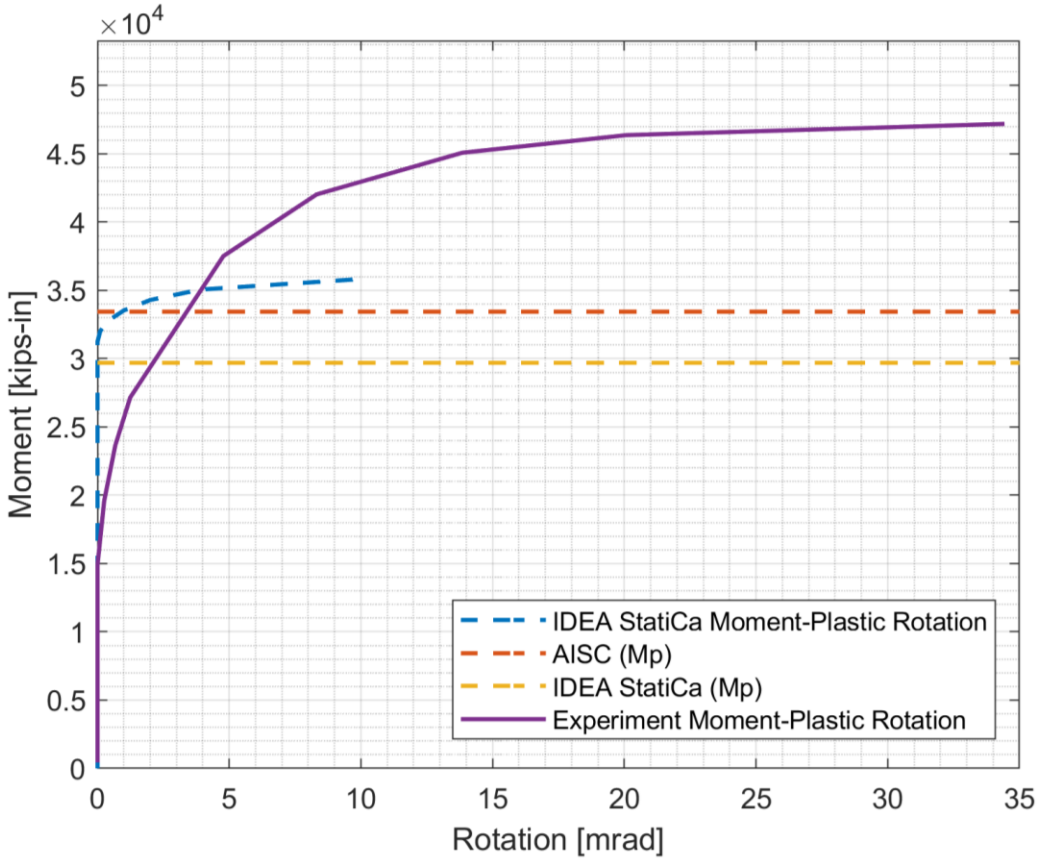

Figure 6.3: Moment (with respect to column centerline) plastic rotation comparison of WUF-W moment connection (baseline model)

In chapter 4, flexural behavior of five tested WUF-B specimens (Lee et al., 1999) were investigated with a total of eight models using two different bolt types: 1) friction, 2) bearing. Flexural moment capacities of the specimens were calculated using IDEA StatiCa and following AISC design procedure and compared (Table 6.4). Since slip critical bolts can be designed as pretensioned

bearing bolts if slip coefficient of faying surface is grater or equal to 0.30 according to AISC 341 (2016), the specimens containing slip critical bolts (e.g., baseline.SC, Var-2.SC, Var-3.SC) can be ignored in the moment strength comparison of IDEA StatiCa and AISC procedure. For the rest of the connections, differences between moment capacities calculated by IDEA StatiCa and AISC vary from -18% to -6% while the average difference is approximately 13%. The reason that IDEA StatiCa calculates more conservative moment strength than AISC procedure can be associated with the weak bond between beam web and column flange. A further examination can be conducted by replacing the shear tab with butt weld along the beam web and obtain a significant improvement in moment capacity following the same procedure in IDEA StatiCa.

For the baseline model, moment plastic rotation was obtained from IDEA StatiCa analysis and compared with the experimentally measured one (Figure 6.4). It should be noted that friction (slip critical) bolts are used for moment rotation analysis while bearing bolts are used for moment capacity analysis. The difference between the curves can be associated with the data extraction process. Since the measured moment rotation curve was extracted from the figure provided in the test report, small errors are inevitable. The difference of post-yielding behavior can be explained with the bilinear material model used by the software.

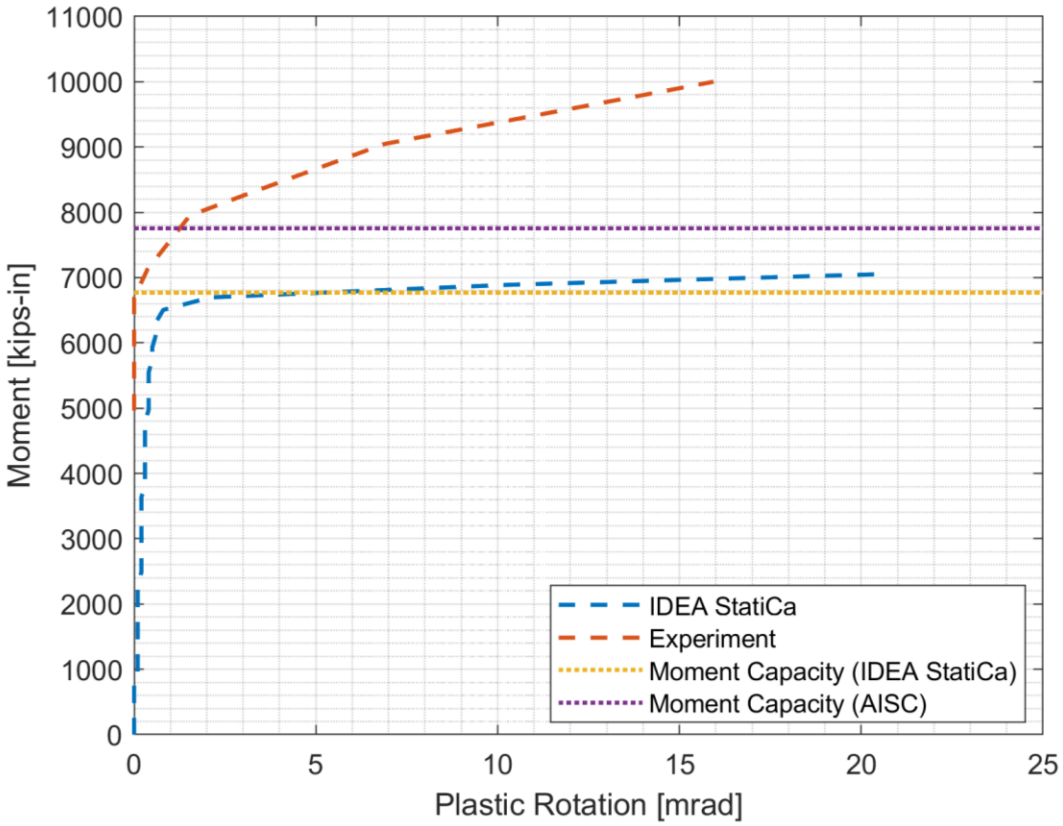

Figure 6.4: Moment (with respect to column centerline) plastic rotation comparison of WUF-B moment connection (baseline model)

Table 6.4: Flexural moment strength of WUF-B moment connections calculated by IDEA StatiCa and AISC procedure (with respect to column face)

Specimen No	AISC moment strength (kips-in.)	IDEA StatiCa moment strength (kips-in.)	IDEA/AISC
Baseline.SC	7,410	6,425	0.87
Var-1	11,831	11,091	0.94
Var-2.SC	15,974	12,116	0.76
Var-3.SC	15,538	11,779	0.76
Var-4	24,286	20,986	0.86
Baseline.X	7,410	6,482	0.87
Var-2.X	15,974	13,063	0.82
Var-3.X	15,538	13,165	0.85

In chapter 5, six tested double-tee connections were examined following AISC design procedure and using IDEA StatiCa. Their moment capacities were calculated, and the results were compared.

Differences between the results vary from -9% to +7% while the average difference is approximately 3% (Table 6.5). Also, the failure modes were estimated reasonably well. Moment rotation analysis was performed through IDEA StatiCa and ABAQUS using two different bolt types (e.g., bearing, friction) since tension-control bolt type is not available in IDEA StatiCa. The curves were compared with the experimentally obtained one performed by Leon (1999) for the baseline model (Figure 6.5). It is observed that moment plastic rotation curve of the test specimen falls between those calculated from IDEA StatiCa analyzes for friction and bearing bolts as expected. Additionally, prequalification checks outlined in AISC 358 were performed for the specimens. For the baseline model, capacity design analysis was performed in IDEA StatiCa, and compared with the one obtained following AISC procedure. It can be concluded that IDEA StatiCa is very capable of calculating moment capacity and determining failure mode of double-tee moment connections. Moreover, it can be added that capacity analysis (e.g., CD) is capable of determining whether the connection has enough strength capacity when plastic hinge occurs in both beams as required by AISC 358 for seismic connections.

Table 6.5: Flexural moment strength of double-tee moment connections calculated by IDEA StatiCa and AISC procedure (with respect to column face)

Specimen No	AISC moment strength (kips-in.)	IDEA StatiCa moment strength (kips-in.)	IDEA/AISC
Baseline	8,749	8,090	0.92
Var-1 (Mill)	4,398	4,702	1.07
Var-1 (Coupon)	5,246	5,278	1.01
Var-2 (Mill)	4,684	4,741	1.01

Var-2 (Coupon)	5,787	5,499	0.95
Var-3	8,802	8,013	0.91
Var-4	8,802	8,013	0.91
Var-5	7,880	7,630	0.97

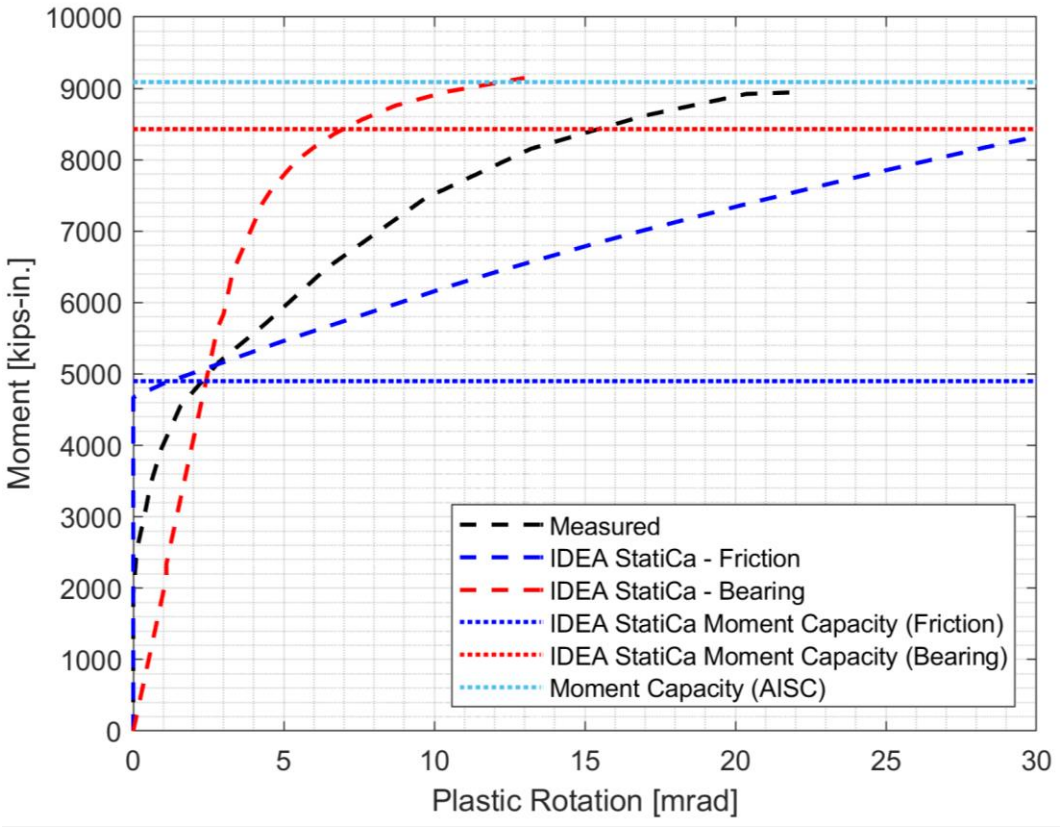

Figure 6.5: Moment (with respect to column centerline) plastic rotation comparison of double-tee moment connection (baseline model)

Overall, there is good agreement among the moment capacities and failure modes obtained from tests, IDEA StatiCa analysis, and AISC design procedure. The recommendations to further improve the software are listed below:

- A new bolt type for tension-controlled/preloaded bolts can be developed and provided to users in addition to bearing and friction bolt types.
- Forces to be applied with "loads are in equilibrium" options can be calculated from IDEA StatiCa for different element lengths and boundary conditions according to user's preferences. In this way, an analysis can be performed for desired condition without other software or additional hand calculation. With the current IDEA StatiCa version (i.e., v22),

to calculate moment capacity of test specimens, the forces at the connection were calculated using SAP2000 by representing test setup conditions (e.g., element lengths, boundary conditions), then those calculated forces were applied in IDEA StatiCa using "loads are in equilibrium" option.

- Incremental loading can be applied automatically and systematically by IDEA StatiCa and the moment capacity can be provided without a need of adjusting the loads and re-run
- Prequalification checks can be performed by IDEA StatiCa
- A better meshing tool can be adapted to the software
- The representation of moment rotation curve can be improved/enriched by providing users tools to adjust font, color, and size of plot.
- Some symbols need to be corrected/adjusted for the American users (e.g., θ instead of ϕ for the rotation according to AISC)